Reprogramming Pediatric Genetic Disorders: Pearson Syndrome, Ring 14 Syndrome, and Fanconi Anemia

Reprogramming Pediatric Genetic Disorders:
Pearson Syndrome, Ring 14 Syndrome, and Fanconi Anemia

A dissertation presented by

Anne Blanche Cresswell Cherry

to the Division of Medical Sciences
in partial fulfillment of the requirements for the degree of
Doctor of Philosophy

in the subject of
Biological Chemistry and Molecular Pharmacology

Harvard University
Cambridge, Massachusetts
April 2014

Dissertation Advisor: Professor George Q. Daley Author: Anne B. C. Cherry

Abstract

Reprogramming Pediatric Genetic Disorders:

Pearson Syndrome, Ring 14 Syndrome, and Fanconi Anemia

The effect of a single genetic mutation can vary greatly between different types of cells. The mutated gene may not be expressed in one tissue but may cause a devastating loss of function in another. To learn about disease mechanisms and generate novel therapies, genetic disorders must be studied in the types of cells where the mutations are most deleterious. Recently, scientists have begun manipulating cellular identity to create the cell types most affected by various genetic diseases. This dissertation describes the experience of generating reprogramming models for three genetic disorders: Ring 14 syndrome, Pearson syndrome, and Fanconi anemia.

Pearson syndrome is a mitochondrial disorder caused by large deletions in mitochondrial DNA (mtDNA). We generated a Pearson syndrome iPS line and an isogenic line that carried only healthy mitochondria. We investigated the effect of the mutant mtDNA on pluripotent cell growth and metabolism, then differentiated both lines into blood cells. Erythroid progenitors carrying the mtDNA mutation showed a clear pathological phenotype associated with the disease.

Ring chromosome 14 causes developmental delay and severe seizures. Until the work described here, there was no opportunity to study cells from ring 14 patients in any cell type other than fibroblasts or peripheral blood. We generated multiple iPS lines that carried the ring chromosome, and were able to identify an isogenic, disease-free control line derived from non-disjunction. R14-iPS cells were then differentiated down a neuronal lineage, marking the first ever neural cells from a ring 14 patient available for study.

Many laboratories have found that Fanconi anemia cells reprogram very poorly. In our non-viral reprogramming system, we were surprised to find that Fanconi cells reprogrammed nearly as well as cells from their wild-type littermates. These results provide new insight into why published attempts to reprogram FA cells have failed.

This dissertation contains these three examples of manipulating cellular identity to learn about rare genetic diseases.

Table of Contents

This dissertation is dedicated to the remarkable parents I have met whose children suffer from rare genetic disorders. Their tenacious bravery and unrelenting pursuit of research provides constant inspiration for my work.

Acknowledgements

It is with immense gratitude that I acknowledge the support and help of my PI, Dr. George Daley. He inspired me, helped me stay on top of my multiple projects, and provided a wonderful laboratory in which to work. He is the most impressive scientist I know, because his scientific brilliance is matched by his geniality—not a common combination. He is capable of always projecting an aura of knowledgeable calm, except when rocking out to karaoke.

The members of my dissertation advisory committee, Dr. Fred Alt, Dr. Johannes Walter, Dr. Keith Joung, and Dr. Alan D'Andrea were invaluable assets over my time here. They constantly pushed me and helped me prioritize the most important experiments. Thank you to my dissertation readers, Dr. Fred Alt, Dr. Len Zon, Dr. Gustavo Mostoslavsky, and Dr. Ann Poduri for their time and consideration.

The members of Dr. Daley's laboratory have supported me throughout the Ph.D. process, both personally and professionally. I would like to start by thanking Dr. Suneet Agarwal, who was the post-doc I worked with during my rotation in Dr. Daley's lab. Dr. Agarwal's excitement over science and surplus of crazy—yet potentially feasible—ideas helped me settle into the lab and work at a bench for the first time. I owe great debts to Dr. Tamer Onder, who taught me to reprogram human cells, and Dr. Juli Unternaehrer, who taught me to reprogram mouse cells. Dr. Lars Mueller was an early inspiration for my work in Fanconi anemia, and continued to be a sounding board as my project evolved. Dr. Thorsten Schlaeger has always been around to answer questions about reprogramming, and the excellent technicians he leads have assisted me on many experiments, especially Phil Manos, Andrew Ettenger, and Alex Devine. Our lab manager Beth Kaleta has helped me at every turn, from learning the minutiae of laboratory life to promoting my newfound interest in crossword puzzles.

I do not have enough words to express my gratitude to Dr. Willy Lensch. Willy was the scientific guru of the Daley laboratory for many years, and until recently becoming the head of Harvard's Stem Cell and Regenerative Biology department. There is not a paper or scientific fact, especially about Fanconi anemia, that Willy does not know. He is always eager to share this knowledge with a listening ear. On top of his considerable scientific expertise, Willy is a wonderful lab companion, always enthusiastic to talk about teaching, weddings, life, science, or cooking recipes. We in the Daley lab miss him like crazy and are glad that he is just across the river.

The Leder Human Biology program, run by Dr. Connie Cepko and Dr. Thomas Michel, provided me with some of my favorite experiences from my graduate school years. I am thankful to have had the opportunity to take the translational courses offered and to observe hematology and pediatric epileptology in a clinical setting.

More recently, the members of the Daley blood subgroup—Linda Vo, Dr. Sam Morris, Dr. Sergei Doulatov, Stephanie Chao, and Dr. Natasha Arora—have helped maintain my sanity with their good (albeit off-color) humor and their constant willingness to lend a hand. Linda Vo in particular has provided invaluable assistance with her always-friendly, incredibly generous weekend "babysitting" of my iPS cells.

I owe my deepest gratitude to my parents, Joyce Cresswell and Dick Cherry, for instilling a love of learning and curiosity in me from an early age. I was a colicky baby, and when they were awake with me in the middle of the nights, they said to each other, "At least she won't cry like this when she's at Harvard." And for the most part they were right—the only exceptions were when 90-day experiments failed. I also would like to thank my brother Scott, for always believing I could do anything I put my mind to.

My aunts, uncles, grandma, cousins, in-laws, and outlaws have always helped me keep my work in perspective. I am blessed to have family members who always want to hear about what I am doing, and who continually inspire me to be a better translational scientist.

Finally, I wish to thank my brilliant and dedicated wife, Elyse Cherry, for her support of my work and my self over the last five years. Her encouragement helped me through the hard times in lab and she celebrated with me in the happy times, and I will forever be grateful.

Scientific Contributions of Collaborators

This work could not have been accomplished without the dedicated and generous work of my many collaborators. One of the best parts of being a member of Dr. Daley's laboratory is the generous spirit of collaboration, exchange of ideas, and experimental assistance. Many of these collaborators have made concrete contributions to the work in this dissertation, as described here.

The introduction and conclusion chapters of this thesis share some of their text with two reviews I have published, one in Cell and the other in the Annual Review of Medicine. Both of these reviews were primarily written by myself and then edited by Dr. Daley.

The text and figures from Chapter 2 are largely drawn from a paper on which I am co-first author that was published last year in Cell Stem Cell. I played a primary role in the writing of the manuscript, experimental and text revisions, and correspondence with editors. The Pearson syndrome project was initiated by Dr. Suneet Agarwal, whose guidance and technical expertise was instrumental in completion of the paper. The original focus of the investigation was on reprogramming Coriell cell lines carrying mitochondrial mutations. I joined the project just after diagnosis of the patient with Pearson syndrome. I took on characterization of the patient's somatic cells and iPS cells, and derivation of the mutant mtDNA-free isogenic control iPS cells, which ended up being the main focus of the published paper. Dr. Agarwal performed many of the Southern blots described in the chapter, and Dr. Paul Lerou was responsible for FISH, immunofluorescence, and the imaging in Figure 2.7. When Dr. Agarwal formed his own laboratory, he hired an excellent technician, Katie Gagne. Ms. Gagne performed the hematopoietic differentiation from PS-iPS lines, grew iPS cells, and ran some of the Southern

blots. Finally, Dr. Mark Fleming performed the blinded pathology analysis of our PS erythroid progenitors. I am very thankful to all of these collaborators for their assistance.

Work presented in Chapter 3 is part of a manuscript that I am currently preparing for submission. I am grateful to Prerana Malwadkar for performing immunofluorescence imaging, and Alejandro de los Angeles for teratoma injections and analysis. Dr. Lorraine Meisner of Cell Line Genetics performed karyotypes and FISH. Finally, I am very thankful to Dr. Didem Demirbas, who performed the neural differentiation of the R14-iPS cells.

In Chapter 4, a wonderful rotation student, Linda Vo, worked with me and assisted in optimization of the reprogrammable mouse system. Dr. Tamer Onder and Dr. Juli Unternaehrer also contributed to my interpretation and understanding of the nuances of reprogramming efficiency. The attempts to reprogram human FA cells during preparation of the 2008 Cell paper were performed by Dr. In-Hyun Park.

To all of my wonderful collaborators, thank you. I could not have accomplished the work described here without your help.

"What an exciting future!"

Howard L. Cherry, MD, upon his retirement
from public service in 1987.

Chapter 1: Introduction and Background

Introduction

When a sperm fertilizes an egg, the genetic material from both gametes combines to form a single nucleus. This nucleus is located in a giant cell called the zygote. Over the next few days the zygote undergoes many cell divisions and eventually becomes a hollow, spherical structure called a blastocyst. Most of the blastocyst will go on to form the placenta, but about a dozen small cells tucked inside the protective outer coating will divide and create first a fetus, then a newborn, then an adult human. These dozen cells are called the inner cell mass. As development progresses, their cellular identities will shift and change, becoming more and more specialized. Genes will be turned on and off, proteins will be generated and degraded, and the cells' functions and behaviors will evolve. Nine months later, those dozen cells will have generated an entire human being: fingers and toes, brain and blood. But sometimes the zygote carries a fateful flaw: tiny errors in its DNA sequence can irreversibly alter the course of that particular zygote's life. This dissertation describes the investigation of three such DNA changes, and how our growing awareness of cellular identity has led to a deeper understanding of the resulting diseases.

If a scientist removes the inner cell mass from a blastocyst, the cells can be nurtured in a laboratory dish. They can reproduce and eventually will generate millions of embryonic stem (ES) cells. Each ES cell retains the ability to form any tissue of the body, and so is termed "pluripotent:" many-potentialed.

The first derivation of human ES cells, accomplished by James Thomson in 1998, captured the imaginations of clinicians and scientists alike (*1*). Cellular pluripotency suggested

revolutionary approaches to learning about and treating human disease. Researchers began developing techniques to coax ES cells to become specialized cell types: heart cells, neurons, insulin-producing pancreatic cells, liver cells, and blood cells. Once these cell types could be made, they promised to become revolutionary new tools for learning about and treating human diseases.

But in the United States, research into this promising avenue of investigation flagged as opposition sprang up from opponents of embryo research. New policies severely limited federal funding of ES cell studies, impeding US scientists' ability to work on this versatile new cell type. With American research hobbled, scientists from around the globe asserted strong leadership positions in the field. Major stem cell research initiatives grew in the United Kingdom, Israel, Singapore, and Japan, fueling the excitement of research communities in these countries (*2*). One flagship center at Kyoto University, the Institute for Frontier Medical Sciences, was founded in 1998 with the goal of advancing the field of regenerative medicine by characterizing ES cells. At this institute, Dr. Shinya Yamanaka began tinkering with ES cells and trying to understand their hitherto unmatched pluripotency. Through an ingenious series of experiments, Dr. Yamanaka and colleagues developed a new technology to convert fibroblasts and other somatic cells into induced pluripotent stem cells (*3*).

Dr. Yamanaka's breakthrough research built upon previous demonstrations that one type of cell could be turned into another by expressing transcription factors specific to the target cell; for example, expression of the muscle-specific transcription factor *MYOD* has been known to convert fibroblasts into muscle progenitor cells since the 1980s (*4*). Dr. Yamanaka and Kazutoshi Takahashi, a graduate student in his lab, hypothesized that they could convert fibroblasts into pluripotent stem cells by overexpression of embryonic transcription factors. To

observe what they anticipated would be a very rare event, they used cells from a strain of mice that carried an antibiotic resistance gene under the control of an embryonic gene promoter (*3*). Cells from this strain of mice would become resistant to antibiotics only if they adopted embryonic-like gene expression. By infecting these cells with retroviruses containing candidate genes, Dr. Yamanaka and Dr. Takahashi hoped to discover combinations of transcription factors that conferred antibiotic resistance by activating an embryonic gene expression program. Their enormous challenge was to identify a combination of genes that could accomplish such a drastic transformation of cellular identity.

Twenty-four genes involved in pluripotent cell identity were chosen as candidates for induction of pluripotency. No single factor was able to induce antibiotic resistance, but when all 24 were transfected at the same time, some rare cells successfully activated embryonic expression patterns and acquired resistance to the antibiotic. When the resistant cells were grown in culture, about half of them demonstrated characteristics of pluripotent stem cells, including morphology, growth rate, and expression of key embryonic genes. These cells were named induced pluripotent stem (iPS) cells.

After the successful initial reprogramming of fibroblasts into pluripotent stem cells, the investigators began to narrow down the field of responsible genes. They infected cells with viruses containing all possible combinations of 23 genes, leaving one gene out each time; those experiments that "failed" identified the genes that were required for embryonic gene expression. This led to the identification of four genes which were indispensable for efficient reprogramming: *OCT4*, *SOX2*, *KLF4*, and *MYC* (collectively termed OSKM) (*3*). These genes are now colloquially referred to as the "Yamanaka factors" and comprise the four genes most commonly used to induce pluripotency.

The initial murine iPS cells were evaluated for pluripotency by multiple assays. First, cell surface markers were investigated, which demonstrated the similarities between iPS and ES cells. Then microarrays comparing gene expression profiles between iPS and ES cells demonstrated that although the cell types were distinguishable, they shared virtually all characteristic expression patterns. Next, teratoma assays showed that the iPS cells were capable of differentiating into cell types of all three germ layers, a crucial test to prove their pluripotency. Finally, the authors established that when iPS cells were injected into blastocysts, they contributed to all three germ layers in developing embryos (*3*). Since the initial report, murine iPS cells' pluripotency has been further confirmed by the birth of live chimeras, germline transmission, and the most stringent test for pluripotency, tetraploid complementation, which entails injecting pluripotent cells into engineered tetraploid embryos and obtaining a complete mouse derived entirely from the iPS cells (*5-8*).

One of the most impressive features of Dr. Yamanaka's discovery was its robust repeatability. Within 18 months of publication of the seminal paper describing mouse reprogramming, three independent laboratories reported successful derivation of human iPS cells, and shortly thereafter two groups produced iPS cells from patients with a multitude of diseases (*9-13*). By mid-2008, it was clear that Dr. Yamanaka's new reprogramming technology had revolutionized how scientists thought of cellular identity. While Drs. Weintraub, Graf, Busslinger, and colleagues had investigated rather modest cell identity changes between mesodermal or hematopoietic lineages, an engineered cell identity change as dramatic as reversion of differentiated cells to pluripotency was not envisioned as plausible before Dr. Yamanaka's work (*4, 14, 15*).

Two main types of pluripotent stem cell now exist: ES cells, derived from the inner cell mass of blastocysts, and iPS cells, created by reprogramming adult cells. ES and iPS cells demonstrate highly similar gene expression and epigenetic regulation and in some cases are functionally interchangeable (*16-19*). However, there are a number of important differences between the two cell types.

First of all, ongoing research into the similarities and differences between iPS and ES cells has made it clear that the two cell types are not completely identical (*17, 20, 21*). During iPS cell generation, reprogramming is often unable to completely eradicate epigenetic markers of the original cell type, which is termed epigenetic memory. These iPS lines retain some epigenetic signatures of their tissue of origin and are most effective at differentiating into the tissue type from which they were originally derived. For example, some iPS lines derived from blood cells differentiate into a hematopoietic lineage more efficiently than do iPS lines derived from skin cells (*16, 18*). This suggests that many iPS cell lines have not reached a true pluripotent state, and further research into the epigenetics underlying reprogramming must be done before iPS cells can be considered as unbiased as ES cells.

Secondly, iPS cells have vastly greater potential for disease research and eventual therapeutics than do ES cells. Before iPS technology, the only ways to obtain human pluripotent stem cells carrying a particular genetic disease was to recruit parents undergoing preimplantation genetic diagnosis and generate ES cells from their discarded blastocysts (*22, 23*). Now, using a reprogramming approach, researchers can generate iPS cells from patients bearing virtually any remarkable genotype. This change is reflected in the large and growing number of disease-specific human pluripotent stem cell lines that have to date been described (*24*). iPS cells also have an important clinical advantage over ES cells: the genome of an iPS cell matches the

genome of the patient from whom it was derived. Thus, if organs or tissues can one day be derived from iPS cells, they will be less apt to face immune rejection when transplanted than tissues derived from allogeneic ES cells (*25, 26*). This advantage may be maintained even in cases where a patient's disease is genetic, if genetic correction can be applied to the cells before transplant (*27*).

Finally, human ES cell isolation requires the destruction of human blastocysts. This concern has led to regulatory, financial, and logistical hurdles for research involving ES cells. In the United States, derivation of ES cells is subject to close regulation by Embryonic Stem Cell Research Oversight Committees, and research funding from the federal government is restricted to a limited subset of ES cell lines that have passed scrutiny by an ethical review committee of the National Institutes of Health (*28, 29*). Derivation of iPS cells does not involve human embryos, so the use of iPS cells raises fewer ethical questions and is subject to less federal oversight (*1, 11*). Thus, in addition to the considerable advantages of iPS cells for disease research applications, they likewise provide significant practical advantages relative to ES cells.

Although a few laboratories still focus on ES cells, the many advantages of iPS cells have made the latter a much more common research tool. For scientists interested in genetic, cell-autonomous disorders, research can be performed on platforms as diverse as epidemiology, human genetics, animal modeling, and *in vitro* cell culture. Each of these approaches provides different kinds of information about the disorder under investigation, and each has its own limitations. The advent of patient-specific stem cells has led to a completely novel platform for studying human disease.

Design and verification of an iPS cell-based disease model

The premise of iPS cell-based disease modeling is simple: differentiate the iPS cell into the cell type affected by the disease and identify a disease-specific phenotype (Figure 1.1). Researchers can then learn about disease mechanisms, search for new drug treatments, or prepare to perform cellular therapy. These goals underlie all iPS cell-based disease models, including those described in this dissertation, but creation and execution of a successful disease model is more complicated than it may first appear. There are five discrete choices to be made: which disease, which control, which target cell type, which differentiation protocol, and which disease-relevant phenotype to investigate.

1) Disease choice. During reprogramming, the cellular epigenome is reset and all environmental conditions are normalized, such that the only disease risk factors carried by the resulting iPS cells are those encoded in its genome (*30, 31*). With this in mind, researchers to date have mostly chosen to create their first disease models either from strictly genetic diseases (e.g., trisomy 21, Shwachman-Diamond syndrome, dyskeratosis congenita) or from a genetic version of a more complex disease (e.g., the SOD1-mutant familial amyotrophic lateral sclerosis, the PINK1-mutant familial Parkinson's disease, the APP-mutant familial Alzheimer's disease) (*32-37*). By ensuring that the iPS cells carry the predisposition to disease, researchers hope to be able to identify a disease-related phenotype when they differentiate the cells.

2) Choice of control. The goal of creating an iPS cell-based disease model is to phenotypically distinguish the disease-bearing cells from the control cells. But results will vary drastically depending on which control cells are used. Unfortunately, different pluripotent cell lines are notoriously variable in their differentiation tendencies and abilities. This is true both

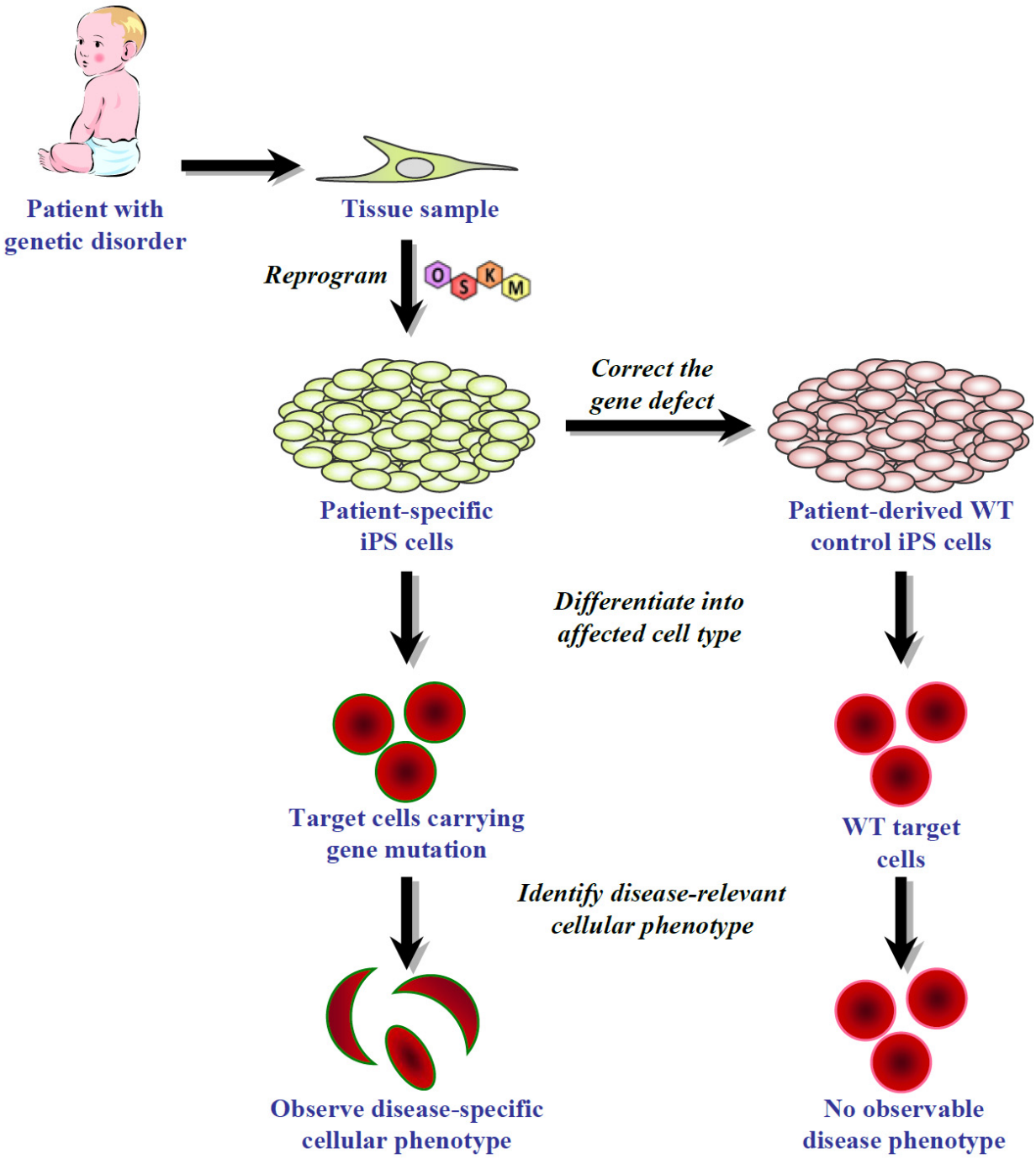

Figure 1.1: Modeling genetic diseases using induced pluripotent stem cells. Patient tissues are reprogrammed, then genetically corrected. The two lines are differentiated into the tissue type affected by the disease. Any difference in phenotype between the two lines is attributable to the gene defect.

between iPS lines generated from different individuals and even between iPS lines generated in parallel from a single patient (*38-40*). For this reason, the best control for any disease model is to correct the disease genotype in the patient's affected iPS line, rendering it genetically wild-type (WT). Any phenotypic discordance observed in cells differentiated from these lines can be immediately ascribed to the disease genotype. Depending on the nature of the disease, correction may be achieved by viral rescue, genome editing, subcloning, or other manipulations. If this can be accomplished, the disease-carrying and the repaired lines are isogenic, distinguishable only by the status of the disease allele or genotype.

3) Target cell type. Genetic diseases manifest differently in different cell types. A mutation that creates a toxic protein in one cell type may be harmless in another—for example, patients with Fanconi anemia endure bone marrow failure but are neurologically normal, while patients with ring 14 syndrome suffer devastating developmental delays but have normal hematopoiesis (*41, 42*). Once the disease is chosen and a control line has been created, researchers must determine which target cell should be used in their model. This choice is influenced by the type of cell most strongly affected in patients, the likelihood of identifying a cell-autonomous phenotype, and the availability of protocols to generate target cell types *in vitro*. Scientists must also consider the best method to verify that the cells they generate are equivalent to the target cells, such as surface markers, transcriptome or epigenetic analysis, or functional assays.

4) Differentiation protocol. In many cases, *in vitro* differentiation protocols are a limiting factor for disease modeling. Even though scientists have worked on directed differentiation approaches for decades, this step is usually the highest hurdle in a stem cell-based model. Differentiation protocols generally attempt to recapitulate the cellular niche present during

embryonic development. Various protocols provide cytokines, 3D organization, mechanical stimuli, exogenous transcription factors, or co-culture with supportive stromal cells in an attempt to induce directed cellular identity changes (*43-47*). Unfortunately, many cell types derived from human iPS cells are not fully differentiated or more closely resemble immature fetal tissue than the mature adult organs affected by disease (*48-53*). In these cases, other cellular identity manipulations may yield better models than approaches beginning with pluripotent cells. One such possibility is transdifferentiation of one somatic cell type to another. This has been particularly successful in the cardiac field, where iPS cell-derived cardiomyocytes remain immature but more adult-like cardiomyocytes have been successfully derived from fibroblasts (*51, 54*). Researchers have been even more successful at generating adult-like cardiomyocytes using *in vivo* cellular identity transformations, but this approach is unlikely to translate into cellular disease models (*55, 56*). In the case of human definitive hematopoietic stem cells (HSCs), a significant part of the reason they have never been successfully derived *in vitro* is likely because researchers lack suitable culture conditions to maintain and expand these evanescent cells. Where appropriate chemical manipulations, ideal starting cell types, or cell culture conditions remain poorly defined, directed differentiation protocols represent a critical rate-limiting step in disease modeling (*57*).

5) Identification of disease-relevant phenotype. The final step in creating a stem cell-based disease model is the identification of a disease-specific phenotype in the resulting cells. In order for a disease model to be informative, its primary phenotype should be directly relevant to the disease, which is why the best cellular phenotypes are those that are also seen in primary patient tissues. These include phenotypes like arrhythmias in cardiomyocytes with long QT syndrome and abnormal glucosylceramide accumulations in macrophages with Gaucher disease

(*58-60*). The importance of a strong, disease-relevant phenotype is two-fold. First, the cellular phenotype is the basis of the model's utility for research on the disease mechanism. As the model is studied, it will provide information about the mechanism by which the cell produces the phenotype. If the phenotype is unrelated to the actual disease, the model will be of no benefit for disease etiology research. Secondly, a strong cellular phenotype can be the basis for a drug screen. If a phenotype can be measured in a high-throughput assay, the model can become a platform for discovery of new therapeutic approaches.

It may be that in certain diseases, no relevant disease-specific phenotype will be forthcoming. This is especially likely in disorders whose basic mechanisms are not yet understood—a cellular phenotype may exist, but scientists have yet to discover what it is. In these cases, the phenotype search itself is likely to yield information critical to understanding the disease process.

Applications of iPS cell-based disease models

Once a model exists for a given disease with an appropriate control, an accurate differentiation protocol, and a biologically-relevant cellular phenotype, it can be put to work understanding disease mechanism, screening for drugs, or eventual cellular therapy (Figure 1.2). Each of these three goals is applicable to different disorders, depending on the nature of the disease and the current state of research in the field.

For disorders where etiology is unclear, patient-specific iPS cell models may confirm current theories or inspire new hypotheses about the origins and progression of the disease (*61*). The opportunity to investigate disease mechanism and phenotypes in the type of cell affected by

the condition—rather than in cell lines or cadaveric samples—is a huge step forward for research on genetic conditions affecting brain, heart, retina, and other inaccessible organs from which scientists cannot obtain living cell samples.

For disorders whose etiology is understood well enough to identify a cellular phenotype, that readout can be used as the basis for a drug screen. As mentioned above, if the *in vitro* phenotype shares a mechanism with its *in vivo* clinical manifestation, a drug that can ameliorate the *in vitro* phenotype may be expected to help a patient. By this logic, once a disease-specific cellular phenotype is identified, iPS technology can provide material for high-throughput drug screens to identify novel therapeutic agents.

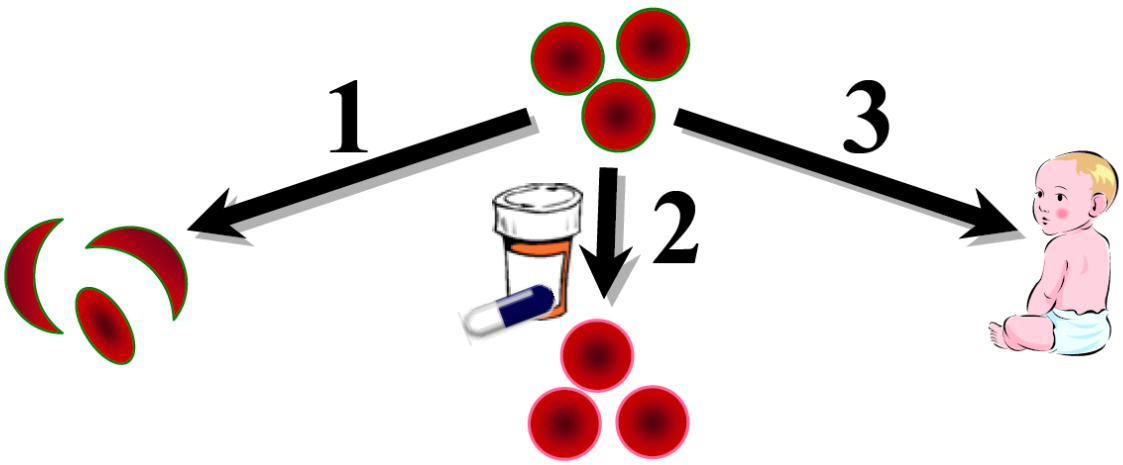

1. Disease mechanism

- Study the processes by which the mutation leads to cellular disease phenotype
- Confirm, disprove, and generate hypotheses of disease etiology

2. Drug screens

- Perform drug screens on the cellular model to identify novel therapeutic approaches
- Test new drugs for toxicity

3. Cellular therapy

- Eliminate the genetic defect
- Differentiate iPS cell into target cell
- Transplant target cell into patient

Figure 1.2: Three applications of iPS cell research.

In addition to identification of new drugs via screens, iPS-derived cells are also expected to facilitate the process of drug development. One of the most common reasons new drug candidates fail clinical trials is due to toxicity to patients' liver, heart, or brain (*62*). By producing human hepatocytes, cardiomyocytes, and neurons *in vitro*, scientists will be able to screen potential drug compounds for toxicity at a much earlier stage of development (*63-65*). Not only is this likely to prevent toxic drugs from reaching clinical trials, but will also give researchers a chance to tweak the molecular makeup of their compound in order to minimize toxicity before investing millions of dollars in moving the drug to the clinic.

Most genetic conditions could reap rewards from the *in vitro* research and drug screens described above. But reprogramming-based cellular transplantation therapy, the most complicated and difficult goal for patient-specific stem cell research, is only an option for a select subset of diseases. Disorders caused by an overabundance of cells (e.g. cancer), widespread cell dysfunction (e.g. Alzheimer's disease), or cellular disorganization (e.g. autism (*66*)), are not candidates for cellular transplantation therapy. Only those rare conditions where the symptoms are caused by lack of a certain group of cells (e.g. bone marrow failure, type I diabetes, Parkinson's disease) could be successfully cured by transplantation of cells from an outside source.

History of clinical stem cell therapy

One stem cell-based therapy is already widely accepted and utilized worldwide: hematopoietic stem cell transplantation. This practice was pioneered by Dr. E. Donnall Thomas in 1959, when he demonstrated that the bone marrow from one identical twin could reconstitute

the blood system of the other twin, who suffered from leukemia (*67*). Initial treatment success was limited to those rare patients who had identical twins, because transplantation of bone marrow from nonidentical donors resulted in severe, systemic attack of the new immune system against the recipient's organs, a condition termed graft-versus-host disease. After ten years of exhaustive research into human leukocyte antigen (HLA) matching and immunosuppression, Dr. Thomas's team successfully performed a bone marrow transplant from one non-twin sibling to another (*68, 69*). This extraordinary feat earned Dr. Thomas a Nobel Prize in 1990 for his contributions to cellular transplantation.

Since 1959, the practice of hematopoietic stem cell transplantation has become widespread. Advanced and inexpensive HLA typing has allowed the collection of millions of potential bone marrow donors in national registries, and an increased understanding of hematology and immunology has lessened the risks associated with transplant. However, even with high-quality HLA matches, bone marrow transplant still carries a treatment-related mortality of 5-20% in the first few months (*70, 71*). The dangers of this period include extreme neutropenia and consequent infections, failure of the transplant to engraft, and acute and chronic graft-versus-host disease. Various features of the transplant determine the likelihood of these complications, including the number of hematopoietic stem cells that are transplanted and the degree of mismatches at both major and minor histocompatability loci. Most patients who survive the transplant itself have a good long-term prognosis, with overall five-year survival rates around 70-80% for non-cancer patients (*72-75*).

Hematopoietic stem cells' robust differentiation potential allows a few hundred milliliters of donor marrow to reconstitute an entire organ in the recipient. Following intravenous infusion, the transplanted hematopoietic stem cells home in on the bone marrow and engraft into the

niches already present there. No cellular organization is required for transplant to occur, making the blood system an attractive starting place for working toward iPS cell-derived cellular therapy. Combined with bone marrow transplant's long history and established clinical efficacy, this advantage makes the hematopoietic stem cell arguably more feasible for clinical application than stem cells from organ systems; however, the quest to convert human pluripotent stem cells into functional, engraftable hematopoietic stem cells has been challenging and has not yet proven successful. This complex task requires a thorough understanding of the developmental events that lead to formation of HSCs in vivo and approaches to mimic these events in the laboratory.

In vitro differentiation of pluripotent cells into blood

Hematopoietic development is strikingly similar in mice and humans, so researchers have turned to the mouse to learn about mammalian blood development. It is hoped that an exhaustive understanding of the signaling, migration, and molecular events in the developing mouse hematopoietic system will inform our ability to direct similar development *in vitro* from human pluripotent stem cells.

In both mouse and human, the first hematopoietic cells are found in the extraembryonic yolk sac. These are referred to as primitive hematopoietic progenitors because the blood cells they produce have more embryonic characteristics than those that arise later in development. This is especially true of early red blood cells, which express embryonic forms of hemoglobin with greater affinity for oxygen, as is appropriate for the hypoxic fetal environment. Around day 10.5 of mouse development, the first HSCs arise in the aorta-gonad-mesonephros region of the developing mouse embryo (*76, 77*). Hemogenic endothelium forms on the ventral wall of the

aorta, squeezing the first true HSCs into the growing circulatory system (*78-80*). These definitive HSCs, possibly along with some primitive progenitors from the yolk sac, colonize the fetal liver (*81*). The main hematopoietic function of the liver appears to be to provide a permissive environment for the HSCs to grow and expand, as their numbers increase greatly at this stage of development (*82*). Finally, HSCs colonize the bone marrow, where they will be responsible for maintaining the immune and blood systems for the rest of the animal's life (*83*).

Two *in vitro* culture systems are currently employed to coax mammalian pluripotent stem cells down the path of hematopoietic differentiation: two-dimensional culture on supportive OP9 stromal cells, and aggregation of differentiating cells into three-dimensional balls of cells called embryoid bodies (EBs) (*84, 85*). In both systems, exogenous cytokines are applied at defined intervals and concentrations to mimic the evolution of cellular identity that occurs during development. If these mouse cells are infected with viruses expressing homeodomain-containing transcriptional regulators like *CDX4* and/or *HOXB4*, the systems create cells that fulfill the definition of HSCs: long-term, multilineage engraftment (*86-88*). However, the activity of these exogenous factors does not appear to be as effective in human lines as it is in the mouse background (*87, 89*). Both EB creation and co-culture with stromal cells lead human pluripotent stem cells to differentiate into the hematopoietic lineage, as measured by robust expression of CD34, CD45, and other hematopoietic markers (*87, 90*). In spite of this, when these cells are transplanted into immunodeficient mice, they fail to generate high-level, multilineage, long-term engraftment (*87*). The reasons for the observed differences between mouse and human pluripotent-to-hematopoietic stem cell differentiation are active areas of inquiry. Achieving stable multilineage engraftment of human HSCs derived from pluripotent stem cells remains a

major goal in hematology research, and must be achieved before patient-specific iPS cells can be used for cellular therapy for bone marrow failure.

Summary of work described in this dissertation

This dissertation focuses on three genetic diseases: Pearson syndrome, ring 14 syndrome, and Fanconi anemia. We manipulated cellular identity to learn more about each of these diseases, by creating iPS cells from patients with Pearson syndrome and ring 14 syndrome, and by studying the reprogramming process in Fanconi anemia cells.

Chapter 2: Pearson syndrome. The presence of a mitochondrial deletion is the well-documented cause of Pearson syndrome, but its effect on pluripotent cellular metabolism and hematopoietic differentiation has never before been studied. Here, we describe creation of Pearson syndrome iPS cells and an isogenic line completely free of disease. We employed these tools to investigate the specific metabolic defects of PS-iPS cells and create *in vitro*-derived Pearson syndrome blood cells. In the erythroid population resulting from this differentiation, we found pathognomonic iron-positive staining specifically in cells carrying the mtDNA deletion.

Chapter 3: Ring 14 syndrome. The single most important question in the field of ring 14 syndrome research is how the presence of the ring chromosome during brain development leads to a seizure disorder. Investigation of this question has been stymied by the complete inaccessibility of relevant cells. Until the work described here, there was no opportunity to study the ring chromosome in any cell type other than fibroblasts or peripheral blood. We report the creation of iPS cells carrying a ring chromosome 14, and observe dynamic changes in the chromosome 14 karyotype over time. Following a non-disjunction event, we identified a

subclone that carried two linear, uniparental disomic copies of chromosome 14. R14-iPS were then differentiated down a neuronal lineage, marking the first neural cells from a ring 14 patient available for study. This project is ongoing, and we are currently comparing differentiation efficiency and neural phenotypes between isogenic iPS lines carrying the ring and carrying disomic chromosome 14.

Chapter 4: Fanconi anemia. Around the world, dozens of attempts have been made to reprogram cells from patients with Fanconi anemia, yet only one of them has succeeded. We set out to investigate this FA reprogramming defect in a secondary murine system, and were surprised to find that the FA cells reprogrammed nearly as well as cells from their WT littermates. These results provide new insight into why published attempts to reprogram FA cells have failed, although an elegant understanding of the problem is still evasive.

Together, these chapters describe three examples of manipulating cellular identity to learn about rare genetic diseases.

Chapter 2: Pearson Syndrome

Introduction

Mitochondrial DNA (mtDNA) mutations are implicated in numerous human disorders ranging from rare multisystem congenital diseases to common acquired degenerative disorders such as Parkinson's disease (*88, 91-95*). No curative therapies exist for mitochondrial disease, and consequently mtDNA mutations cause significant morbidity and mortality (*96*).

In congenital mtDNA disorders, a mixture of normal and mutant mtDNA, termed heteroplasmy, is inherited from the oocyte at fertilization and partitioned differentially in tissues during embryogenesis (*88, 97*). The degree and distribution of heteroplasmy in adult tissues determines the severity and marked phenotypic heterogeneity of the disease. Pearson marrow pancreas syndrome, also called Pearson syndrome (PS), is a congenital multisystem disorder caused by large deletions in the mitochondrial genome and is characterized by life-threatening bone marrow failure and metabolic derangements (*98, 99*). The cause of the hematopoietic failure in PS is unknown, and experimental models to reproduce tissue-specific defects in PS and other mtDNA disorders are needed.

Cybrids, the mitochondrial mutation research tool

Because mtDNA sequences are difficult to manipulate in cells, cybrid (cytoplasmic hybrid) cell lines have been the most common model for studying mitochondrial disorders (*100, 101*). Cybrids are created by fusion of cytoplasts harboring mutant mtDNA with a cell depleted of mitochondria, called ρ0 (rho-naught) cells. The resulting cybrid contains the nucleus of the

ρ0 cancer cell line and the mutant mitochondria of interest. Cybrids have provided insights into the role of mtDNA in cancer, the effects of specific mtDNA mutations, and inter-species mitochondrial complementarity (*95, 101*). However, the cybrid approach is heavily dependent upon the cell type chosen to receive the affected mitochondria. When different ρ0 cell lines are used as the nuclear donor, experimental results vary dramatically (*102, 103*). This is widely recognized as the most severe limitation of cellular research into mitochondrial disorders.

Pearson syndrome mutations have been studied only using cybrids created from ρ0 cancer cell lines (*104, 105*). Because cell type-specific mitochondrial function is crucially relevant to disease processes, an experimental system in which the effects of mtDNA mutations could be studied in specific human cell types would be of great value. We have created such a system for blood, and it is proof-of-principle for similar applications in other organs.

Reprogramming cells that carry deleted mtDNA

Somatic cells can be directly reprogrammed using defined genetic factors to yield iPS cells, which have the capacity to differentiate into any tissue (*11-13, 106*). Direct reprogramming allows the creation of patient-specific pluripotent cells that retain the cytoplasmic contents of donor cells, including disease-associated mtDNA. We sought to generate iPS cells carrying mutant mtDNA in order to investigate tissue-specific effects of mitochondrial dysfunction. We describe the derivation of iPS cells bearing a pathogenic mtDNA deletion from a patient with PS. We observed changes in heteroplasmy during culture of PS-iPS cells, which allowed us to isolate isogenic iPS cells with undetectable levels of mutant mtDNA. Comparison of PS-iPS cells with varying degrees of heteroplasmy *in vitro* revealed defects in growth and mitochondrial function, and directed differentiation into the hematopoietic lineage

revealed a tissue-specific phenotype characteristic of PS. Our results demonstrate that reprogramming of somatic cells from patients with Pearson syndrome can yield patient-identical pluripotent stem cells varying in mtDNA heteroplasmy, providing unique tools to study tissue-specific effects of mtDNA mutations.

Materials and Methods

Patient material

Biological samples were procured under protocols approved by the Institutional Review Board at Boston Children's Hospital. Standard histological evaluations were performed by the Department of Pathology, Boston Children's Hospital.

DNA isolation

Genomic DNA was isolated from peripheral blood or bone marrow using the QIAamp DNA Blood Maxi Kit or the DNeasy Blood and Tissue Kit (Qiagen). DNA was isolated from fibroblast and iPS cell lines by SDS/Proteinase K lysis followed by phenol/chloroform extraction and ethanol precipitation.

Cell lines and culture

Pearson syndrome patient bone marrow-derived fibroblasts (PS-Fib) were isolated by plating 150 uL of liquid bone marrow in DMEM/15% FCS. Media was changed every three days until outgrowths appeared (approximately two weeks), and thereafter cells were expanded by routine trypsinization and subculture. Cells were characterized for mutant mtDNA at passage

two. Pearson syndrome fibroblasts (GM04516) and lymphocytes (GM04515) and Kearns-Sayre syndrome fibroblasts (GM06225) and lymphocytes (GM06224) were obtained from the Coriell Institute for Medical Research.

Long range PCR

Long range PCR to detect mitochondrial DNA deletions was performed by amplifying 100-500 ng of template DNA using the Expand Long Template PCR system (Roche Diagnostics) according to manufacturer's instructions. The deletion locations were mapped using PCR, restriction digests, and Sanger sequencing. Nucleotide positions were assigned per the revised Cambridge Reference Sequence of human mitochondrial DNA. Sequence analysis was performed using data from www.mitomap.org.

Mitochondrial DNA FISH

Templates for probes were amplified by PCR. COMMON probe was labeled with digoxigenin using the DIG-Nick Translation Mix (Roche) and CHBMDF1 FISH probe was labeled using the Biotin-Nick Translation Mix (Roche). Fibroblasts were prepared on coverslips as previously described (*107, 108*). COMMON and CHBMDF1 probes were simultaneously hybridized on the coverslips in 50% formamide, 2X SSC by heating to 85° C for 2.5 minutes followed by incubation at room temperature overnight. Coverslips were washed in TBS 0.05% Tween (TBST) and incubated in TBST with 0.05% W/V Blocking Reagent (Roche) with FITC conjugated anti-Dig and Alexa Fluor 594 conjugated streptavidin at room temperature for one hour. Coverslips were washed in TBST, dehydrated and mounted in Prolong Gold (Invitrogen), and analyzed by epifluorescence microscopy.

Heteroplasmy determination by quantitative real-time PCR

Quantitative real-time PCR measurements were performed using 30 ng of template DNA and Brilliant SYBR Green QPCR Master Mix (Stratagene) with primers CHBMDF1F and CHBMDF1R for the mutant mtDNA species and WTmitoF and WTmitoR for all mtDNA molecules. Primer pairs were verified for linear amplification over a 100-fold range of input DNA.

Single-cell multiplex real-time PCR

Primer pairs and probe sets were optimized and validated for sensitivity and specificity. Fibroblasts were collected by trypsinization and single cells were FACS sorted into individual wells of a 96-well qPCR plate containing 10 uL of 10% SideStep Lysis buffer. Amplification was performed with appropriate negative and positive controls using primers/probes at the concentrations described above with Brilliant II QPCR Master Mix in a Stratagene MX3000P QPCR system, and results were graphed and scored as described in the figure legends.

Mitochondrial complex quantity and activity assays

Quantification of complex I, complex IV, frataxin and PDH was performed using the MetaPath MitoDisease 4-Plex Dipstick Array (MitoSciences, Abcam) according to manufacturer's instructions. Complex I, III and IV activity were respectively determined using the Complex I Enzyme Activity Dipstick Assay Kit, Cyt C Reductase Human Profiling ELISA Kit, and Complex IV Enzyme Activity Dipstick Assay Kit (MitoSciences, Abcam) (*46*). A standard curve was established for each assay using a range of normal fibroblast protein concentrations. 0.5 and 5 ug of protein extract were used for each sample in duplicate for

MetaPath quantity assays. 1 and 10 ug of protein extract were used for each sample in duplicate for complex I and IV activity assays. Quantification was performed by scanning the dipsticks followed by image analysis using Adobe Photoshop as described in the manufacturer's instructions. 34 ug protein extract was used in triplicate for the complex III activity assay, and quantification was performed using a microplate reader. Results are shown as normalized to quantity or activity of complexes in WT cells.

Direct reprogramming and iPS cell characterization

Derivation, culture, characterization and differentiation of iPS cells was as described (*109*) with modifications to protocol as noted in the text. iPS lines were cultured on irradiated MEF feeder cells or hESC-qualified Matrigel (BD Biosciences). PS-iPS cells were generally passaged every 6-7 days, with manual removal of differentiated cells under a dissecting microscope, release of colonies with Collagenase IV (Invitrogen) or Dispase (Stem Cell Technologies), and fragmentation and collection using a cell scraper. Teratomas were formed as described (*109*) by intramuscular injection of iPS cells in immunodeficient mice under approved animal use protocols. Histology was performed at the Dana-Farber Harvard Cancer Center Rodent Histopathology core facility.

Immunostaining of iPS cells

iPS lines were grown on glass coverslips and stained with: (1) OCT4 rabbit polyclonal antibody (1:300; Abcam) with Alexa-Fluor 488 chicken-anti-rabbit secondary antibody (1:1000; Life Technologies); (2) SSEA4 mouse monoclonal antibody pre-conjugated to Alexa Fluor 647 (1:100; BD Biosciences); (3) NANOG rabbit polyclonal antibody (1:200; Abcam) with Alexa-

Fluor 488 chicken-anti-rabbit secondary antibody; (4) TRA-1-60 mouse monoclonal antibody (1:100; Millipore) with Alexa-Fluor 594 goat-anti-mouse secondary antibody (1:1000; Life Technologies); (5) TRA-1-81 mouse monoclonal antibody (1:100; Millipore) with Alexa-Fluor 594 goat-anti-mouse secondary antibody.

Reverse-transcription PCR

RNA was made using Trizol, and cDNA was made with Superscript III (Invitrogen), according to manufacturer's protocols. PCR was performed using gene-specific primers using SYBR green SsoAdvanced polymerase (Bio-rad).

Southern blots

10 ug of genomic DNA was digested with NcoI, separated on a 0.6% agarose gel and transferred to a positively charged nylon membrane. For evaluation of heteroplasmy, hybridization was performed using a probe corresponding to nucleotide 14840-15261 (cytochrome b) of the mitochondrial genome, which detects a 7.5 kb band from the intact mitochondrial genome and a 5 kb band from the deleted mitochondrial genome in the PS patient. Hybridization was performed with Rapid-Hyb buffer (GE Healthcare) according to manufacturer's instructions. Each reprogramming retrovirus contains an IRES-GFP cassette and a single NcoI restriction site, which was used for proviral integration pattern analysis. The proviral integration patterns were determined by cutting with NcoI and probing Southern blots with a GFP probe.

Live-cell imaging

iPS cells were plated as single cells on Matrigel (BD Biosciences) in mTESR medium (Stem Cell Technologies) in a glass bottom dish (MatTek) on a microscope outfitted with a thermo/CO2-regulated chamber and a computer-controlled motorized stage. Images of iPS colonies were obtained at 6-hour intervals in a tiled array and stitched to form a single composite image. The surface area of the colony was measured using Elements AR (Nikon) software. Growth analysis ended at 6 days or when the colony grew into an adjacent colony or when the colony outgrew nine low-power fields.

Mitochondrial membrane potential

iPS cells were incubated in hES cell medium containing 7 nM tetramethylrhodamine, ethyl ester (TMRE) (Invitrogen) and 100 nM MitoTracker Green (MTG) (Invitrogen) for 90 minutes. Immediately prior to imaging, this medium was replaced with phenol red-free hES cell growth medium containing 100 nM TMRE. Live cells were imaged by epifluorescence microscopy.

Extracellular flux analysis

Extracellular flux analysis was performed using the Seahorse platform as previously described (*110*). PS-iPS cells cultured on Matrigel were trypsinized to single cells and plated onto Seahorse 24-well analysis plates at a density of 50,000 single cells per well in mTESR media containing 10 uM compound Y-27632 (Sigma). Each cell line was assayed in quadruplicate. One day later, the cells were analyzed for OXPHOS function (Injection 1: 20 uM oligomycin; Injection 2: 3 uM CCCP; Injection 3: 10 uM antimycin and 10 uM rotenone) and

glycolysis function (Injection 1: 250 mM glucose; Injection 2: 20 uM oligomycin; Injection 3: 1.5 M 2-DG). The listed injection concentrations are 10x the final concentration. Results were normalized for protein concentration in each well and analyzed by Seahorse XF24 software.

To quantify extracellular flux analyses, background signals were removed by subtracting final OCR or ECAR values from signals. Standard deviations were calculated by analytically combining averaged data points and their errors from each well into a composite distribution, and then summing the variances of the estimated signal and background distributions. Figure 2.8 C and E were normalized to PS-iPS1 to account for expected inter-experiment variability in raw data. Significant differences in basal respiration rates were identified by t-test of the normalized data (n = 12) averaged over three replicates. Percentage of oxygen used for ATP production and glycolysis activity and the appropriate standard deviations were calculated using Taylor series approximations of the mean and variance of the ratio of random variables.

Hematopoietic colony forming assay and sideroblast quantification

iPS cells were collected as large aggregates and resuspended in EB differentiation medium (80% DMEM, 20% FCS (Stem Cell Technologies 06900), 50 ug/ml ascorbic acid, 0.2 ug/ml holo-transferrin) on low attachment dishes. After one day, cytokines were added: hSCF (300 ng/ml), hFlt3L (300 ng/ml), IL-3 (10 ng/ml), IL-6 (10 ng/ml), G-CSF (50 ng/ml), BMP4 (50 ng/ml). Media containing cytokines was replaced every three days for 14-16 days, as described (*111*). EBs were dissociated and an equal number of cells was plated in MethoCult GF H4434 complete methylcellulose medium (Stem Cell Technologies). After 14-16 days of hematopoietic differentiation, CFU colonies were counted by an experienced observer who was blind to the identity of the samples. For sideroblast quantification, CFU-GEMM and BFU-E

picked from methylcellulose were washed in PBS, plated on glass slides by Cytospin, and stained using Prussian blue. Erythroid cells without and with iron deposits were scored by a hematopathologist who was blind to the sample identity.

Studies and Results

Induced pluripotent stem cells from a patient with Pearson syndrome

A three year-old patient presented at Boston Children's Hospital with transfusion-dependent anemia from birth, metabolic acidosis, pancreatic exocrine insufficiency, insulin dependent diabetes mellitus, hypothyroidism, and transfusion-related iron overload. Examination of the patient's bone marrow showed vacuolated hematopoietic precursors and ringed sideroblasts, which are erythroid progenitors containing inappropriate iron granules in their mitochondria (Figure 2.1 A). Together with her clinical presentation, these findings suggested the diagnosis of Pearson syndrome. We confirmed this diagnosis by identifying a 2501 base pair deletion in a subset of the patient's mtDNA from peripheral blood and bone marrow (Figure 2.1 B and C). The deletion from base pairs 10949-13449 interrupts the mitochondrial oxidative phosphorylation (OXPHOS) complex I NADH dehydrogenase genes *ND4* and *ND5*, and also deletes three tRNAs (L_{CUN}, S_{AGY}, and H) that are necessary for translation of all products of the mitochondrial genome (including required components of OXPHOS complexes I, III, IV, and V). We derived a primary fibroblast culture from the patient's bone marrow (PS-Fib, Figure 2.1 D), which carried mutant mtDNA in a proportion similar to that found in the patient's blood and bone marrow (60-80% of all mitochondrial genomes). By mtDNA FISH and single-cell multiplex PCR analyses, we determined that over

95% of cells in the fibroblast population harbored the mutated DNA species (Figure 2.2 A-C). As expected, we found quantitative and functional defects in OXPHOS complexes I, III, and IV in PS-Fib fibroblasts compared to wild-type (WT) fibroblasts (Figure 2.2 D, E). These results describe patient-specific somatic cells carrying the characteristic genetic and functional defects of a mtDNA deletion disorder.

The PS-Fib line was infected with retroviruses encoding *OCT4*, *SOX2*, *KLF4*, and *MYC*. No pluripotent colonies had emerged after the typical 3-4 weeks of culture under human ES cell conditions. However, continued culture for 8-12 weeks yielded 1-3 colonies, which displayed the morphological and functional characteristics of pluripotent stem cells (Figure 2.3). The same

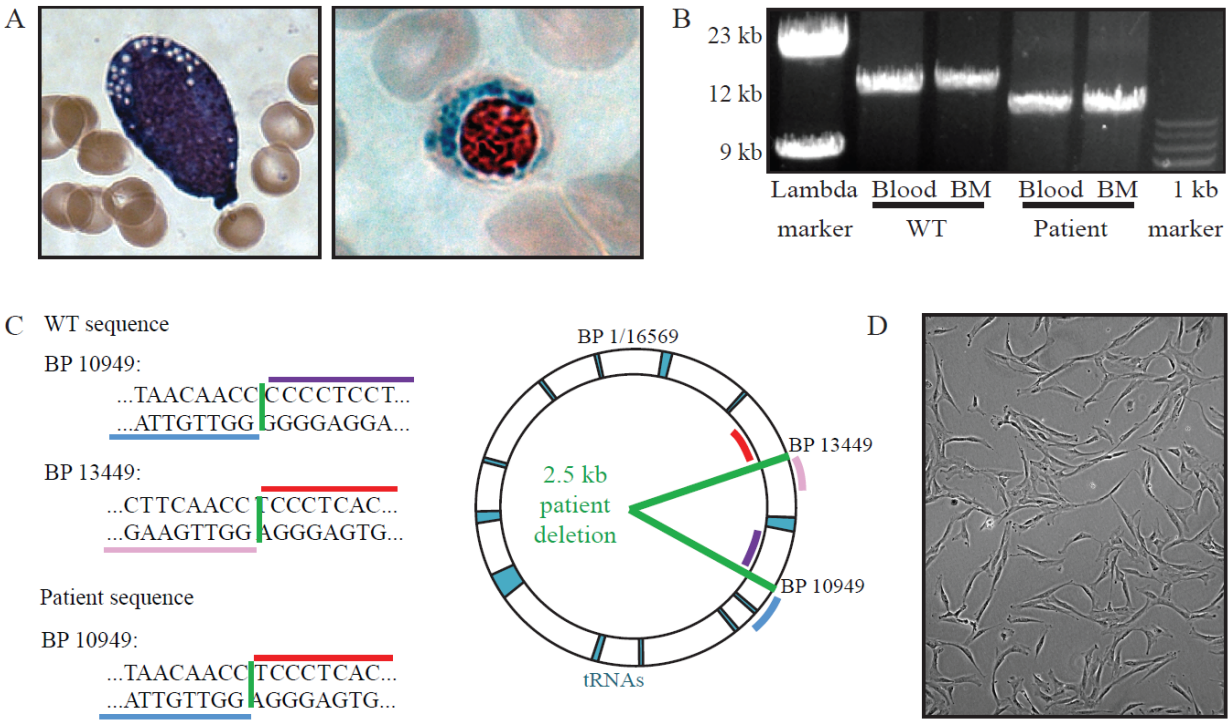

Figure 2.1: Diagnosis of a patient with Pearson syndrome. (A): A vacuolated hematopoietic precursor (left, hematoxylin and eosin stain) and ringed sideroblast (right, Prussian blue stain) from the patient's bone marrow aspirate. (B): Mitochondrial genome long range PCR revealing the patient's large mitochondrial deletion. (C): Sequence surrounding the breakpoint and its position in the genome. (D): PS-Fib, the patient bone marrow-derived fibroblast line that was reprogrammed to create the PS-iPS cells (40x).

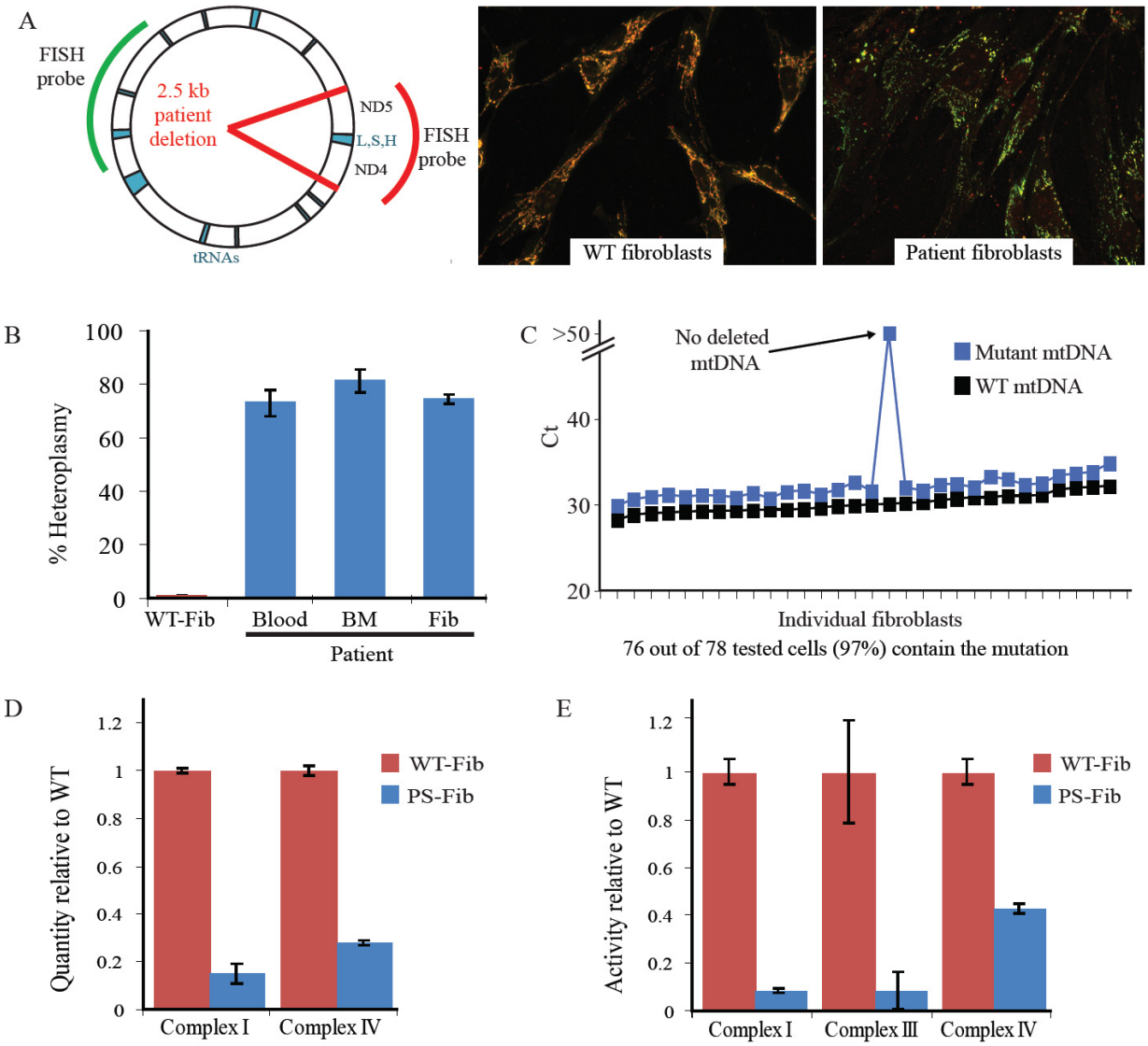

Figure 2.2: Characterization of PS fibroblasts. (A): Location of the patient's 2.5 kb mutation in the mitochondrial genome and fluorescence in situ hybridization comparing WT and patient fibroblasts. The red probe covers a stretch of the mtDNA lost in the patient while the green probe covers an unaffected region. (B): Heteroplasmy of patient peripheral blood, bone marrow, and bone marrow-derived fibroblasts as measured by qPCR. (C): Multiplex qPCR performed at the single cell level on the patient's bone marrow derived fibroblasts. (D): Quantification of electron transport chain protein complexes by sandwich ELISA. Quantity is normalized to frataxin. (E): Activity of electron transport chain complexes. Complex I activity is measured by a nitrotetrazolium blue-based assay, complex III and complex IV activity are measured by cytochrome c assays coupled to horseradish peroxidase and diamino benzidinetetrachloride staining. All error bars indicate standard deviation.

low efficiency and delayed kinetics of iPS cell derivation were observed in three independent reprogramming experiments from this patient's cells. We focused our analyses on three Pearson syndrome iPS clones (PS-iPS, clones 1-3), each derived from an independent reprogramming experiment.

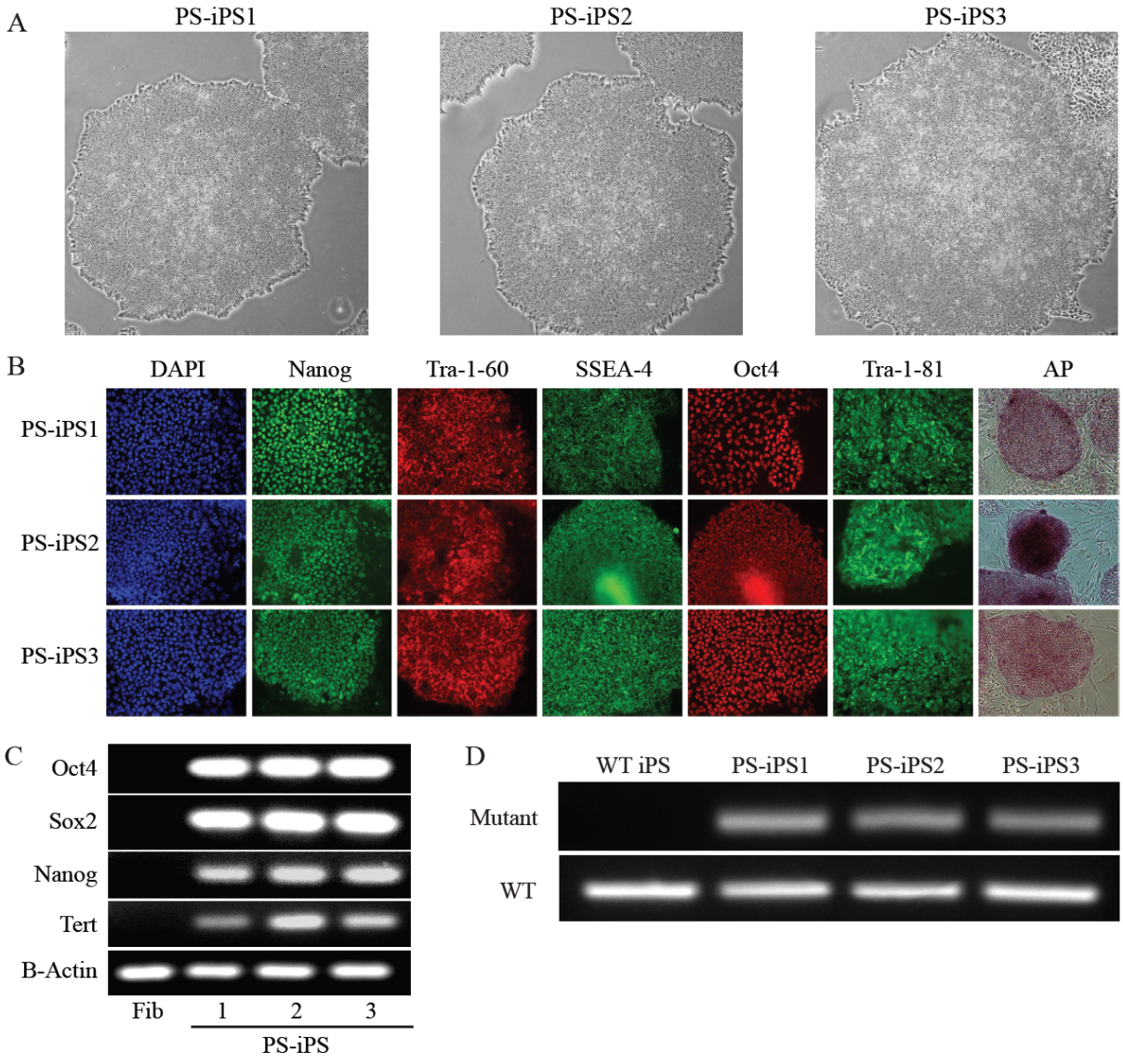

Figure 2.3: Generation of PS-iPS cells. (A): Brightfield images of Pearson syndrome iPS (PS-iPS) cell lines 1, 2, and 3 grown on Matrigel (40x). (B): Immunofluorescence staining for human pluripotency markers (100x). (C): RT-PCR of pluripotency associated genes demonstrates expression in PS-iPS lines but not in the patient's bone marrow derived fibroblasts. (D): Mitochondrial PCR of PS-iPS lines using primers specific for the patient's mutation (upper) or primers that amplify an unaffected region of the mitochondrial genome (lower).

PS-iPS clones demonstrated ES-like cell morphology and self-renewal under ES cell culture conditions (Figure 2.3 A). They expressed high levels of genes associated with pluripotency, as measured by immunofluorescence and RT-PCR (Figure 2.3 B and C). All iPS clones carried the pathological mtDNA deletion found in the parent fibroblasts as demonstrated by PCR using primers flanking the deletion junction (Figure 2.3 D). Each line was capable of *in vitro* differentiation into embryoid bodies and, when injected into immunodeficient mice, showed the capacity to yield teratomas that included tissues from all three embryonic germ layers and differentiate into embryoid bodies during *in vitro* culture (Figure 2.4). These data demonstrate the derivation of human iPS cell lines from a patient with Pearson syndrome.

mtDNA heteroplasmy in PS-iPS varies as a function of passage

In early passage PS-iPS cells, initial burdens of deleted mtDNA varied between 55-70%

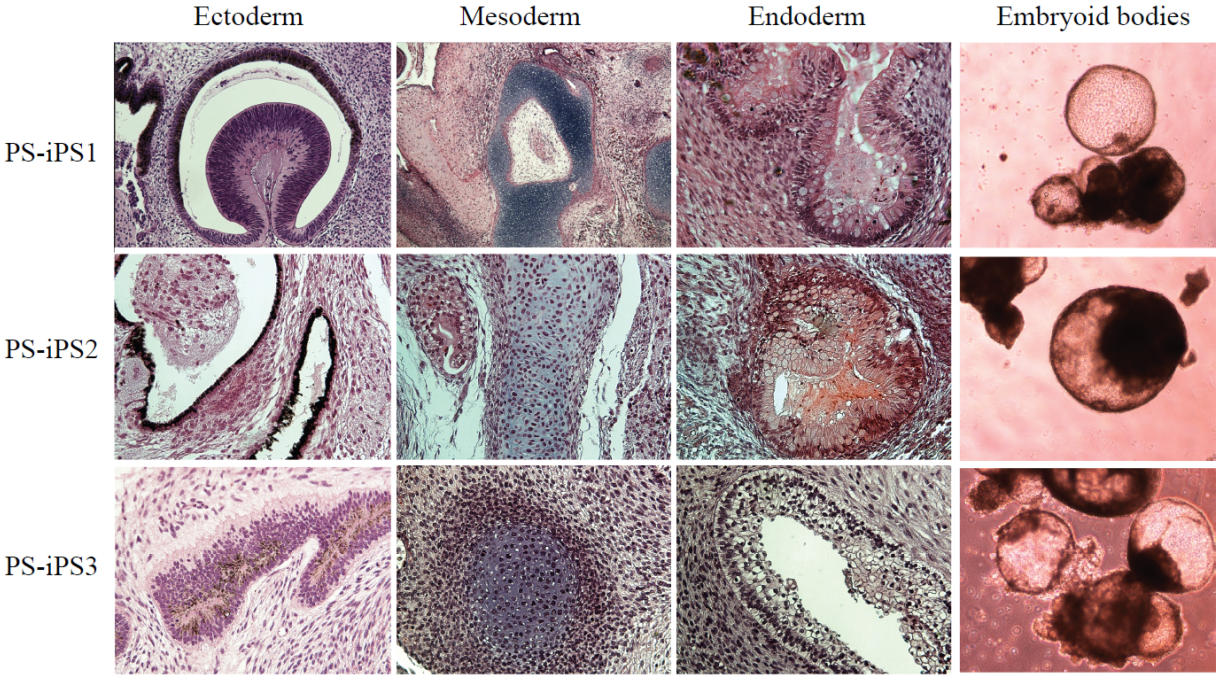

Figure 2.4: PS-iPS differentiation. All three PS-iPS lines formed teratomas *in vivo* containing all three germ layers. In addition, each line could be induced to differentiate into embryoid bodies *in vitro*.

when assessed by Southern blot and qPCR (Figure 2.5). As expected, the PS-iPS cells could be continually propagated well beyond the point of senescence compared to the original fibroblast population. When we analyzed the degree of heteroplasmy during culture, we found that the clones behaved differently from each other: heteroplasmy in PS-iPS3 remained unchanged at approximately 50%, but PS-iPS1 and PS-iPS2 purged mutant mtDNA over time. Upon continued culture of PS-iPS1, we obtained iPS cells with undetectable levels of the mutant mtDNA genome (Figure 2.5 B and C). Importantly, proviral integration analysis performed on each PS-iPS line showed a unique pattern that was maintained across passages, demonstrating that each line was clonally descended from a single fully reprogrammed PS-Fib cell (Figure 2.6). In the case of PS-iPS1, this analysis also demonstrates that the late passage, disease-free cells arose by loss of the mutant mtDNA species from the earlier highly-heteroplasmic clone. These data demonstrate clonal variation in changes in mtDNA heteroplasmy during culture, and derivation of mutation-free iPS cells from a patient with a mtDNA deletion disorder.

Functional characterization of PS-iPS cells

With isogenic, pluripotent cell lines that varied only in their degree of mtDNA heteroplasmy, we attempted to ascertain the effects of mitochondrial function on pluripotent cell growth and differentiation *in vitro*. When we used time-lapse imaging to compare colony growth between isogenic iPS lines with and without mutant mtDNA, we found that early passage PS-iPS1 cells containing 30% deleted mtDNA grew significantly more slowly than isogenic late passage PS-iPS1 cells which were purged of deleted genomes (Figure 2.7 A-C). These differences in growth were not attributable to different rates of spontaneous differentiation, as

Figure 2.5, on following page: Characterization of PS-iPS cell heteroplasmy. (A): Changes in heteroplasmy over passage number as measured by Southern blot (quantification of blots in this figure). (B): Changes in heteroplasmy over passage number as measured by qPCR. (C) Southern blots of PS-iPS1. Upper blots are probed for wild-type and mutant mtDNA. Lower blots show a retroviral integration pattern created by viruses encoding reprogramming factors. Black lines indicate individual blots. Left panel shows a single blot probed for wild-type and mutant mtDNA (upper) and virus integrations (lower). Right panel shows two independent blots probed for wild-type and mutant mtDNA (upper) and virus integrations (lower). (D): Southern blot of PS-iPS2 probed for wild-type and mutant mitochondrial DNA. (E): Southern blot of PS-iPS3 probed for wild-type and mutant mitochondrial DNA.

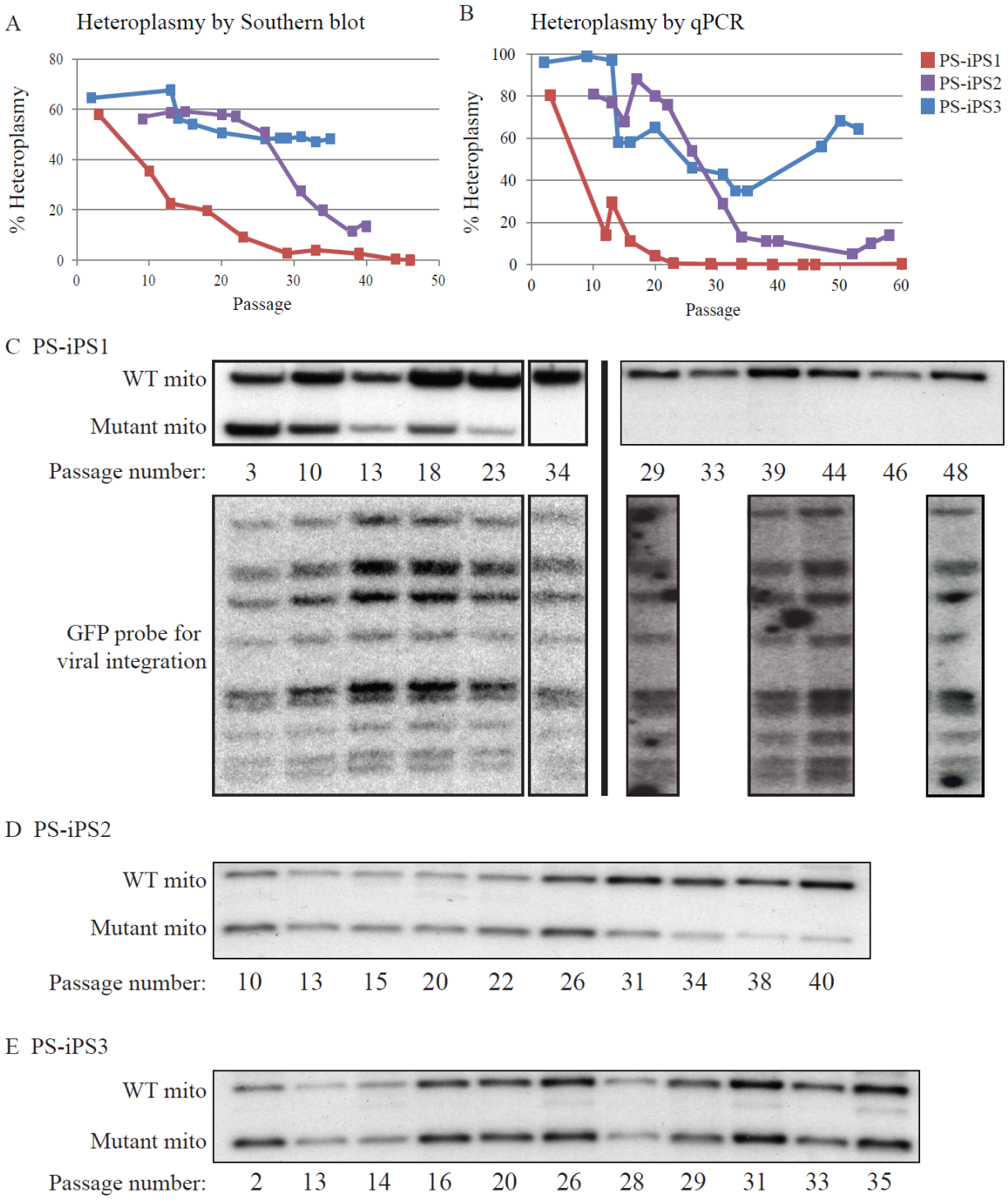

Figure 2.5: Characterization of PS-iPS cell heteroplasmy (Continued)

judged by our observation of cellular and colony morphology during the experiment. We also found that iPS cells that did not carry mutant mtDNA maintained a higher mitochondrial membrane potential than isogenic culture of iPS cells carrying 30% mutant mtDNA (Figure 2.7 D and E). These results show the restoration of mitochondrial function and growth after elimination of mutant mtDNA in cultured PS-iPS cells.

To investigate the physiological basis of the growth defect in the cells, we analyzed mitochondrial respiration and glycolytic function by measuring oxygen consumption and media acidification rates (Figure 2.8). iPS cells carrying about 60% mutant mtDNA (PS-iPS3) showed a 50% lower baseline oxidative respiration rate compared to iPS cells carrying low or no mutant mtDNA (Figure 2.8 A and C). This significant oxygen consumption defect could be caused by either impaired electron transport chain (ETC) function or by an uncoupling of ETC from ATP synthase activity. To distinguish between these possibilities, we added oligomycin to inhibit ATP synthase (Injection 1, OM). Upon oligomycin addition, all three lines reduced their oxygen consumption by similar degrees (64-76%, no significant difference, Figure 2.8 A and D), indicating that ATP synthesis efficiency is equivalent between lines. These results suggest that the decreased oxygen consumption found in iPS cells with a high burden of mutant mtDNA likely results from impaired ETC function.

We next measured glycolytic rates in PS-iPS cells with varying levels of mutant mtDNA. Glycolysis activity was assessed by measuring the extracellular acidification rate (ECAR) which varies depending on the cells' production of lactate, a metabolic byproduct of glycolysis. To measure glycolysis levels, cells were starved, then glucose was added to the media (Figure 2.8 B, Injection 1 Glu). PS-iPS3 showed a trend toward higher glycolytic activity compared to iPS cells with negligible or low burdens of mutant mtDNA (PS-iPS1 and PS-iPS2),

but the differences did not achieve statistical significance in aggregate analysis of replicates (Figure 2.8 E). Taken together, the extracellular flux analyses suggest that pluripotent stem cells carrying heavy burdens of deleted mtDNA are defective in oxygen consumption due to reduced ETC function, which may be partly compensated for by an increase in glycolytic activity.

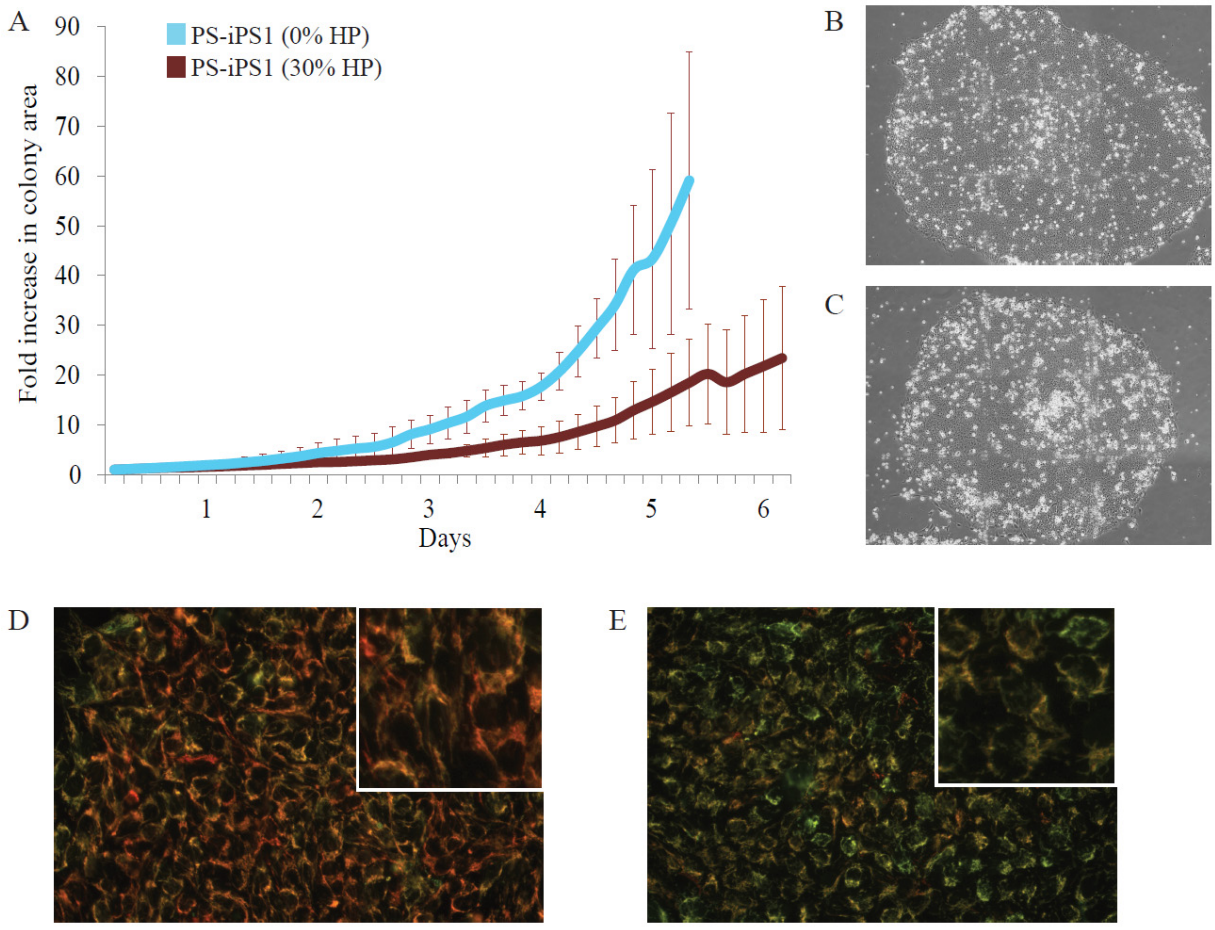

Figure 2.7: PS-iPS cell deficits. (A): PS-iPS1 growth in culture with and without mutant mtDNA, measured simultaneously by live cell imaging. Fold size increase is relative to size at day 0. (B): Example image of 0% heteroplasmy colony from live cell imaging. (C) Example image of 30% heteroplasmy colony from live cell imaging. D & E: Mitochondrial membrane staining with MitoTracker Green (stains all mitochondrial membranes) and TMRE (stains high membrane potential). (D) PS-iPS1 with 0% heteroplasmy (40x). (E) PS-iPS1 with 30% heteroplasmy (40x). Insets in both panels are 100x.

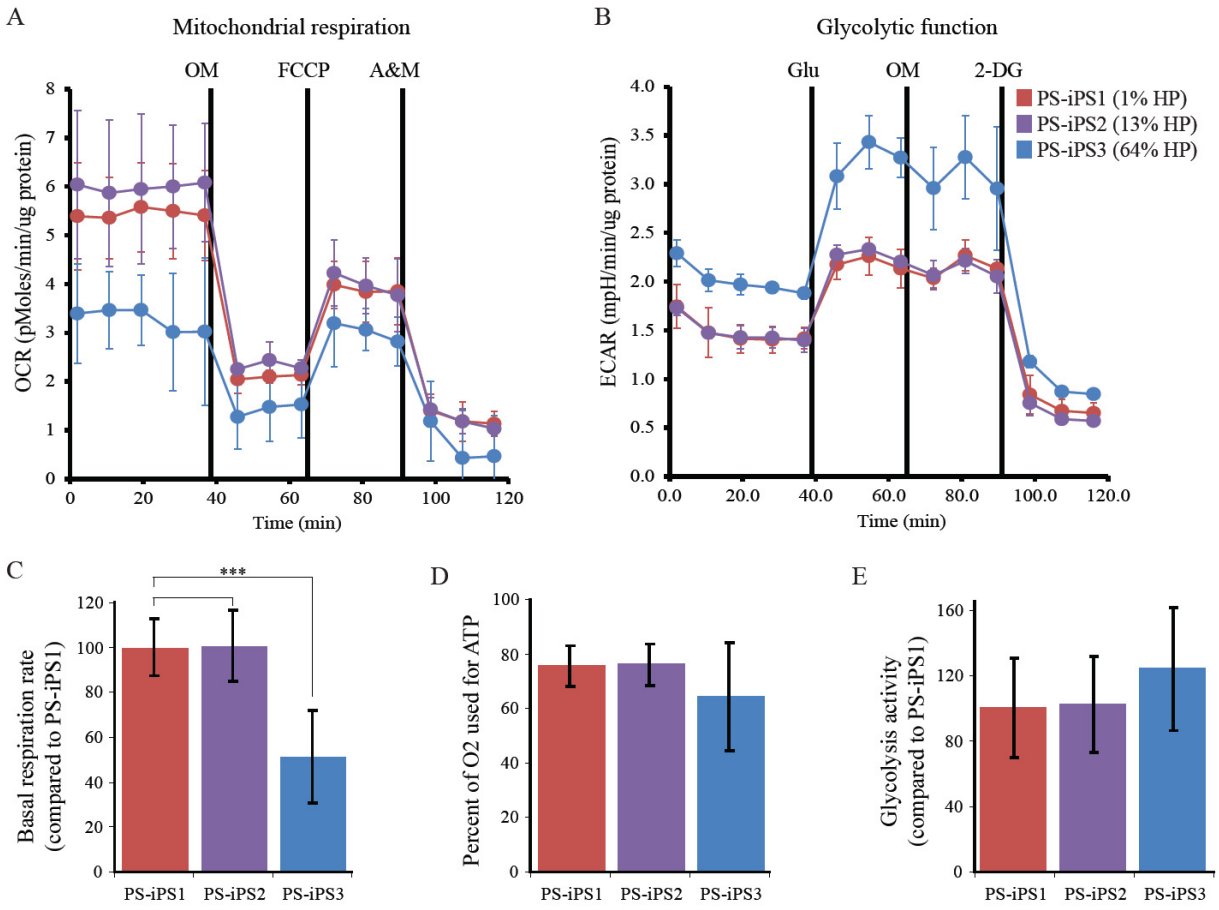

Figure 2.8: Metabolism of PS-iPS cells. (A): Representative data from extracellular flux analysis of oxygen consumption. Solid black lines indicate time of chemical injections: the ATP synthase poison oligomycin (OM), mitochondria uncoupler FCCP, and mitochondrial poisons antimycin and rotenone (A&M). (B): Representative data from extracellular flux analysis of glycolytic function. Cells begin in relative starvation before the first injection of glucose (Glu). The second injection is oligomycin (OM), followed by the glycolysis inhibitor 2-Deoxy-D-glucose (2-DG). (C): Quantification of basal oxygen consumption (respiration) compared to PS-iPS1, *** indicates $p < 0.0001$, n=3. (D): Quantification of the percentage of oxygen which is used to drive ATP synthase, n=3. (E): Quantification of glycolysis activity, compared to PS-iPS1, n=2. All error bars indicate standard deviation.

Hematopoietic differentiation of PS-iPS cells

Given the hematologic deficits in Pearson syndrome patients, we next assessed the capacity of PS-iPS cells to form hematopoietic progenitors *in vitro*. We generated EBs from PS-iPS cells in the presence of mesoderm- and hematopoiesis-inducing factors, followed by dissociation and suspension in methylcellulose containing hematopoietic factors. We found that all PS-iPS lines were capable of forming progenitor colonies with typical myeloid, erythroid and mixed myeloid-erythroid morphology, verified at the single cell level by Wright-Giemsa staining (Figure 2.9 A). We were unable to detect statistically significant differences among PS-iPS lines carrying varying degrees of mutant mtDNA, possibly due to high intrinsic variability in ES-derived hematopoietic colony forming assays, but we noted a trend towards reduced numbers of colonies in samples carrying deleted mtDNA (Figure 2.9 B, n = 4 differentiation experiments).

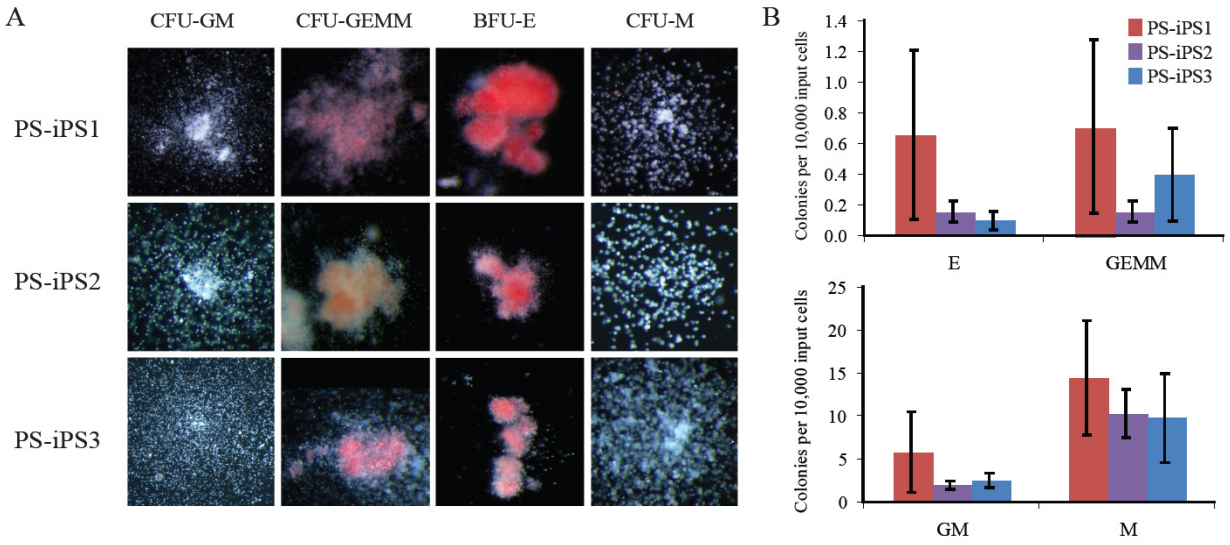

Figure 2.9: Hematopoietic differentiation of PS-iPS cells. (A): Images of hematopoietic colonies derived from each PS-iPS line (25-63x). (B) Quantification of hematopoietic colony forming efficiencies, n=4. (E = BFU-erythroid; GEMM = granulocyte, erythroid, macrophage, megakaryocyte; GM = granulocyte, macrophage; M = macrophage)

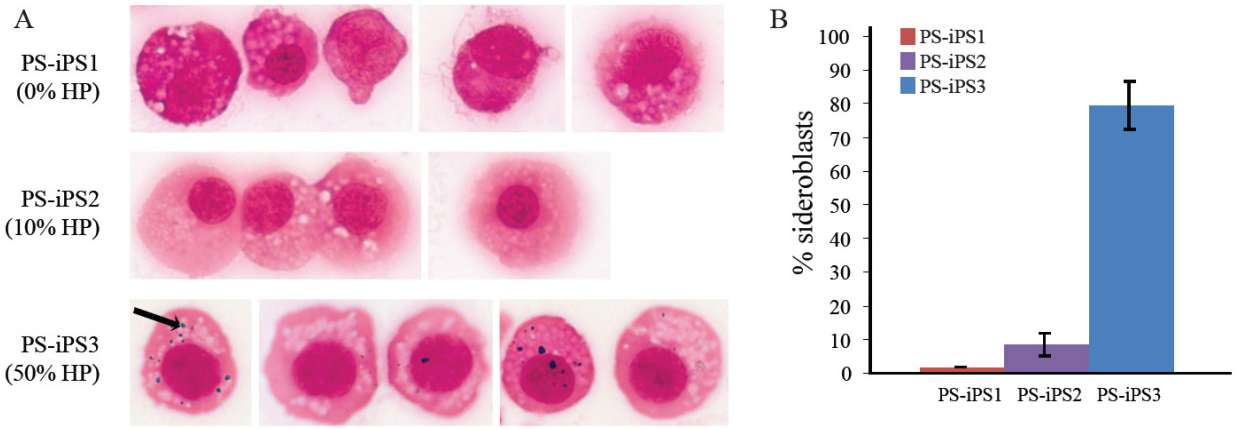

Figure 2.10: Sideroblastic erythroid progenitors. (A): Erythroid progenitors derived from PS-iPS cells, stained for iron with Prussian blue. The arrow indicates an example iron granule (1000x). (B): Blinded quantification of sideroblasts, scored as percent of erythroid progenitors containing visible iron granules on Prussian blue stain.

To investigate whether sideroblasts were present, we performed iron staining on the hematopoietic cells isolated from the methylcellulose cultures. PS-iPS3 cells, which carry a significant burden of mutant mtDNA, yielded high numbers of erythroid precursors with pathologic iron granule deposition compared to PS-iPS cells with less mutant mtDNA (Figure 2.10). Collectively, these results demonstrate the recapitulation of a tissue-specific phenotype by directed differentiation of iPS cells carrying mutant mtDNA, and the amelioration of the phenotype in mutation-free, patient-identical iPS cells derived *in vitro*.

Reprogramming cells from other patients with mtDNA deletion syndromes

We obtained fibroblasts from two other patients suspected to have mitochondrial disease from the Coriell repository: one with symptoms consistent with Pearson syndrome (GM04516), and one with the later-onset variant Kearns-Sayre syndrome (GM06225). We confirmed these clinical diagnoses by detection and mapping of mtDNA deletions in both lines (Figure 2.11 A). The burden of mutant mtDNA at a population level in the skin-derived fibroblasts was low: 6%

Figure 2.11, on following page: iPS lines from two other patients with mtDNA deletions. (A): Detection of mutant mtDNA in cells from a Pearson syndrome patient (PS; GM04516) and a Kearns-Sayre syndrome patient (KSS; GM06225) by long range PCR. The location of each mutation is illustrated in the schematic. (B): Demonstration of pluripotency in iPS cell lines derived from PS (GM04516) and KSS (GM06225) by immunofluorescence and teratoma analysis (40-100x). (C): PCR evaluation of iPS clones for the presence of the mutant species of DNA. "Deleted" primers covered the deletion junction for each patient. Patient fibroblasts (F) and lymphocytes (L) are included in multiples lanes as positive controls, all other lanes are individual iPS clones. Asterisk (*) denotes true positive, filled circle (•) denotes false positive, determined on subsequent testing. 61 independent iPS cell clones were analyzed for PS (GM04516) and 21 independent iPS cell clones for KSS (GM06225).

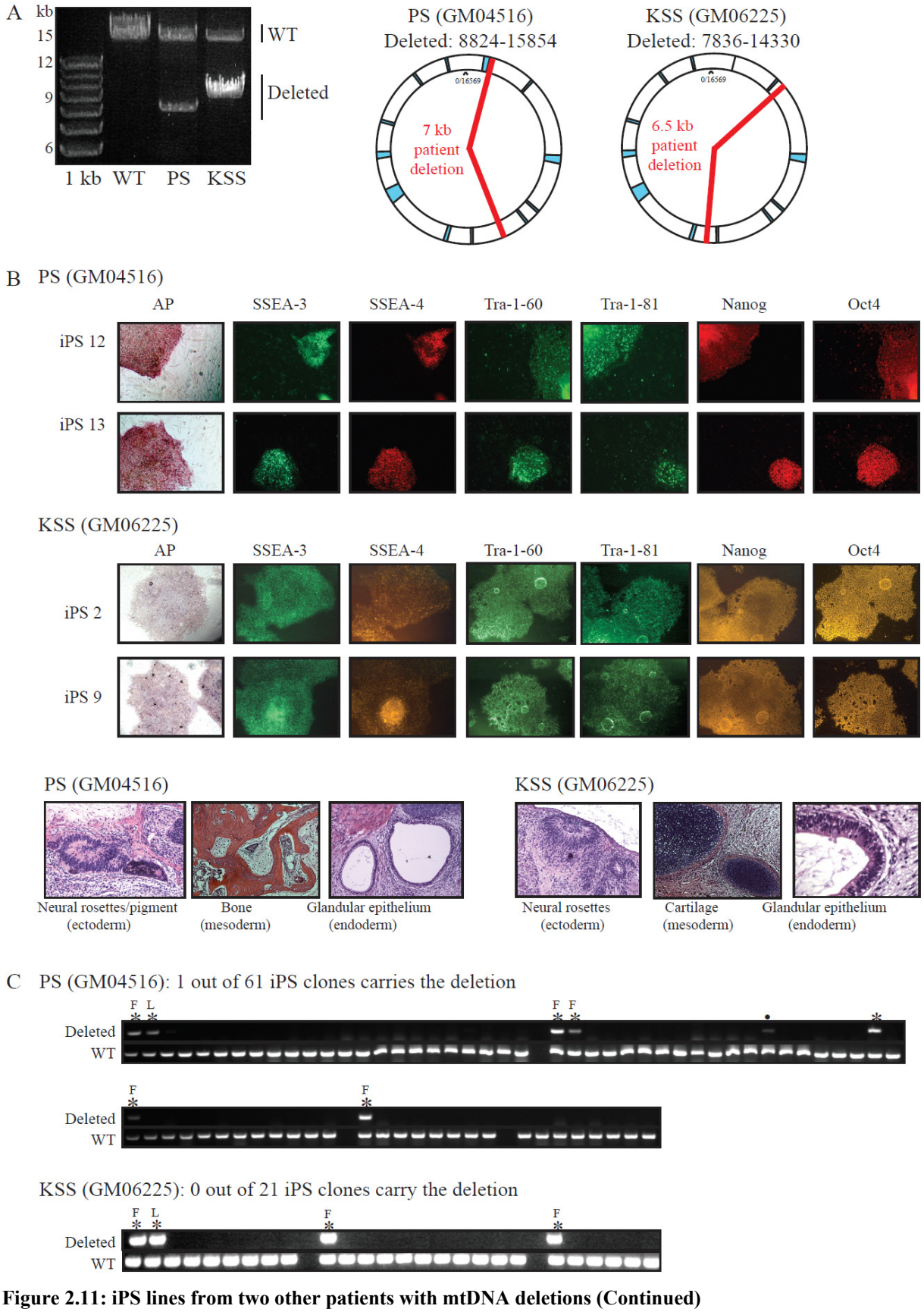

Figure 2.11: iPS lines from two other patients with mtDNA deletions (Continued)

for GM04516 and 3% for GM06225. We reprogrammed these samples as described above and obtained with relatively high efficiency and normal kinetics several iPS cell lines bearing the hallmarks of pluripotency (Figure 2.11 B). However, of the resulting lines, nearly none carried the mtDNA mutation: only 1 of 61 lines derived from GM04516, and 0 of 21 lines analyzed from GM06225 (Figure 2.11 C). The reprogramming efficiencies and proportion of lines carrying the mtDNA deletion of samples from all three patients are documented in Table 2.1. Collectively, these data demonstrate the efficient derivation of disease-free patient-specific iPS lines from patients with a low burden of a mosaic genetic abnormality.

Table 2.1: Reprogramming kinetics and efficiency for three cell lines with mtDNA mutations.
Cumulative results of at least three independent reprogramming experiments per cell line. Pearson syndrome, PS; Kearns-Sayre syndrome, KSS.

Fibroblast cell line (Disease)	Deletion size	Genes/*tRNAs* Affected	% mutant mtDNA in fibroblasts	Time to iPS colonies (weeks)	Reprogramming efficiency (%)	iPS clones with deletion	% mutant mtDNA in + iPS cells
PS-Fib1 (PS)	2.5 kb	ND4/5 $L_{CUN}/S_{AGY}/H$	60-80	8-12	0.002	5/5	55-70
GM04516 (PS)	7.0 kb	ATPase 6, COIII, ND3/4/4L/5/6, cytb $G/R/L_{CUN}/S_{AGY}/H/E$	6	3-4	0.1	1/61	20
GM06225 (KSS)	6.5 kb	COII/III, ATPase 6/8, ND3/4/4L/5/6 $K/G/R/L_{CUN}/S_{AGY}/H$	3	3-4	0.05	0/21	N/A

Discussion and Future Directions

Mitochondrial diseases are a unique category of genetic disorders. Each cell contains tens or hundreds of copies of the mitochondrial genome, which are inherited randomly during cell division. From a zygote that carries a mix of healthy and mutated mtDNA, random partitioning means that some tissues will be heavily affected by the mutation while others may show little or no defect. Mitochondrial function varies widely in different cell types of the body and therefore mitochondrial disorders in patients manifest with myriad syndromes and conditions. In the case of mtDNA defects, symptoms also depend on the deletion size and location, the severity of the heteroplasmy, and the mosaic of cell types affected. Such heterogeneity makes mitochondrial disorders a challenge to diagnose, treat, and study.

Most cellular research on Pearson syndrome, a rare multisystem mitochondrial DNA deletion disorder, has been performed in the cybrid system, where cytoplasts containing mutant mtDNA are fused to ρ0 nuclei from cancer cell lines. But as can be predicted from using nuclei with vastly different cellular identities, cybrid systems are notorious for producing results that mimic the behavior of the ρ0 cell instead of the cell type affected by the disease (*102, 103*). The advent of direct reprogramming technology has created new possibilities for the study of mitochondrial disorders by making it possible to study the mtDNA mutation in the relevant cell type.

We have generated pluripotent stem cell lines by direct reprogramming of somatic cells from a patient with Pearson syndrome. iPS cells carrying mutant mtDNA were derived with low efficiency and delayed kinetics, and showed impaired mitochondrial function and growth. These PS-iPS lines were found to carry the mtDNA mutation. During culture, heteroplasmy varied

between PS-iPS cell lines, allowing us to isolate pluripotent cells with the same nuclear genome but without mutant mtDNA.

PS-iPS cells with and without the mtDNA deletion were differentiated towards the hematopoietic lineage *in vitro* and were capable of generating erythroid and myeloid colonies. Moreover, differentiation of cells from the PS-iPS line with the highest mutant mtDNA burden yielded erythroid cells with inappropriate iron deposits which are characteristic of Pearson syndrome. The pathological finding of iron inclusions in erythroid progenitors is pathognomonic of the disease, suggesting that it arose from a disease-specific mechanism. Thus, we were able to observe a mitochondrial disease phenotype in a cell lineage affected in the human disease.

The study of mitochondrial disorders in iPS cells may also provide insight into mitochondrial function and mtDNA dynamics in stem cells in general. Human pluripotent stem cells are reported to rely primarily on glycolysis for ATP production and to harbor immature, cristae-poor mitochondria (*112-115*). Consistent with a relative lack of reliance on OXPHOS, we found that PS-iPS cells carrying high levels of deleted mtDNA could be generated and propagated. However, the kinetics of iPS derivation from fibroblasts with high mutant mtDNA burdens were delayed, and growth of iPS colonies with high levels of mutant mtDNA was decreased. Fibroblasts samples from two other patients generated iPS clones with normal kinetics and efficiency, and the resulting lines were free of deleted mtDNA. This is likely due to low heteroplasmy in the initial fibroblast population but possibly also because of selection against clones carrying the mtDNA deletion. Furthermore, in two of our PS-iPS lines, we observed a decline in heteroplasmy over time, suggesting that mutant mtDNA is selected against during rapid proliferation over many population doublings in the pluripotent state.

Given the inclusion of glucose in fibroblast and iPS culture medium, and the reportedly largely glycolytic state of human pluripotent cells (*113, 115-117*), these findings are somewhat unexpected and suggest that intact OXPHOS machinery may be required for optimal reprogramming of somatic cells and growth of pluripotent cells. In keeping with these observations, a recent report shows that the OXPHOS machinery is active in pluripotent cells but uncoupled from ATP production, leading to speculation that mitochondrial activity is required for as yet undefined homeostatic functions in human pluripotent stem cells (*118*). Moreover, our analysis of metabolism in PS-iPS cells showed a decrease in mitochondrial respiration in PS-iPS cells carrying high levels of mutant mtDNA compared to those without mutant mtDNA, revealing a basal level of oxidative activity that may serve a role in pluripotent cell homeostasis. The availability of isogenic iPS cells and derivatives carrying varying levels of deleted mtDNA, as described here, will provide a valuable platform to study the role of mitochondrial function in reprogramming of somatic cells, and growth and differentiation of human pluripotent cells.

This work opens up many questions for future investigation. Notably, in one of our PS-iPS cell lines, mtDNA heteroplasmy was maintained at high levels over more than fifty passages (approximately 1 year) in culture. Our observations are consistent with independent findings of variable heteroplasmy in iPS cells derived from patients with MELAS, a disorder caused by mtDNA point mutations (*119*). We speculate that infrequent epigenetic or genetic changes, possibly including viral integrations, may enable rare iPS clones to tolerate heteroplasmy-induced mitochondrial dysfunction. Identification of these events could provide insights into the mechanism of disease and possibly inspire new treatments. This question could be approached by investigating whether the integration sites of the reprogramming viruses in this line provide

insight into its tolerance of heteroplasmy, and to compare epigenetic profiles between lines that tolerate and do not tolerate heteroplasmy.

In order for mtDNA disease iPS lines to eventually be used in a clinical setting, scientists will need to be able to control the fluctuation of heteroplasmy in culture. We attempted multiple approaches to manipulate heteroplasmy (hypoxic culture, uric acid, rapamycin; data not shown) but were unable to identify culture conditions that affect heteroplasmy. One possible approach would be to replace glucose in the media with galactose, which has been previously shown to select against cells with oxidative defects (*120*).

Finally, it is interesting to consider that the observation of decreased heteroplasmy in rapidly-dividing pluripotent stem cells *in vitro* may be reflective of changes in mutant mtDNA in stem cells *in vivo.* Pearson syndrome patients generally show spontaneous improvement in hematologic disease and immune function over the course of years, but worsening of neuropathy and myopathy (*121, 122*). In patients with other mtDNA disorders, mutant mtDNA is found as the predominant species in post-mitotic skeletal muscle fibers, but depleted in mitotic cells such as blood cells and skeletal muscle satellite stem cells (*123, 124*). Although the mechanisms driving these differences are largely unknown, selection against mutant mtDNA in dividing stem cells has been proposed as an explanation (*121*). If similar forces are at work in the PS-iPS lines, further *in vitro* studies may yield insights into methods to promote the extinction of mutant mtDNA species in specific tissues in patients. The PS-iPS cells we generated here could be the basis of a drug screen for previously-unknown compounds that promote extinction of heteroplasmy. This type of screen could have wide-ranging clinical applications, as all cells in a patient's body would benefit from decreased heteroplasmy levels.

Conclusion

This chapter describes the creation of iPS cells that carry varying burdens of mutated mtDNA from a patient with Pearson syndrome. These isogenic lines provide a new tool for *in vitro* studies of mitochondrial dysfunction. iPS cells offer a valuable complement to cybrid techniques because disease-carrying and disease-free iPS lines can be directly differentiated into specific tissue types to illuminate the pathophysiology of mtDNA disorders, and possibly to screen drugs that will support impaired cell-type specific functions. Mutation-free iPS cells are also a potential source of healthy, autologous tissue-specific progenitors for patients with mitochondrial diseases, although significant hurdles remain in the translation of iPS based cellular therapy. By exploiting their capacity for self-renewal and pluripotency, PS-iPS cells will be a valuable tool to understand tissue-specific pathophysiology and innovate treatments for patients with Pearson syndrome and other mitochondrial genetic disorders.

Chapter 3: Ring 14 Syndrome

Introduction

Ring 14 syndrome is a rare genetic condition, with fewer than one hundred cases diagnosed globally since its discovery in 1971 (*125*). It occurs when the fourteenth chromosome is circularized, usually through loss of genetic material on both ends of the chromosome and subsequent end fusion via non-homologous end joining. The ring 14 clinical syndrome typically presents with intellectual disability and severe drug-refractory epilepsy that begins within the first year of life, and it often associated with a distinctive facial appearance, retinitis pigmentosa, and microcephaly (*126, 127*). Interestingly, epilepsy is also associated with ring chromosomes 17, 18, 19, 20, and 21 (*128-136*).

Mosaicism in ring 14 syndrome

Many patients are mosaic for the ring chromosome: not all cells in their body contain the same genotype. Ring 14 mosaicism occurs in two main types, which are reflective of the origin of the ring chromosome. As a zygote, the majority of patients likely had one linear and one ring chromosome 14. Upon development, the ring chromosome was present in every cell unless it was lost, so these patients are mosaic for ring 14 and monosomy 14. In the smaller group of patients, the ring likely arose early in development but after the single-cell stage. In this case, the patient is mosaic for ring 14 and disomy 14 and may thus have regions or even whole organs that do not carry the ring chromosome. Interestingly, the only known ring 14 patient who does

not have severe intellectual disability falls into this latter category, suggesting the disomic mosaicism may have lessened the severity of the syndrome (*42*).

Types of ring 14 chromosomes

Ring 14 chromosomes are divided into three categories. In some cases, only telomeric and nucleolar organizing sequences have been lost; these are said to be "complete" rings. In others, more substantial coding regions are missing from the ring, resulting in "deleted" rings (*137*). In still others, the rings exhibit a mixture of deleted and duplicated regions, termed "complex" ring chromosomes. To investigate how the ring chromosome causes symptoms of ring 14 clinical syndrome, multiple groups have compared phenotypes between ring 14 patients with complete rings and deleted rings. Developmental delay and drug-resistant focal epilepsy, the most severe symptoms of ring 14 syndrome, appear in all cases of ring 14 syndrome regardless of the category of ring chromosome. On the other hand, the distinctive ring 14 facial appearance is associated only with deleted rings, specifically those with a deletion greater that 0.65 Mb (*42*).

Disease mechanisms in ring 14 syndrome

The etiology of epilepsy in ring 14 syndrome is not yet understood. The two most commonly proposed explanations are heterochromatin spreading on the ring chromosome causing functional neuronal haploinsufficiency of key chromosome 14 genes, and mitotic instability of ring chromosomes leading to epilepsy through an unknown mechanism (*137*). Unfortunately, due to the inaccessibility of affected neurons, researchers have been unable to investigate directly which explanation is responsible for the clinical findings.

In an attempt to distinguish between these two possibilities, researchers have compared the frequency of seizures between ring 14 patients and individuals who carry non-ring deletions on 14q. Four groups have conducted such studies, and their combined findings show that 42% of patients with proximal 14q deletions, and 13% of patients with distal 14q deletions, suffer from seizures (*126, 138-141*). The modest frequency of seizure in patients with linear 14q deletions could indicate that genes on 14q may be able to induce seizure upon haploinsufficiency, lending credence to the hypothesis that ring 14 syndrome epilepsy is caused by chromatin spreading, especially in proximal regions. However, none of the studies found rates of seizure with deletion anywhere close to seizure frequency in ring 14 patients (average of 98%). This, along with the preponderance of epilepsy in rings of other chromosomes, indicates that the presence of a ring chromosome itself may cause seizures.

Ring 14 syndrome is so rare that comparison studies such as these are severely limited by the number of patients who partake, and so are unfortunately restricted in the conclusiveness of their results. A more direct tool to analyze the function and behavior of ring 14 chromosomes in human neural cells would be more useful for understanding the mechanisms by which ring 14 causes seizure. Our goal in the study described here was to create such a tool.

Generation of ring 14 iPS cells

We reprogrammed cells from two ring 14 patients. One starting sample was mosaic for ring 14 and disomy 14, and all of the resulting iPS lines from this patient demonstrated disomy 14 with no ring chromosomes. The other patient fibroblast sample was mosaic for ring 14 and monosomy 14. All iPS lines derived from this patient carried the ring chromosome (R14-iPS).

We observed that over time in culture, the R14-iPS cells tended to lose the ring chromosome, while monosomic cells became more common. R14-iPS cells with a high percentage of ring chromosomes were differentiated down a neuronal pathway, representing the first neural cells available for study from a ring 14 patient. We were also fortunate enough to capture a nondisjunction event in one of the R14-iPS lines, resulting in a disomy 14 iPS line isogenic to the R14-iPS cells. As this study continues, the isogenic disomic line will be used as a control to investigate the effect of the ring chromosome on neuronal differentiation.

Materials and Methods

Patient material

The Galliera Genetic Bank (Galliera Hospital), member of the Network Telethon of Genetic Biobanks (Project No. GTB12001), funded by Telethon Italy and International Association Ring14 provided us with specimens.

Cell lines and culture

Ring 14 patient fibroblasts were grown in DMEM/10% FCS. Media was changed every two days and cells were expanded by routine trypsinization and subculture. iPS cells were grown either on irradiated murine embryonic fibroblasts (MEFs) with human ES media (DMEM:F12, beta-mercaptoethanol, glutamine, bFGF, and non-essential amino acids) or grown on matrigel and fed with mTeSR. All medias contained 100 IU penicillin and 100 ug/mL streptomycin except where otherwise noted. iPS cells were fed daily except for the day after

passage when they were left to sit undisturbed. iPS lines were passaged by collagenase while on MEFs or dispase while on matrigel, and picked by hand when necessary.

Reprogramming of ring 14 patient samples

Cells were reprogrammed using the three Yamanaka episomes, each with two genes on the pCXLE vector: *OCT3/4* and sh-*p53*; *SOX2* and *KLF4*; *LIN28* and *L-MYC*. These were prepared using endotoxin-free megapreps (Qiagen). Fibroblasts were trypsinized and counted. 500,000 cells of each line were spun down. The Amaxa nucleofection kit was utilized as described by the manufacturer, using program p-022 for the nucleofection. After nucleofection, the cells were placed in one well of a 6-well plate, in antibiotic-free DMEM/10% FCS media. Media was changed the following day to include antibiotics. On day 6 after nucleofection, the wells were split onto MEFs at two ratios: 1:36 and 5:36. The day following the split, the media was changed to hES media and fed daily hES until picking. From days 20 - 25, iPS colonies were identified and picked by hand into 6-well plates with MEF feeders. Picking was done in hES media containing 10 uM compound Y-27632 (Sigma) to prevent apoptosis. Picked colonies were passaged by hand with individual colony cutting. Ten iPS lines were established from Patient 1 (R14-iPS lines 1 - 10, seven of which were eventually karyotyped), and eight from Patient 2 (R14-iPS lines A - H, five of which were eventually karyotyped).

G-banded karyotyping

Cells were plated on MEFs in T25 dishes 2-4 days before submission for karyotyping. All G-banded karyotyping was performed by Cell Line Genetics. Unless otherwise stated, 20 cells were counted in karyotype.

Fluorescent in situ *hybridization (FISH)*

Cells were plated in T25 dishes 2-4 days before submission for FISH. FISH was performed by Cell Line Genetics, using probes for the telomeres and a probe for part of chromosome 14 present in both the linear and ring chromosome. The pattern of telomere and non-telomere probe allowed for distinction between disomic, monosomic, and ring 14 cells. Unless otherwise stated, 20 cells were counted in each FISH assay.

Microsatellite analysis

DNA was collected from iPS cell lines grown on matrigel. Samples were submitted to the Centre for Applied Genomics at the Hospital for Sick Children in Toronto, Canada for analysis.

Immunostaining of iPS cells

Performed as described in Chapter 2.

Subcloning of R14-iPS cells

In order to create clonal R14-iPS lines, with specific karyotypes, R14-iPS line E was incubated in hES media containing 10 uM compound Y-27632 (Sigma) for 30 minutes, then washed with DMEM:F12 and treated with accutase at 37 degrees for 15 minutes, with occasional pipetting. Cells were strained through a 40 um filter, then spun down. After being resuspended in hES with Y-27632, the cells were strained again, resulting in a suspension of single cells as verified on a microscope. These cells were plated at low density (15 - 100 cells per cm^2) on MEFs and returned to the incubator. 48 hours later they were fed regular hES media, then media

was changed every day following. Very small colonies began to appear 7 days after splitting, and most were large enough to pick by day 12 - 14. Colony picking proceeded by hand as described above.

Neural induction and maturation of R14-iPS cells

Neural differentiation was performed by dual SMAD inhibition as described previously (*142, 143*). In short, R14-iPS cells were plated as single cells in mTeSR1 media. They were treated with Noggin (R&D/Peprotech) or ALK2/ALK3 inhibitor LDN-193189 and SB431542 (Tocris Bioscience) in knockout serum replacement based media and they were transitioned into N2 media (Neurobasal with 0.5x B27, 1x N2 and 2 mM Glutamax) over ten days. Following dual SMAD inhibitor treatment, cells were passaged and expanded in N2 media with bFGF (Life Technologies). Neural rosettes were imaged on day 29 of differentiation. Neural progenitors were imaged on day 34 of differentiation after the cell mixture was depleted of neural crest cells by CD271 microbeads (Miltenyi) and enriched for PSA-NCAM+ cells.

Studies and Results

Comparison of ring 14 mosaicism between two patients

In order to distinguish between the effect of the ring and the effects of deleted coding sequences, we chose to create iPS cells only from patients that carried non-deleted rings. We obtained dermal fibroblasts from two patients with ring 14 syndrome. In both patients, the chromosomal breakage and rejoining occurred between 14p12 and 14q32.3 (Figure 3.1 A). As measured by karyotype, the sample from Patient 1 contained 4% ring 14 and 96% disomy 14,

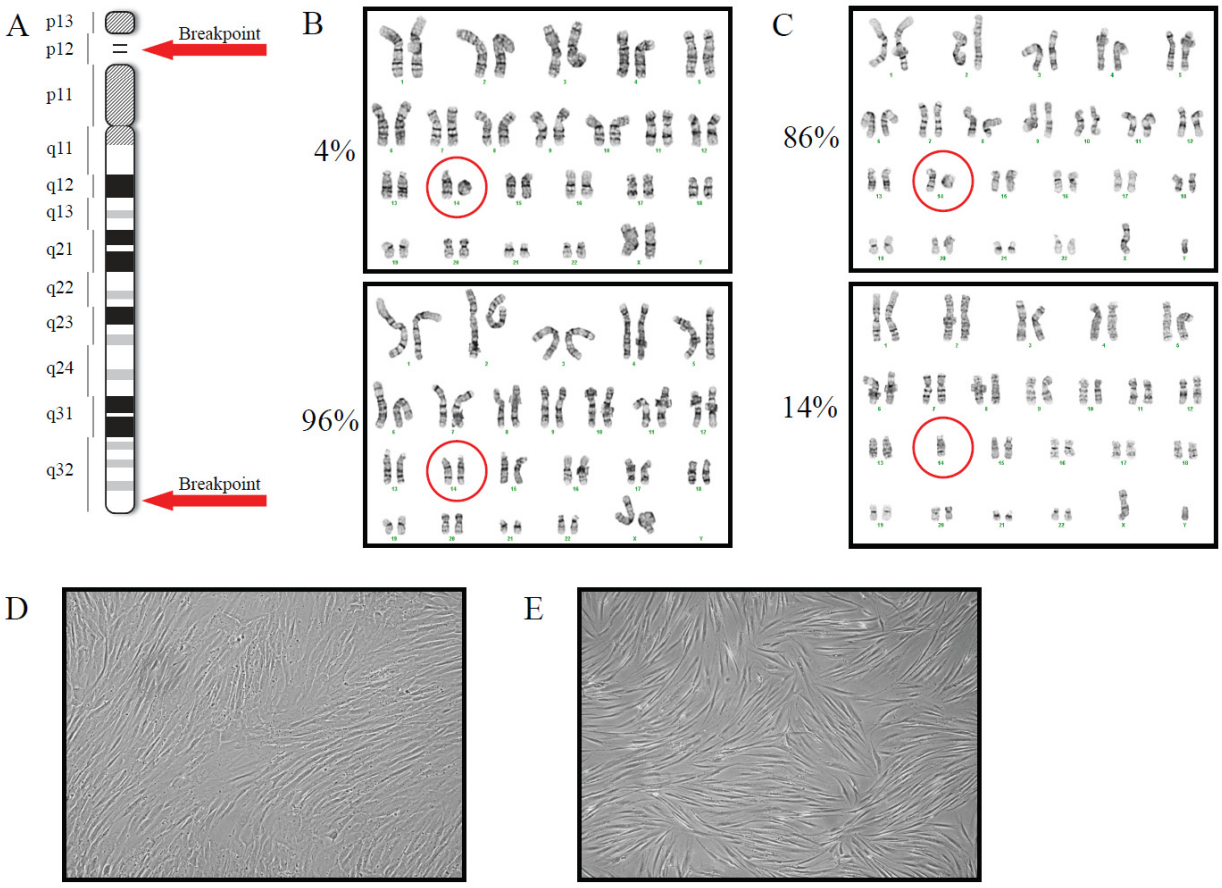

Figure 3.1: Fibroblasts from two patients with ring 14 syndrome. (A) Both patients have complete rings, with breakpoints at 14p12 and 14q32.33. (B) Patient 1 fibroblast karyotypes. (C) Patient 2 fibroblast karyotypes. (D) Brightfield image of Patient 1 fibroblasts (40x). (E) Brightfield image of Patient 2 fibroblasts (40x).

while the sample from Patient 2 carried 86% ring 14 and 14% monosomy 14 (Figure 3.1 B and C). Both fibroblast samples grew normally (Figure 3.1 D, E).

Generation of iPS cells carrying a ring chromosome 14

After confirming the presence of the ring, we initiated reprogramming. 500,000 fibroblasts were nucleofected with reprogramming episomes containing *OCT3/4, KLF4, SOX2, MYC, LIN28*, and sh-*p53*. Reprogramming proceeded normally and colonies were picked around three weeks after nucleofection (Figure 3.2 A). Out of seven iPS lines assayed from Patient 1, all were disomic and none carried the ring chromosome. On the other hand, all of the five tested

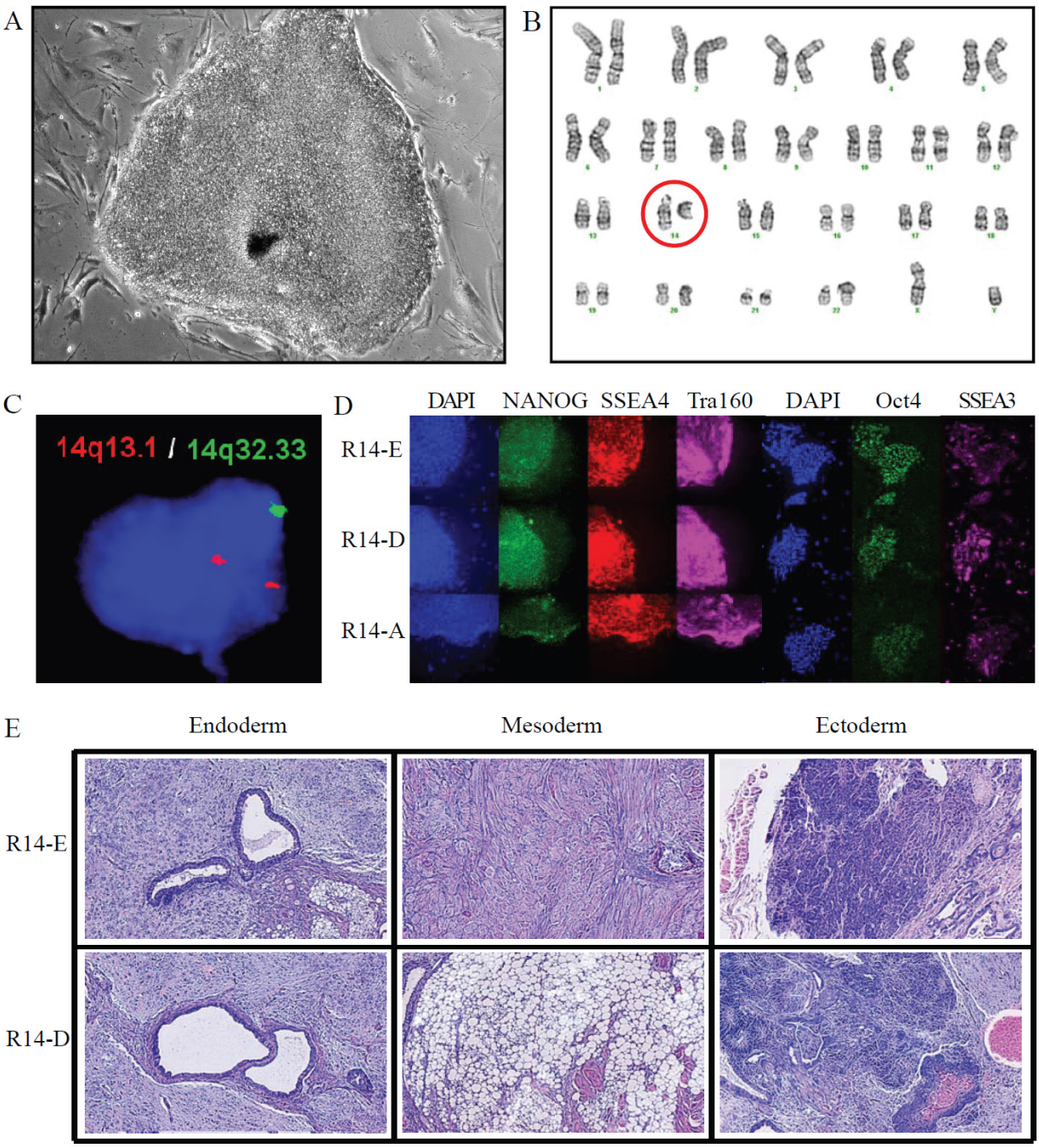

Figure 3.2: iPS cells carrying ring chromosome 14 from Patient 2. (A) Brightfield image of a R14-iPS colony grown on MEFs (40x). (B) R14-iPS cell karyotype. (C) Visualization of the ring chromosome in an iPS cell by fluorescent *in situ* hybridization. The red probe hybridizes to 14q13.1, which is present in both the ring and the linear chromosome. The green probe hybridizes to 14q32.33 sequence beyond the breakpoint, so is not present in the ring chromosome. (D) Immunofluorescence staining for human pluripotency markers (100x). (E) Teratomas from R14-iPS lines show differentiation into all three germ layers.

iPS lines derived from Patient 2 carried ring chromosome 14 (Figure 3.2 B). We were able to visualize the ring chromosome in the pluripotent cell using fluorescent *in situ* hybridization (FISH) with probes against chromosome 14 telomeric sequence and a region of chromosome 14 present on both the ring and the linear chromosome (Figure 3.2 C). Although these numbers are small, they are consistent with the hypothesis that cells with disomy 14 reprogram better than cells with ring 14, which in turn fare better than cells with monosomy 14.

Of the five iPS lines from Patient 2 that carried the ring chromosome, three were selected for further characterization. R14-iPS cells were positive for pluripotent cell surface markers including NANOG, SSEA4, TRA160, OCT4, and SSEA3, and were able to form teratomas that contained cells from all three germ layers (Figure 3.2 D, E). These results show the derivation of human iPS cells carrying a ring chromosome 14.

Changes in R14-iPS karyotype over time

Given that the frequency of ring chromosomes may change over time *in vivo*, we wondered whether the iPS cells would show a selection against the ring during *in vitro* culture. We karyotyped the R14-iPS lines at passage 3 and again at passage 15 or 17 (Figure 3.3). Two of the lines displayed the behavior we had expected: early passage cultures carried the ring

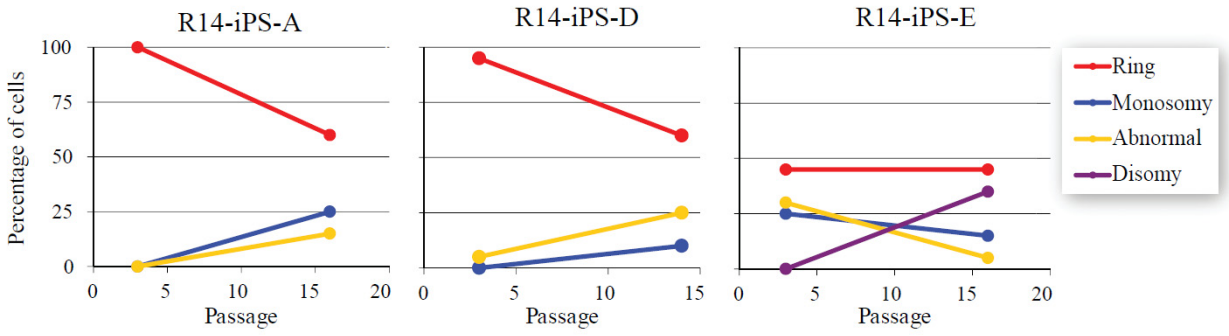

Figure 3.3: R14-iPS karyotype dynamics. Changes in chromosome 14 karyotype status over approximately three months in culture. "Abnormal" refers to a karyotype that contains translocations or chromosomal loss or gain. These aberrations are often associated with enhanced growth *in vitro*.

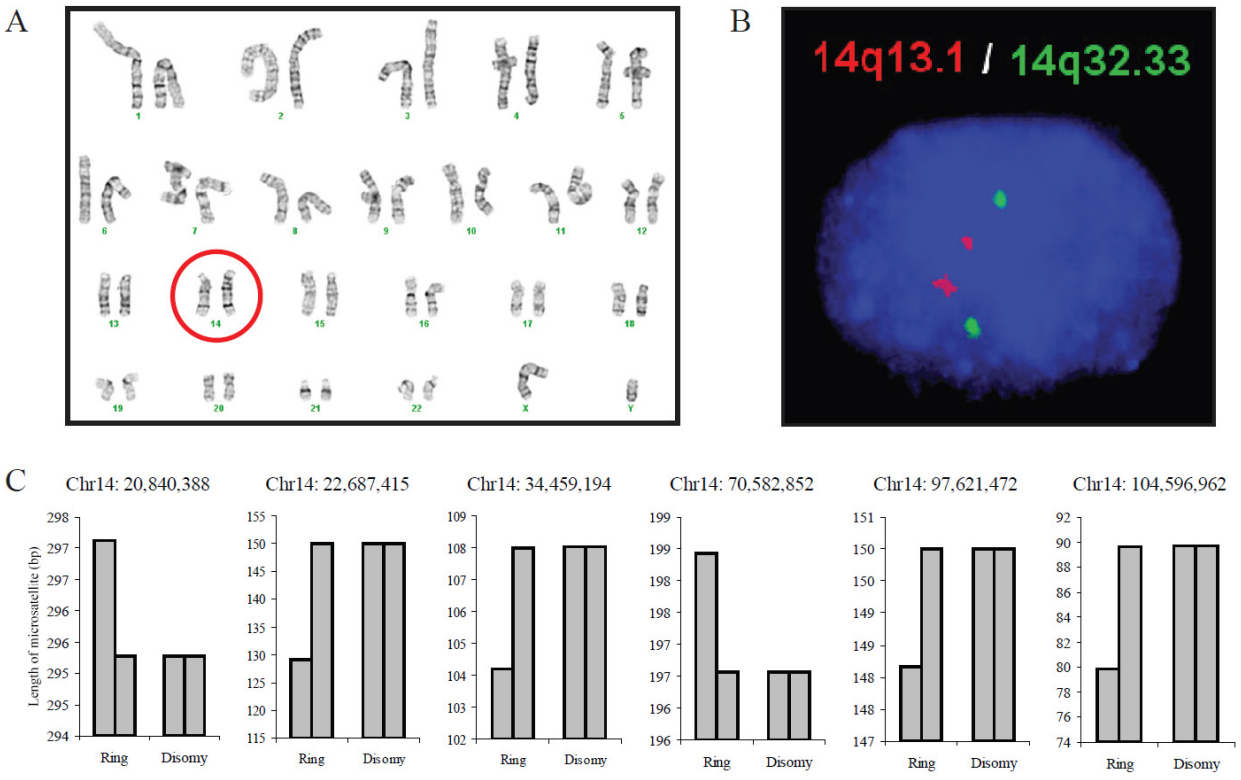

Figure 3.4: Spontaneous uniparental disomy. (A) Karyotype of spontaneous disomy in a ring 14 patient-derived iPS cell. (B) Visualization of disomic chromosome 14 in an iPS cell by fluorescent *in situ* hybridization. (C) Genotyping analysis of six microsatellite markers along chromosome 14 confirms uniparental disomy. Each bar represents one allele from that sample.

chromosome in every cell, but over the three months of passage, ring chromosomes were slowly lost and monosomic cells (or karyotypically aberrant cells) became more prevalent. One R14-iPS line manifest a less stable karyotype during early passage in which ring 14, monosomy 14, and aberrant chromosomes were all strongly represented. After continued cell culture, the karyotype normalized. The percentage of ring and monosomic chromosomes were unchanged, while the aberrant karyotype population was completely replaced by a novel species: cells disomic for normal chromosome 14 (Figure 3.4 A).

Isolation of a disomic control line

The ideal control for experiments testing the behavior of R14-iPS cells would be an iPS line isogenic to the R14 line, but carrying disomy 14 instead of a ring. This would allow for experimental comparisons in which the only difference between inputs would be the presence or absence of the ring; the cell line and the DNA gene dosage would be the same between both conditions. Any observed phenotypic differences could then be immediately ascribed to the presence of the ring chromosome. In pursuit of such a line, we subcloned the R14-iPS cells that showed spontaneous disomy, and we were able to isolate a line that carried exclusively disomy 14 (Figure 3.4 B). PCR analysis of microsatellites on chromosome 14 confirmed that the second copy of linear chromosome 14 arose from spontaneous uniparental disomy (Figure 3.4 C).

All told, we observed five species of chromosome 14 in our iPS cells (Figure 3.5). Not only did we see monosomy and disomy, but also a double ring (twice the genetic material of a normal ring) and a species with one linear chromosome and two discrete rings. These findings underscore the mitotic instability of the ring chromosome.

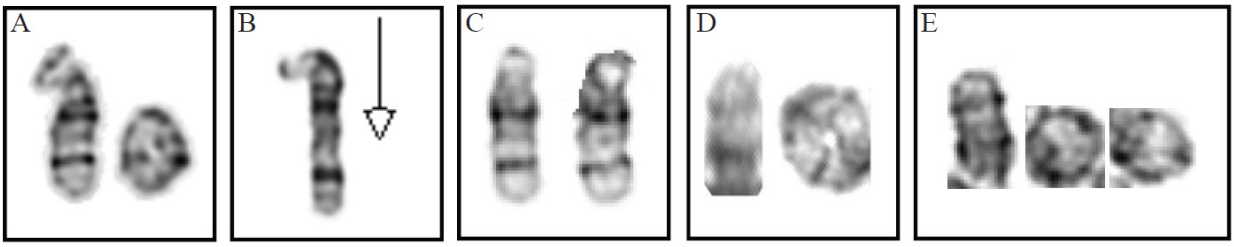

Figure 3.5: Genomic instability of the ring chromosome. We observed five species of chromosome 14: (A) Ring 14 (B) Monosomy 14 (C) Disomy 14 (D) Double ring 14 (E) One linear, two rings 14.

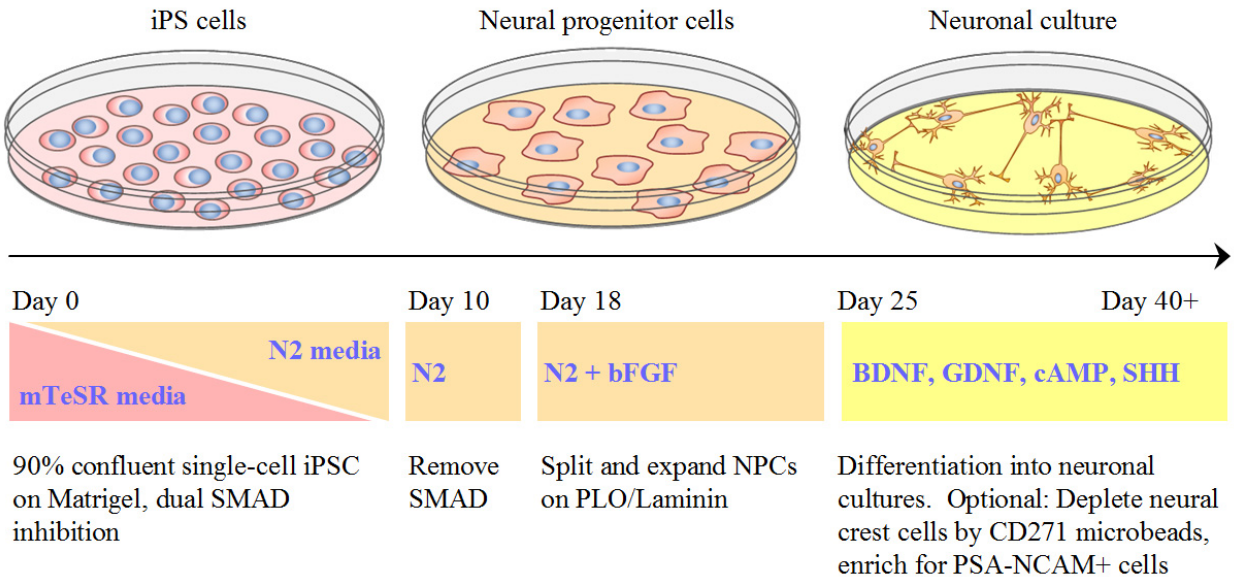

Figure 3.6: Neural differentiation schema.

Neural differentiation of R14-iPS cells

As ring 14 syndrome's primary symptoms affect the central nervous system, we decided to differentiate the R14-iPS down a neural pathway. The dual-SMAD inhibition protocol is illustrated in Figure 3.6. R14-iPS cells were able to form neural progenitor cells, neural rosettes, and cells with neuronal morphology that stained positive for the neuron-specific marker beta III tubulin (Figure 3.7). As our investigation continues, we will differentiate the R14-iPS and the disomic control line in parallel and perform more extensive characterization of the resulting cells. This will provide insight into the effect of the ring on neuronal development.

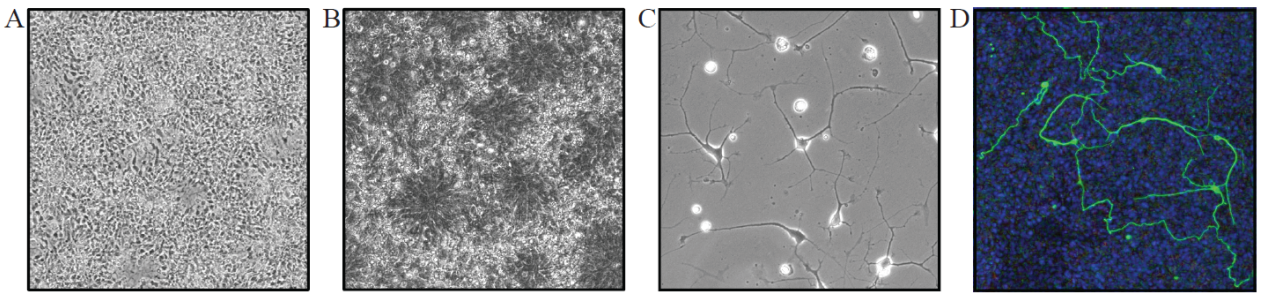

Figure 3.7: Neural cells derived from R14-iPS. R14-iPS cells of origin carried about 70% ring chromosome, 30% monosomy. (A) Neural progenitor cells. (B) Neural rosettes. (C) Cells with neuronal morphology. (D) Neural cells stained for Hoechst (blue) and neuron-specific beta III tubulin (green).

Discussion and Future Directions

Of the three disorders described in this dissertation, the least is known about ring 14 syndrome. The complete inaccessibility of brain cells has prevented researchers from investigating even the most basic questions about how such a drastic chromosomal disturbance manifests itself as epilepsy and developmental delay. Two hypotheses are frequently discussed in the literature to potentially explain the ring 14 phenotypes: the spreading of centromeric heterochromatin to compromise haploinsufficient genes, and the presence of the ring chromosome itself. Evidence for the former possibility lies in the genes present near the centromere after chromosome 14 circularization: *DICER, IGH, FOXG1,* and a large microRNA cluster. Evidence for the latter possibility comes from the presence of seizures in patients with other ring chromosomes (*128-136*).

So far, scientists have only had a single analytical tool to bring to bear on this question: phenotypic comparisons between patients with various sizes and locations of genetic deletions, with or without a ring chromosome. Unfortunately, the small size of these studies has prevented them from reaching any definitive conclusions about how the ring chromosome 14 leads to developmental delay and seizure.

Our work here has created iPS lines that carry a ring chromosome 14. Fibroblasts from a patient mosaic for ring and disomy 14 yielded only iPS lines with two normal copies of chromosome 14, while fibroblasts from a patient mosaic for ring and monosomy 14 reprogrammed exclusively into pluripotent cells that carried the circularized chromosome. The R14-iPS cells grew normally in culture, and over time we noticed a tendency for the ring chromosome to be lost, much as has been previously documented in patients. We differentiated

R14-iPS cells carrying the ring chromosome down a neural lineage and observed neural rosettes and neuronal morphology.

As expected, the ring 14 lines demonstrated mitotic instability. Five different arrangements of chromosome 14 were observed during our study, including the appearance of normal, disomic cells in one iPS line. After this unexpected finding, we were able to isolate iPS cells that differed only in their chromosome 14 genotype: ring or disomy.

The appearance of a disomic subpopulation of cells in our culture was surprising. These 46, XY cells could not have arisen from a small population in the starting fibroblasts, because each iPS line is derived from a single reprogrammed cell. Therefore, the disomic cells must have been generated during *in vitro* culture. Since regions of the teleomeres and nucleolar organizing regions are deleted in the ring chromosome, it is implausible that the second linear copy of chromosome 14 could result from a ring opening. This is underlined by microsatellite analysis demonstrating that the two linear chromosomes are derived from uniparental disomy. This finding confirms that a nondisjunction event occurred, resulting in a duplication of the entire non-ring chromosome. We suspect that this event occurred in a monosomic cell, as there is no evidence of cells with two linear chromosomes and one ring, but we cannot rule out this possibility. The 46, XY clone's ascendance suggests that disomic iPS cells enjoy a selective advantage over those carrying the ring chromosome.

After we observed dynamic karyotypes and disomy appear in our culture, a paper was published in Nature in March of this year that reported findings highly similar to ours, albeit on different ring chromosomes. Bershteyn et al. generated iPS cells from a patient with ring chromosome 17 (*144*). They found that the ring chromosome was quickly lost with passage. The selection against ring chromosome 17 in the iPS cell stage was much stronger than the

selection we observed against ring chromosome 14, as they did not even find the ring in some of the initial lines they examined. After documenting the disappearance of the ring chromosome 17, the authors observed appearance of a disomic population and confirmed its origins as uniparental disomy. They then repeated the experiments in cells containing ring chromosome 13, and found much the same results.

The Bershteyn et al. paper suggests that our findings of ring chromosome 14 dynamics in iPS cells are likely to be generalizable to all ring chromosomes. While being upstaged by such a publication is a risk of working in a fast-moving and exciting field, the paper did not make any effort to differentiate the iPS lines into the cell types affected by the disorders. We anticipate extending our studies to include such differentiations prior to submission of our manuscript. We have already generated neuronal cells from a R14-iPS line, and now that we have isogenic lines from a ring 14 patient that differ only in the presence or absence of the ring chromosome, we are poised to make the next step. As we did in Pearson syndrome, the next project in this disease will be to differentiate both the R14-iPS and the disomic iPS into the cell type most strongly affected by the disease—in this case, neurons. We will compare differentiation efficiency at each step of the process. Since some types of epilepsy are attributable to an imbalance of glutamatergic and GABAergic neurons in the central nervous system, we will investigate whether the R14-iPS cells produce a skewed ratio of Glu:GABA neurons upon differentiation. It is our belief that this differentiation data will give our data a high impact, complementing the recent Nature paper.

There are three exciting future directions for this project. The first is described above, differentiation of the cells into neurological cells and investigation of the GABAergic and

glutamatergic neuron populations. We expect to accomplish this goal before the paper will be submitted in the next few months.

The next exciting investigation for this project would be based on recent work in Dravet syndrome. Dravet syndrome is a severe epilepsy condition caused by *de novo* mutations in the voltage-gated sodium channel gene *SCN1A*. As a channelopathy, it was the first epilepsy syndrome to be studied in human iPS cells. Three different research groups published patient-specific iPS cell-based models of Dravet syndrome in 2013 (*145-147*). Each group generated iPS cells from patients with Dravet syndrome, then differentiated them into neurons and attempted to identify electrophysiological phenotypes in the resulting cells.

Before these studies were released, all previous work in mouse models, electrophysiological studies in *Xenopus*, and overexpression assays in human cell lines agreed that *SCN1A* mutations uniformly led to reduction in sodium currents. Thus, the reigning mechanistic explanation was that *SCN1A* mutations caused epilepsy by impairing firing efficacy of GABAergic interneurons. The recent work in iPS cells revealed a very different story, and underscores the impact that cell type can have on the phenotype of a given genetic mutation. The three Dravet iPS modeling papers suggest that *SCN1A* mutations actually fall into two distinct categories with completely different disease mechanisms. The first type of mutation indeed impairs action potentials in GABAergic neurons (*145*). But the second, and more common type, in fact increases sodium currents by 2-3 fold in both glutamatergic and GABAergic neurons (*146, 147*). These findings revolutionized scientists' understanding of Dravet syndrome and demonstrate the vital importance of studying genetic mutations in the appropriate cell type.

In addition to gaining insight into the mechanism of Dravet syndrome, these papers demonstrate that electrophysiology can be used to investigate genetic epilepsy syndromes on a single-cell level. Once neurons have been generated that contain ring chromosome 14, it will be fascinating to investigate their electrophysiological properties on the cellular level. Whole-cell current clamp measurements can be used to investigate cellular response to stimulation, and voltage clamp assays can provide information about the number and type of voltage-gated ion channels present in the cells. Expansion of heterochromatin is a cell-autonomous process, and if it is the main cause of seizures in ring 14 syndrome, we would expect to see electrophysiological differences between R14 and WT neurons. Effects of a ring chromosome on cell division and mitotic stability, on the other hand, are more likely to manifest as cellular disorganization or impairment of cellular connection. If these are the main causes of R14 epilepsy, we would expect to observe phenotypes on the population level, not on a cell-autonomous scale.

The third exciting research prospect would be to break open the ring chromosome using genome editing techniques. This could be accomplished using CRISPR/Cas9 technology to introduce a double strand break in the ring chromosome, then adding telomeric sequence to the break site either by homologous recombination or by capitalizing on the cell's propensity for NHEJ-based repair. If ringbreaking were successful, this cell line would be an excellent addition to the model. It would allow us to distinguish more precisely between phenotypic effects caused by the presence of the ring, heterochromatin disparities between ring and linear chromosomes, and the effect of genetic material lost during ring formation.

Conclusion

Understanding the pathophysiology of inborn genetic disorders requires a research tool that allows researchers to study the disease in the affected cell type. The complete inaccessibility of brain tissue has prevented scientists from investigating even the most basic questions about how ring 14 and other ring chromosomes manifest as treatment-resistant epilepsy, so the goal of our study was to produce neural cells from a patient with ring chromosome 14. We have accomplished that goal. These cells will provide researchers with a new tool to investigate the etiology of seizure and developmental delay in ring 14 syndrome, and especially to determine the relative importance of heterochromatin spreading and ring effects for these symptoms.

Chapter 4: Fanconi Anemia

Introduction

Fanconi anemia (FA) is the most common inherited cause of bone marrow failure. Mutations in any of more than a dozen genes can cause the same clinical picture, including skeletal abnormalities, cancer predisposition, and bone marrow failure. Bone marrow failure is in a rare class of disorder: those that could, one day, be cured by a transplant from a patient's own iPS-derived cells. In fact, because the liquid blood organ needs no matrix, organization, or shape, many researchers believe that iPS-derived cellular therapy will be more feasible in the blood system than in some other organs. With the goal of cell therapy in mind, when laboratories across the globe were first reprogramming cells from patients with all kinds of disorders, many groups attempted to reprogram cells from FA patients. None were successful.

Why not? We have investigated this question with multiple experimental approaches and have numerous interesting findings, but a single comprehensive explanation is still evasive. It was our initial belief that FA cells' inability to reprogram suggested a fundamental role for the Fanconi DNA repair pathway in the reprogramming process. Our results call this hypothesis into doubt, and suggest that perhaps the FA proteins are required for an earlier step in the process than we had anticipated. We hope that the work described in this chapter will contribute to the eventual solution of the puzzle.

Molecular phenotype of Fanconi anemia

Fanconi anemia is a clinical syndrome that can be caused by homozygous mutation of any of fifteen different genes, named *FANCA*, *FANCB*, *FANCC*, *etc*. Most of these genes are located on autosomal chromosomes, and so demonstrate an autosomal recessive inheritance pattern, although *FANCB* is on chromosome X and manifests accordingly. About 66% of Fanconi anemia is caused by mutations in *FANCA*, followed by about 12% each in *FANCC* and *FANCG* (*148*). The rest of the genes combine to comprise the other 10% of cases. The cause of this unequal distribution is not well understood, although the *FANCC* mutation is associated with the Ashkenazi population and so is more common in that group (*149*).

The FA proteins are members of a DNA repair pathway responsible for removing accidental covalent crosslinks between DNA strands. First, FANCM identifies the presence of DNA crosslinks and causes assembly of eight FA proteins into the FA core complex (*150, 151*). The core complex then ubiquitinates FANCD2 and FANCI, which form a heterodimer (*152*). This heterodimer directs a nuclease to induce a double strand DNA break at the site of the crosslink, and the FA complex oversees translesion synthesis and homologous recombination to repair the break (*153*). Mutation of any single FA protein prevents the pathway from resolving DNA crosslinks, which is believed to be the reason that mutations in many different genes result in such similar clinical syndromes.

In the laboratory, mitomycin C or nitrogen mustard are commonly used to induce crosslinks for investigation. But the primary source of DNA crosslinks in a physiological setting has been hard to identify. Recent studies have used double knockout animals to investigate which pathways are cooperative with FA. Interestingly, animals missing a Fanconi gene are highly sensitive to loss of a gene responsible for breaking down aldehydes (*154*). Aldehydes are

common products of metabolism and are also encountered in the environment. They are highly reactive moieties that can form DNA adducts and cause crosslinks (*155*). The importance of this pathway in clinical Fanconi anemia was underscored by a recent investigation in Japan, where mutations in acetaldehyde dehydrogenase are common. Patients who suffered mutations in both pathways showed more severe phenotypes, including bone marrow failure within the first few months of life (*156*). These studies support endogenous aldehydes as a leading cause of genotoxcicity in FA patients.

FA clinical syndrome

Fanconi anemia is usually diagnosed in the first decade of life, although rare patients have been diagnosed in their thirties or later (*157, 158*). About two-thirds of patients are diagnosed soon after birth due to skeletal abnormalities, including thumb hypoplasia and congenital scoliosis. The remaining 1/3 are usually diagnosed upon hematological involvement (*159*). Pancytopenia usually begins to occur around age seven and soon progresses to full bone marrow failure, frequently converting to myelodysplastic syndrome or acute myeloid leukemia.

Given the inexorable progression towards bone marrow failure, physicians begin looking for an HLA-match as soon as patients are diagnosed with FA. Unfortunately, less than a quarter of all FA patients have access to a matched, unaffected sibling donor, and many pass away from bone marrow failure or failure of an unrelated bone marrow transplant (*160*).

In addition to skeletal abnormalities and hematological complications, FA is a cancer predisposition syndrome. As the FA pathway is required at the molecular level to repair DNA damage, mutation in a FA gene causes DNA mutations and chromosomal abnormalities to accumulate over time. The cumulative risk of cancer (leukemia or solid tumor) in a FA patient is

about 40% by age 48 (*161, 162*). Part of this risk is caused by the bone marrow transplants that most patients experience in their youth; Fanconi patients are uniquely sensitive to many of the drugs used in conditioning regimens, increasing their chances of later malignancies.

Attempts to reprogram: the FA reprogramming defect

In 2008 our laboratory, while successfully using viruses to reprogram cells from patients with ADA-SCID, Gaucher disease, Duchenne and muscular dystrophies, Down syndrome, Parkinson disease, Diabetes type I, Swachman-Bodian-Diamond syndrome, and Huntington disease, tried to reprogram cells from six different FA patients (*10*). None were successful (Table 4.1). The following year, the Belmonte group in Spain published their work in FA reprogramming. They found that cells from Fanconi patients could be reprogrammed into iPS lines, but only if the gene defect was corrected before reprogramming began. They were unable to reprogram any somatic cells carrying a defective FA pathway into expandable iPS lines (*163*).

In 2012, Dr. David Williams published an extensive study of reprogramming in FA mouse cells (*164*). They found that FA cells could be reprogrammed using viruses, but at greatly reduced efficiency compared to wild-type cells. The authors identified elevated levels of gamma-H2AX in the FA cells after infection, and suggested that there may be a threshold level

Table 4.1: FA cell lines for which reprogramming was attempted during preparation of our laboratory's 2008 Cell paper.

Complementation Group	Coriell number	Tissue	Age	Gender
FANCA	GM16632	Skin Fibroblast	13 Y	Female
FANCC	GM00449	Fibroblast	6 Y	Female
FANCG	GM02361	Fibroblast	14 Y	Male
FANCA	GM00369	Fibroblast	6 Y	Male
FFANCC	GM16754	Skin Fibroblast	3 Y	Female
FANCD2	GM16633	Fibroblast	7 Y	Male

of acceptable gamma-H2AX for reprogramming. However, infection caused the gamma-H2AX levels to increase by the same amount in both FA and WT cells. This finding suggested that the observed higher levels of gamma-H2AX after infection are due to baseline differences, not reprogramming. If a threshold is indeed involved, it is not mediated through p53 pathways, as the authors observed no difference in p53, p21, or p19 levels between WT and FA cells during reprogramming. Thus, the cause of the FA reprogramming defect is still unclear.

Hypothesized role of FA proteins in reprogramming

The reprogramming cocktail contains powerful transcription factors. Two of them, *KLF4* and *MYC*, are notorious oncogenes. It is well documented that expression of *OCT4, SOX2, KLF4,* and *MYC* results in genomic trauma, especially double strand breaks (DSBs) in DNA (*164-166*). The cell has two main ways of repairing DSBs: homologous recombination (HR), which is highly accurate, and the more error-prone non-homologous end joining (NHEJ). In wild-type cells, HR is employed whenever possible in order to avoid mutations caused by NHEJ (*167*). But in Fanconi cells, NHEJ has been shown to be aberrantly hyperactive, resulting in DNA damage and chromosomal breakage (*168, 169*). This suggests that FA proteins are responsible for prioritizing HR over NHEJ when the cell chooses a repair pathway. Thus, in cells where the FA pathway is non-functional, DNA damage accrues not only through failure to repair crosslinks, but also through inappropriate choice of NHEJ over HR.

When genomic damage is found in a cell, whether in the form of DSBs or replication forks stalled at DNA crosslinks, cellular signaling prevents further cell division until the damage has been repaired. These signals include activation of the p53 and Chk1/2 pathways. Although the role of Chk1/2 in reprogramming has not been studied, p53 is known a strong inhibitor of the

process (*170-172*). Together with the role of FA in controlling DNA repair, this information led us to form the following hypothesis to explain the FA reprogramming defect: expression of OSKM induces DNA breaks. In normal cells, the FA proteins help ensure they are repaired via HR, but in Fanconi cells, overactive NHEJ results in increased genomic damage. This, along with the initial damage, activates DNA damage signaling pathways, which in turn prevent reprogramming.

Materials and Methods

Generation of the reprogrammable FANCC-/- mouse (Figure 4.3)

We purchased mouse stock number 011004 from the Jackson Labs. This mouse was homozygous for two transgenes: the reprogramming factors *OCT4*, *SOX2*, *KLF4*, and *MYC* integrated at the *COL1A1* locus under control of the dox responsive element, and *rtTA* integrated at *Rosa26*. Together, we refer to these two transgenes as "inducible OSKM" or "iOSKM." We obtained *FANCC*-/- mice through a kind gift of Dr. David Williams. The *FANCC*-/- mice were bred with the 011004 mice to create triple heterozygous transgenics. Because *FANCC*-/- mice suffer from impaired fertility, we bred the heterozygotes back with the iOSKM mice to obtain mice homozygous for iOSKM and heterozygous for *FANCC*. These mice were then bred to each other to produce embryos for MEF derivation: approximately one quarter of the resulting embryos were WT for *FANCC*, and one quarter were *FANCC*-/-. These littermates were compared in all reprogramming experiments.

Murine Embryonic Fibroblast (MEF) collection

iOSKM, *FANCC*+/- mice were set up in timed matings and checked for plugs the following morning, then removed from the male's cage. On day 13 or 14 after mating, females were palpated to determine pregnancy. Pregnant females were sacrificed according to our laboratory's animal protocol. The uterine horns were removed and placed in a dish of PBS with penicillin and streptomycin on ice. In a tissue culture hood, the embryos were removed from the uterus and dissected out of its membranes and placenta. With multiple PBS rinses, forceps were used to isolate the torso and limbs, the main sources of embryonic fibroblasts. Mechanical and enzymatic (trypsin, collagenase IV, hyaluronidase V, and DNAse) methods were used to reduce the tissue to single cells. These were then put through a 40 um sieve and plated in DMEM/10% FCS media, one embryo per 10-cm tissue culture dish. These MEFs were then expanded and passaged as usual fibroblasts. During dissection, extra tissue from each embryo was placed into lysis buffer for genotyping.

Collection of fibroblasts and keratinocytes from neonatal mice

Neonatal mice were anesthetized with CO2 and then sacrificed. Pup bodies were submerged in 70% ethanol for 15 seconds to decontaminate them, then rinsed in PBS. Feet were removed and used for genotyping. An incision was made along the back, allowing the skin to separate from the body wall. The skin sheet was then rinsed in PBS and transferred into dispase, where it sat overnight at 4 degrees. The next day, excess dispase was washed off and then forceps were used to pull apart the epidermis from the dermis with forceps. Neonatal fibroblasts come from the pink dermis, while the white epidermis is the source of keratinocytes.

Keratinocytes: the epidermis was transferred into TrypLE Select (Invitrogen) with basal layer facing down, and incubated 20 - 30 minutes at room temperature. CnT media (Cellntech) was added, the epidermis was mechanically agitated in order to loosen the keratinocytes. After collecting all cells, they were seeded at 40,000 cells per cm^2 in CnT media, in flasks coated in retronectin. Media was changed every other day. Keratinocytes were reprogrammed in the same fashion as fibroblasts (see below), except in CnT media instead of DMEM/10% FCS.

Fibroblasts: the dermis was transferred into 0.25% trypsin and incubated at 37 degrees for 10 minutes. The cells were spun down and resuspend in DMEM/10% FCS medium. Media was changed every other day.

Reprogramming blood

Retro-orbital bleeds were used to collect 100 uL of peripheral blood per mouse as described in our animal protocol. Reprogramming of blood cells was performed as described by Stadtfeld et al. (*173*).

Reprogramming iOSKM* FANCC+/+ *and* FANCC*-/- MEFs

Five independent reprogramming experiments were completed comparing littermate animals with varying Fanconi C genotypes. They are described here by their labels in Figure 4.5. In experiment B, 100K cells per replicate were reprogrammed. At the split on day 3, 50K cells were plated per technical replicate. In experiment C, 100K cells per replicate were reprogrammed. All wells were split 1:4 on day 3. In experiment D, 600K cells per replicate were reprogrammed. At the split on day 3, 15K cells were plated per technical replicate. In experiment E, 40K cells per replicate were reprogrammed. At the split on day 3, 15K cells were

plated per technical replicate. In experiment F, 100K cells per replicate were reprogrammed. At the split on day 3, 15K cells were plated per technical replicate. Cells were fixed on day 24 - 28 and stained for *SSEA1*. Stained plates were scanned, and colony counts were performed by ImageJ analysis.

Calculating reprogramming efficiency: colonies per original input cell

On day 3 during murine reprogramming, the cells are trypsinized, counted, and re-plated onto feeders. Because some input cells grow more quickly than others, each line has a different total number of cells by day 3 after reprogramming has begun. In most of our experiments, we plated the same number of cells onto feeders on day 3 for all of the reprogramming lines, regardless of how many cells were present. We found that this approach of normalizing the number of cells plated on day 3 was superior to its alternative (a fixed split ratio), because it usually resulted in similar fibroblast growth and colony density per well by the end of the experiment.

For example, cell lines A and B both may have 40K input cells plated on day 0. These would receive doxycycline for 3 days, then be trypsinized and counted. Line A may have a total of 300K cells, while line B may have a total of 150K cells. Each of these lines would be plated in triplicate, with 15K cells per well of a 6-well plate. The excess cells would be discarded. This approach introduces a split factor: line A was split 1:20, and line B was split 1:10. If the average number of colonies in the line A wells is equal to that of the line B wells, we would conclude that line A reprograms with twice the efficiency of line B.

To calculate the number of colonies per input cell, one must first extrapolate the total number of colonies that the line would have produced if all of its day 3 cells had been plated at

the target density (and not discarded). This can be calculated by dividing the average colonies per well by the number of cells plated per well on day 3. This number is then multiplied by the total number of cells present in that line on day 3, whether or not they were actually plated.

$$\textit{Extrapolated total number of colonies} = \frac{\textit{Average colonies per well} * \textit{Total number of cells on day 3}}{\textit{Cells plated per well on day 3}}$$

The extrapolated total number of colonies, divided by the number of input cells, provides the most basic "colonies per input cell" measure that is used in the left-hand panels of the efficiency figure.

$$\textit{Colonies per input cell} = \frac{\textit{Average colonies per well} * \textit{Total number of cells on day 3}}{\textit{Cells plated per well on day 3} * \textit{Number of input cells}}$$

Calculating reprogramming efficiency: colonies per cell plated on day 3

As described in the text, measuring colonies per input cell can bias reprogramming efficiency towards input cell lines with high proliferation rates. To minimize this effect, we also report the average number of colonies per cell plated on day 3. This is a much more straightforward measure:

$$\textit{Colonies per plated day 3 cell} = \frac{\textit{Average colonies per well}}{\textit{Cells plated per well on day 3}}$$

Because no cells are discarded in this measure, it is not an extrapolated number. This measure is reported in the right-hand panels of the efficiency figure.

Reprogramming samples from human Fanconi patients

Cells from two FA patients were a kind gift from Dr. Alan D'Andrea's laboratory. Both samples grew well as fibroblasts and were reprogrammed by episome and iPS lines established as described above in Chapter 3.

Western blotting of FANCD2

Mouse-anti-human FANCD2 antibody FI17 was used at 1:1000 (Santa Cruz). Mouse-anti-human vinculin antibody H-10 was used at 1:1000 (Santa Cruz). Samples were run on a 7.5% gel. HRP-conjugated secondary antibody was used at 1:2000, and visualization of HRP used Pierce ECL kit.

Mitomycin C sensitivity testing

Mitomycin C (MMC) was resuspended in water. Fibroblasts were plated at a density of 1250 cells / cm^2 in DMEM/10% FCS media. The next day, media was replaced by media containing 0, 5, 15, 50, or 200 nM MMC. Media was changed every 2 days for 1 week. BCA kit (Pierce) was used to determine total protein concentration per well, and each cell line was normalized to the amount of protein present in the untreated wells. Each treatment group contained 8 replicates.

Studies and results

We set out to test our hypothesis of the role of FA proteins in reprogramming by generating an ideal experimental reprogramming system: an inducible Fanconi mouse. Much of the variability in viral reprogramming assays is attributable to the method of reprogramming: when the four factors are carried by different viruses, the insertion sites and copy numbers of each factor vary greatly between target cells. Additionally, the viruses insert their DNA into the genomes of the recipient cells, a process that may be particularly traumatic for cells with compromised DNA repair pathways. With these considerations, we designed a system to investigate the Fanconi reprogramming defect that would minimize experimental noise and provide strong efficiency.

Reprogrammable mouse

The secondary reprogramming system is illustrated in Figure 4.1. *OCT4, SOX2, KLF4,* and *MYC* are integrated at the *COL1A1* locus under the control of a dox-inducible promoter, whose *rtTA* activator is integrated at the *ROSA26* locus (*174*). In every cell of this mouse, addition of doxycycline induces expression of the four reprogramming factors (inducible OSKM, iOSKM). This system is termed "secondary" because the cells went through a pluripotent stage during generation of the mouse, so their subsequent reprogramming by doxycycline is their second pluripotent incarnation.

We analyzed a number of experimental parameters of this system. We found that reprogramming efficiency is highly dependent upon the number of copies of both the transcription factor cassette and the rtTA activator, with cells homozygous for both transgenes

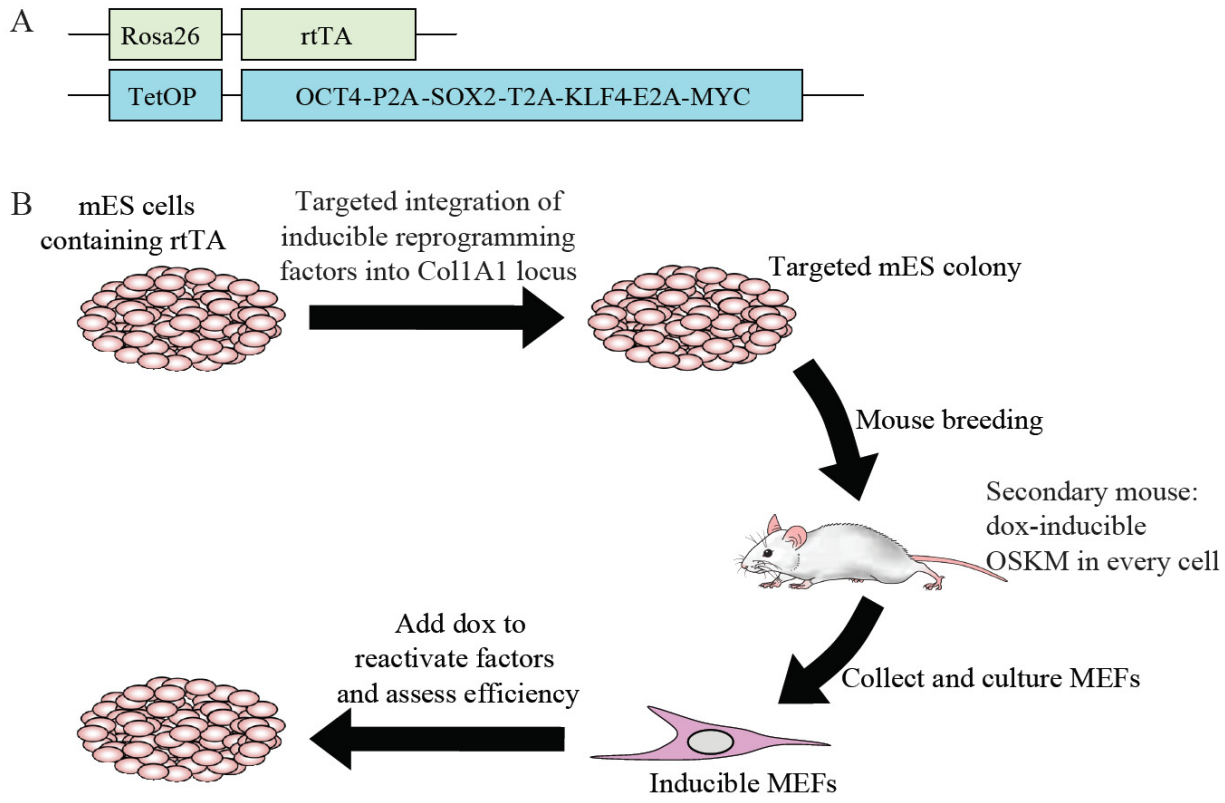

Figure 4.1: Secondary reprogramming system. (A) Two transgenes were targeted into the mouse genome. (B) Derivation of the secondary mouse and collection of reprogrammable MEFs.

reprogramming much better than heterozygotes (Figure 4.2 A). As expected, we were able to create iPS cells from many starting tissue types: MEFs, neonatal fibroblasts, peripheral blood, and keratinocytes (Figure 4.2 B). For ease of experimentation, we decided to pursue our studies using fibroblasts. To determine the best type of cell to start with, we compared reprogramming efficiency between MEFs and neonatal fibroblasts, as well as MEFs derived from different ages of embryo. Using this system, MEFs reprogrammed significantly better than neonatal fibroblasts, and there was no difference between MEFs collected from embryos at e13.5 and e14.5 (Figure 4.2 C, D). We investigated the effect of cell density on reprogramming efficiency, and found that day 3 splits of 10,000 - 35,000 cells resulted in good and not overcrowded

Figure 4.2, on following page: Optimization of secondary system. (A) Effect of copy number of iOSKM and rtTA on reprogramming (25K split). (B) Brightfield and Nanog-stained images of iPS colonies derived from the blood and keratinocytes of the secondary mouse. (C) Comparison of reprogramming between murine embryonic fibroblasts (MEFs) and neonatal fibroblasts. (D) Comparison of reprogramming between MEFs derived from e13.5 and e14.5 day old embryos. (E) Effect of split density on reprogramming, 5 ug/mL. (F) Effect of doxycycline concentration on reprogramming (15K split).

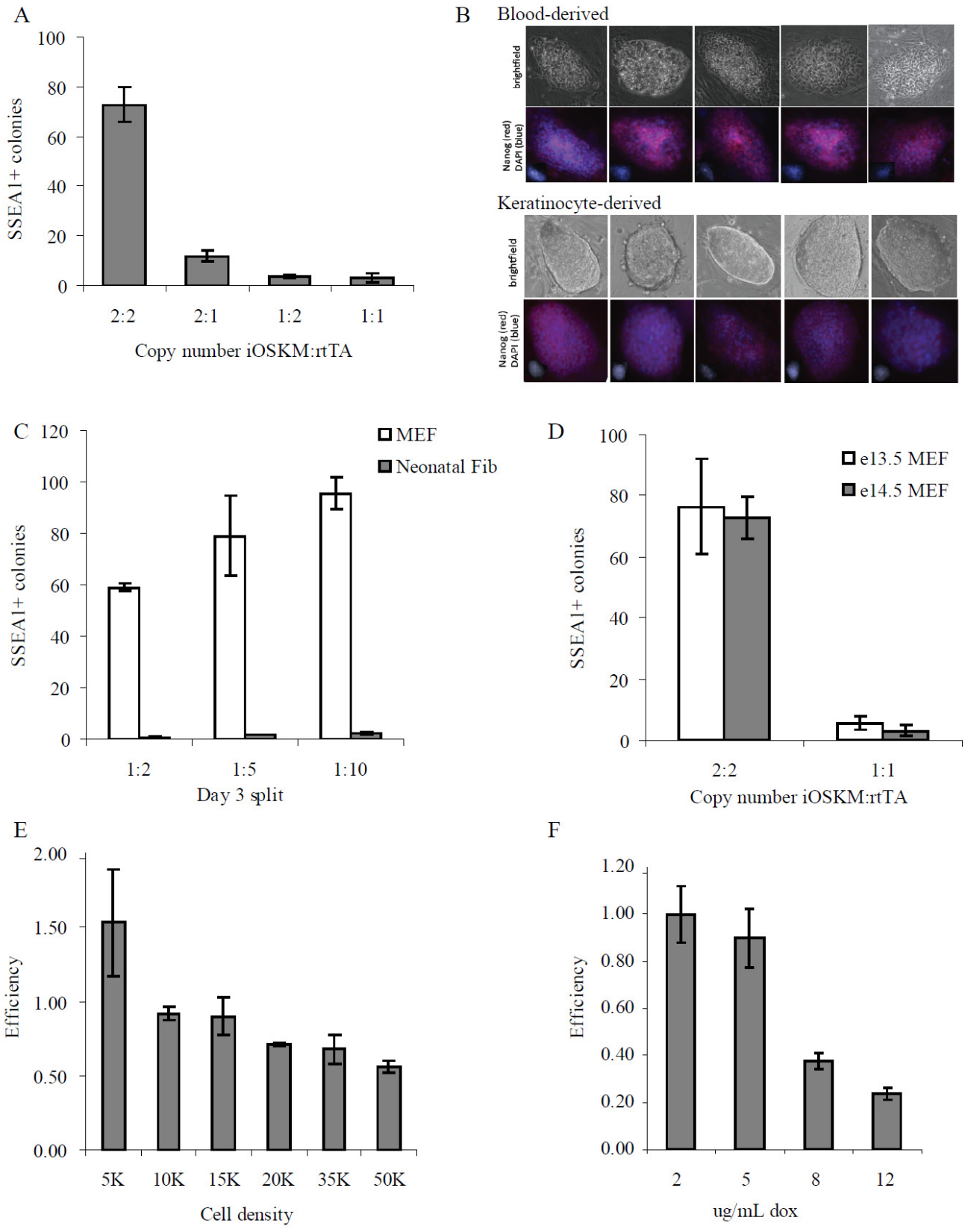

Figure 4.2: Optimization of secondary system (Continued)

reprogramming efficiency (Figure 4.2 E). Finally, we found that 2 or 5 ug/mL of doxycycline provide the best reprogramming (Figure 4.2 F).

FANCC *knockout cells in secondary reprogramming*

We bred a *FANCC* knockout transgene into the secondary reprogramming mouse strain. Because homozygous FA mice show severely impaired fertility, we maintained our *FANCC* knockout mouse colonies as heterozygotes (Figure 4.3). Murine embryonic fibroblasts (MEFs) from mice homozygous for the iOSKM cassette and rtTA were collected and genotyped to identify *FANCC*-/- and *FANCC*+/+ littermates. These MEFs were plated and grown in doxycycline for three days. On day 3 of reprogramming, they were split onto feeder cells and then switched into mouse embryonic stem cell media. Reprogramming efficiency was measured by SSEA1 staining at day 21.

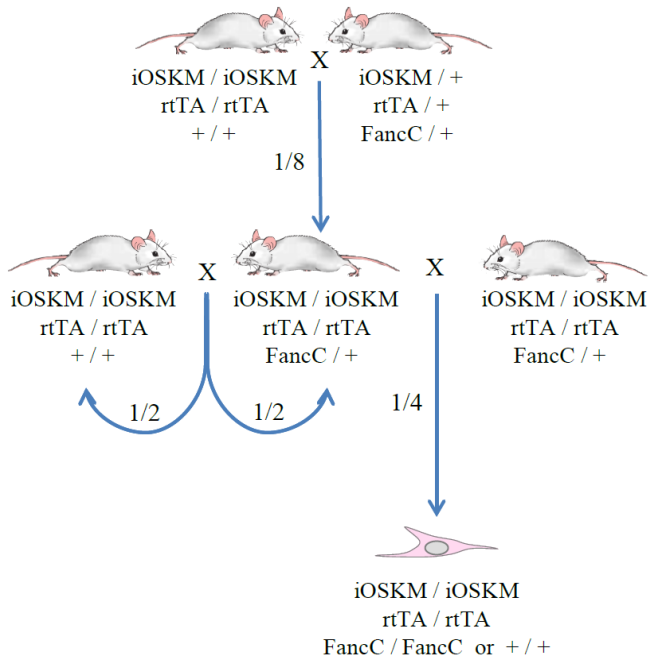

Figure 4.3: Breeding schema for Fanconi secondary mice. The target cell for experimentation was iOSKM homozygous, rtTA homozygous, and either *FANCC*+/+ or *FANCC* -/-.

Murine reprogramming protocols, including the one described here, prevent culture overgrowth by splitting on day 3. We have observed that individual MEF lines divide at very different rates. While measuring MEF proliferation, up to a 7-fold difference in cell number can be seen after only two days in culture. Especially in secondary reprogramming, where every cell is exposed to doxycycline, a raw increase in the number of fibroblasts in the

first few days of culture has the potential to distort the final number of colonies (*175*). Because of this effect, a strong null hypothesis when investigating secondary reprogramming efficiency is that a sample "reprograms" with good efficiency simply because the input cells divide faster.

One way to minimize the impact of differential fibroblast growth is to measure efficiency as the number of colonies per cell plated during the day 3 split. This approach removes any effect on efficiency caused by three days of fibroblast growth. Measuring colonies per day 3 cell, however, introduces its own form of error, in that a true reprogramming enhancement or defect whose primary mechanism is enhancing early fibroblast growth will not be seen. Thus there are two ways to measure secondary reprogramming efficiency: colonies per input cell and colonies per cell plated on day 3. The former is vulnerable to swings in efficiency due to fibroblast growth rate, while the latter can overlook changes in efficiency caused by changes in growth rate. Neither of these measures is fully informative, but by comparing the two we can determine whether an observed difference in secondary reprogramming efficiency is attributable to differential early growth rates or to an effect later in the reprogramming process. For this reason, we report efficiency data as both (extrapolated) colonies per input cell and colonies per cell plated on day 3. Please see the methods section for greater explanation of how the (extrapolated) colonies per input cell and colonies per cell plated on day 3 were calculated.

In order to perform the day 3 efficiency analysis, the total number of cells in each condition was counted at the split. This resulted in an accurate measure of fibroblast growth during the first three days of reprogramming, which we investigated after observing higher-than-expected inter-experimental variability. Interestingly, for a given cell on day 3, we could compare its history of growth with its future chances of reprogramming. All MEFs were

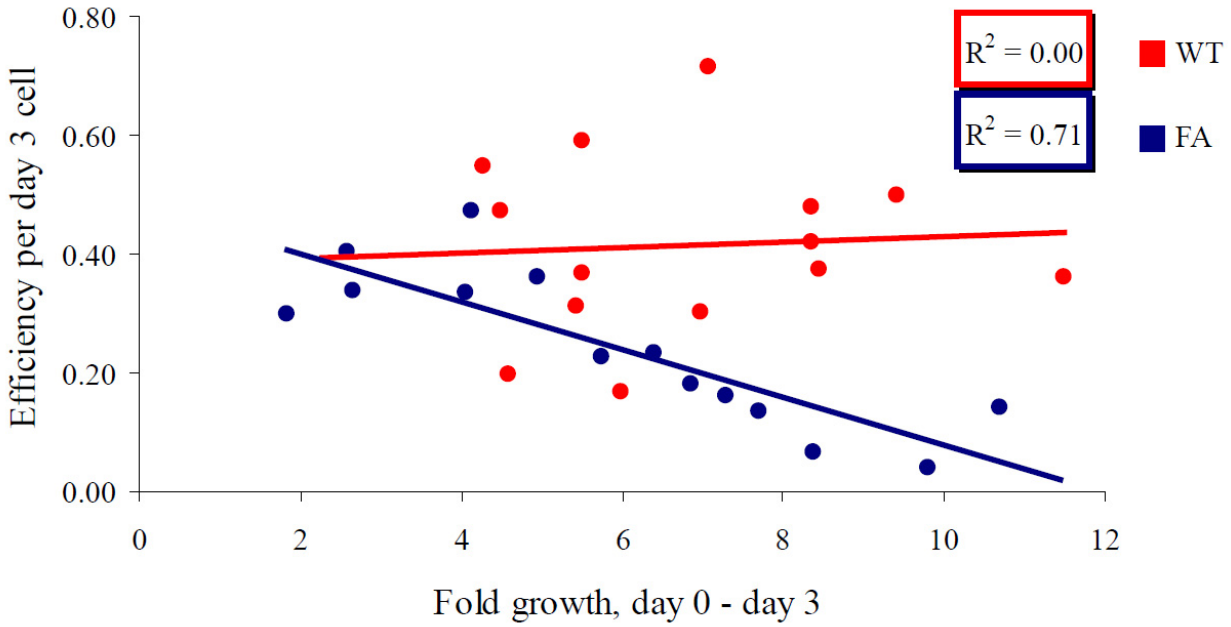

Figure 4.4: Effect of early proliferation on eventual reprogramming efficiency. Each dot represents one biological replicate.

between passages 2 and 4 upon reprogramming. A striking difference between WT and FA cells emerged from this analysis (Figure 4.4). In the WT culture, growth rate was not strongly correlated with reprogramming efficiency. But in the FA culture, the highest efficiencies were seen in experiments with the lowest initial growth rates, and high early growth rates were associated with the lowest reprogramming efficiency. This suggests that for *FANCC* knockout cells, a recent history of active proliferation impedes the reprogramming process.

Despite this apparent disadvantage, we did not observe a reliable defect in *FANCC* knockout MEF secondary reprogramming efficiency compared to wild-type MEFs (Figure 4.5). In some experiments, FA cells reprogrammed better than WT cells; in others, they performed more poorly. We observed much higher levels of variability than expected from literature descriptions of this technique, both between experiments and between replicates. There was no clear reprogramming defect in the FA cells, especially when efficiency was measured as colonies per cell plated on day 3 (Figure 4.5, right panels).

Figure 4.5, on following page: Fanconi secondary reprogramming efficiency. Left panels: extrapolated efficiency measured as colonies per input cell. Right panels: efficiency measured as colonies per cell plated at the split on day 3. (A) Compiled experimental data. (B - F) Individual experiments.

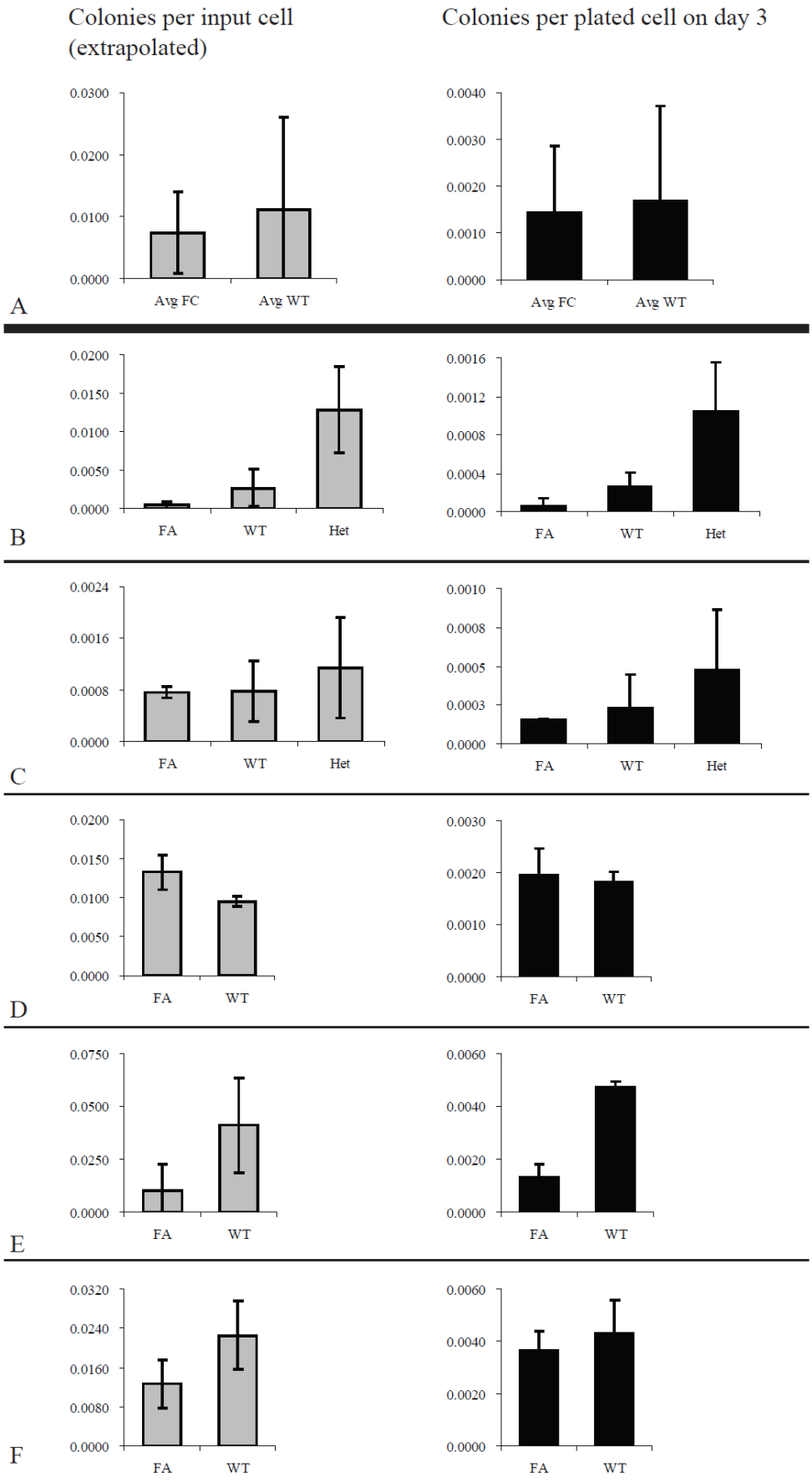

Figure 4.5: Fanconi secondary reprogramming efficiency (Continued)

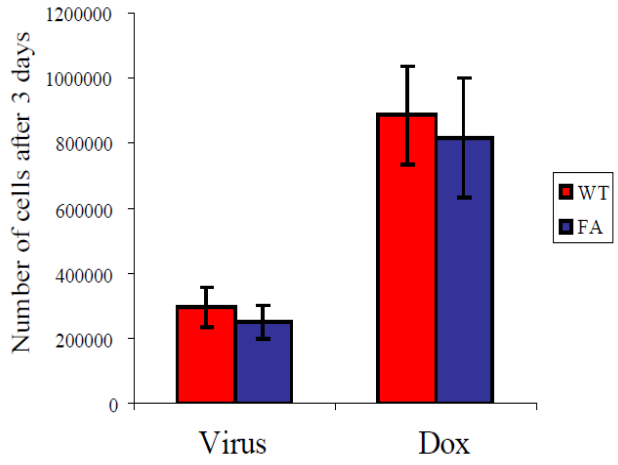

Figure 4.6: Effect of reprogramming method on cell growth. Total number of cells was counted three days after induction of reprogramming either by virus or by addition of doxycycline.

The reprogramming proficiency of secondary FA cells—even in the face of inverted growth effects—surprised us. Previous publications had demonstrated a severe reprogramming defect in Fanconi cells. Our findings led to two possible interpretations: first, that *FANCC* knockout in mice does not cause the same reprogramming defects as knockout of other Fanconi genes, or second, that the cause of the published FA reprogramming defect was absent from our system. One such possible cause could be viral infection.

Given the negative association between FA growth and reprogramming, we tested whether growth rates differed between secondary fibroblasts exposed to viruses or doxycycline. We directly compared the growth rates of WT and FA secondary MEFs three days after doxycycline addition or lentiviral OSKM infection (Figure 4.6). In both WT and FA secondary cells, doxycycline induced significantly more proliferation than infection with OSKM lentivirus. Accordingly, if FA cells specifically fail viral reprogramming, it is not due to an increase in early proliferation.

Episomal reprogramming of human samples

Unfortunately, the *FANCC*-/- secondary system is unable to distinguish between the possible explanations for the lack of a severe reprogramming defect. To investigate further, we turned to human samples. We obtained cells from two FA patients, one with a mutation in

FANCD1 and the other missing *FANCD2*. We reprogrammed these human cells using a non-integrating episomal approach in normoxia and were surprised to find that by three weeks after nucleofection, dozens of colonies were visible on the plates from both patient samples. Those from Patient 1 seemed to show better morphology, while those from Patient 2 tended to look more transformed. Many colonies were picked from each patient sample, and iPS lines were easily established from 20/22 of the Patient 1 colonies and 3/5 of the Patient 2 colonies (Figure 4.7 A). The estimated reprogramming efficiency was 0.035% from Patient 1 and 0.001% from Patient 2. A recent comparison study by our laboratory found the average episomal reprogramming efficiency from 12 non-FA lines to be about 0.015%, suggesting that Patient 1 reprogrammed at least as well as most WT lines.

Upon western blotting of the resulting iPS cells, lines derived from Patient 1 samples appeared to have restored function of the FA pathway (Figure 4.7 B). We believe this is an instance of a previously described phenomenon in which mutant FA genes can recombine or spontaneously correct to produce a functional copy of the gene, thus rescuing the FA phenotype during *in vitro* fibroblast culture (*176, 177*). Cells from Patient 2, however, maintained their FA identity, as evidenced by the total lack of FANCD2 protein and sensitivity of the fibroblasts to MMC (Figure 4.7 B and C). We wondered whether the observed ease of reprogramming was due to the presence of p53 knockdown in the episomal system. Although we were not able to investigate this question directly, loss of p53 has been shown to lead to highly irregular karyotype (*172*). We established three lines of iPS cells from Patient 2 and selected one for further characterization, including an analysis that demonstrated a normal karyotype (Figure 4.7 D).

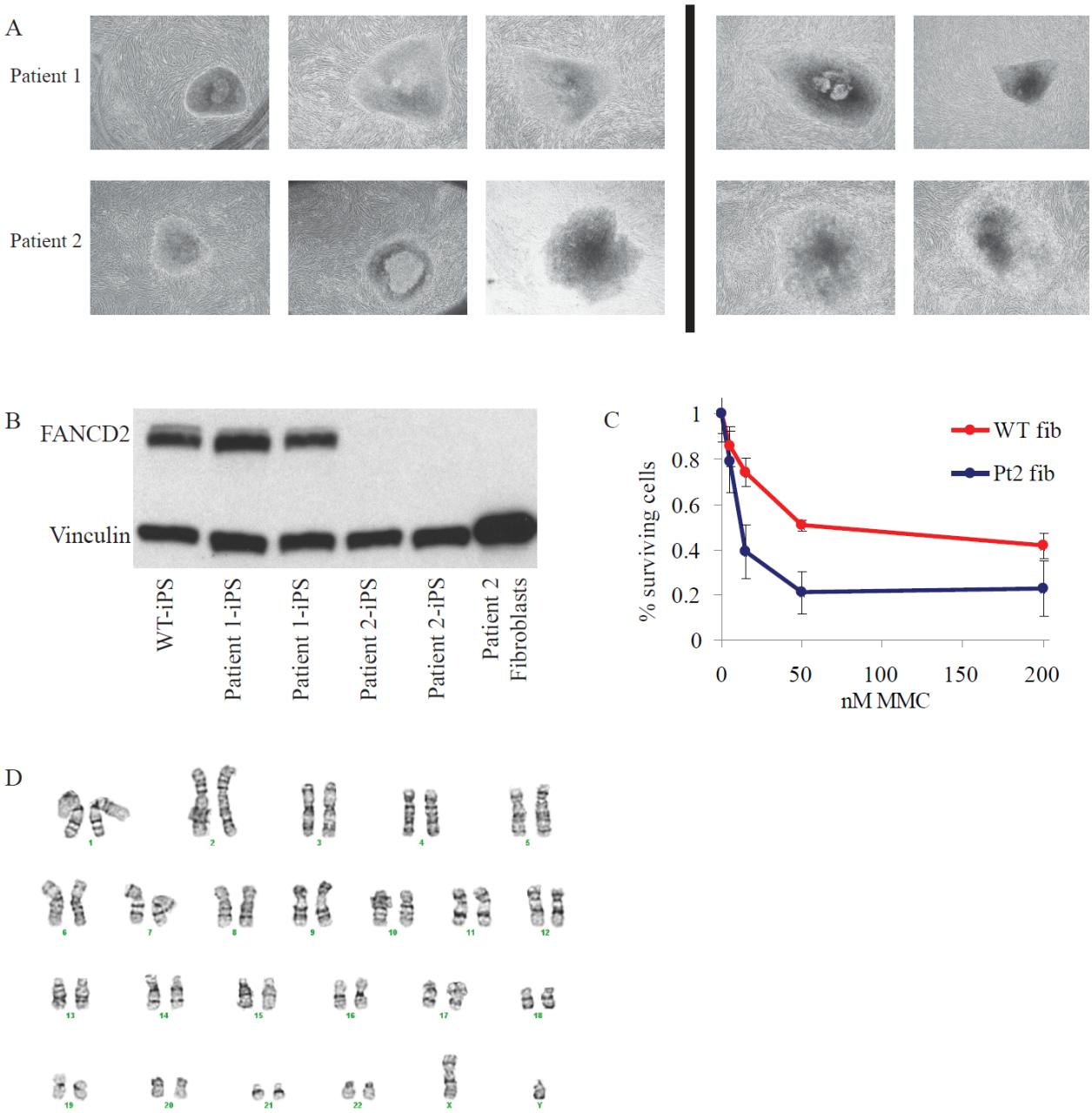

Figure 4.7: iPS cells derived from human FA patients. (A) Brightfield images of iPS colonies on the reprogramming plate (passage 0) from both patients (40x). Colonies on the left side of the divider successfully formed iPS lines; colonies on the right side of the divider did not. (B) Western blot for FANCD2. Heavy upper band demonstrates restoration of FA pathway activity in Patient 1 iPS lines. (C) Mitomycin C sensitivity of fibroblasts from Patient 2 compared to WT. (D) Karyotype of FA-iPS line derived from Patient 2.

We were impressed by how easily we could derive FA-iPS cells using non-integrating episomal reprogramming methods. Unfortunately, obtaining patient samples is often a limiting factor in Fanconi anemia research, and we have been unable to obtain samples from other patients for investigation. Thus while our data are provocative, they are not sufficient to conclude that episomal reprogramming of FA cells is definitively more efficient than viral reprogramming.

In addition to the successful episomal reprogramming of a human patient line, we designed and generated a *FANCC* synthetic modified RNA that restored function of the Fanconi pathway in *FANCC*-/- human cells (See Appendix). It is our hope that this tool, combined with viral and non-integrating reprogramming, will contribute to the eventual elucidation of the cause of the FA reprogramming defect. Once the cause is understood, researchers will be able to generate patient-specific FA-iPS cells. Eventually, these cells could be used as a source of autologous stem cells for Fanconi patients who do not have a matched bone marrow donor.

Discussion and Future Directions

The purpose and function of Fanconi anemia genes have been determined by years of *in vitro* work, and now a relatively clear picture has emerged: loss of any gene involved in the resolution of DNA crosslinks will result in FA. Some clinical aspects of the disease are even understood on the molecular level, such as endogenous aldehyde damage to DNA and p53's role in hematopoietic stem cell depletion, while others such as skeletal abnormalities remain mysterious (*178, 179*). Because bone marrow failure is one of a handful of disorders that could be cured by cell transplantation, there is much interest in derivation of patient-specific iPS cells.

However, FA patient cells appear to be resistant to reprogramming by viruses carrying *OCT4, SOX2, KLF4,* and *MYC*.

Laboratories around the world have attempted to reprogram cells from human Fanconi anemia patients (*10, 163, 180*). Only two human FA-iPS cell lines have ever been published, one of which carried a severely abnormal karyotype (*180*). The question of why FA cells are so hard to reprogram has intrigued scientists: the mere demonstration that corrected patient cells—essentially wild-type cells—could be reprogrammed was published in the journal Nature (*163*). Mueller et al. found that murine FA cells can be reprogrammed, albeit at lower efficiency than WT cells (*180*). We attempted to generate an ideal experimental system for investigating the FA murine reprogramming defect: the secondary reprogrammable mouse is described as fast, efficient, and reliable, with no variation due to copy number differences or insertion site effects.

The secondary murine system is touted as a low noise, high efficiency system, so we were disappointed to observe considerable inter-experimental variation. When we attempted to identify why some of the experiments seemed to reprogram more efficiently than others, we noted that the fibroblast growth rate during the first three days of reprogramming varied significantly between cell lines and between experiments. We were struck by the observation that *FANCC* knockout MEFs which spontaneously underwent intense proliferation reprogrammed more poorly than those that grew slowly. WT reprogramming efficiency, on the other hand, was not correlated with fibroblast growth rate during the first few days of reprogramming. We wondered whether the effect of proliferation on FA reprogramming efficiency could be the underlying reason for the FA defect reported in viral systems. This theory would predict that viral OSKM transfection induces more proliferation than does activation of the secondary system. However, we observed that secondary MEFs proliferated

significantly more after addition of doxycycline than they did after infection with viruses carrying *OCT4*, *SOX2*, *KLF4*, and *MYC*. Thus, the published FA reprogramming in viral systems is not likely due to FA cells' sensitivity to proliferation.

The effect of cellular proliferation on reprogramming is an area of intense research, and most studies suggest that proliferation is correlated with improved reprogramming efficiency (*175, 181*). Our surprising observation of an inverse correlation between early growth and reprogramming efficiency in FA cells is particularly interesting in light of paper published by Dr. Jun Lu's laboratory in February of this year (*182*). The authors used continuous live-cell imaging to study inducible reprogramming from MEFs and murine hematopoietic cells. They identified a subpopulation of input cells that gave rise to nearly exclusively iPS colonies. These cells were characterized by extremely rapid cell division, and thus called ultrafast cells. Because most of the reprogrammed colonies were derived from ultrafast cells, the overall reprogramming efficiency was tightly correlated to the number of ultrafast cells in the starting sample. This number could be increased by knockdown of p53, suggesting that the previously-described effect of p53 knockdown on reprogramming may be mediated through its effect on the ultrafast cell population. This work suggests that an investigation of the cell cycle profile of day 3 reprogramming FA cultures could provide insight in to the trend seen in Figure 4.4.

We originally hypothesized that the FA reprogramming defect occurred because the FA proteins play a vital role in DNA repair during the reprogramming process. However, this hypothesis was not fully borne out by our data. When the *FANCC* knockout mice were bred into the homozygous secondary reprogramming mouse background, we were surprised to find that the *FANCC*-/- MEFs reprogrammed with nearly the same efficiency as cells from their WT littermates. This unexpected finding suggested two possible alternate hypotheses: either *FANCC*

cells reprogram with better efficiency than other Fanconi anemia genotypes, or the cause of the published reprogramming defect was absent from our system.

One figure in the paper from the Williams laboratory drew our consideration: the authors observed that although *FANCC*-/- cells showed a moderate reprogramming defect, *FANCA*-/- cells were more severely impaired. This finding is surprising given the FA molecular pathway: FANCA and FANCC are two members of the same core protein complex, and FANCA has never been found to have any functions independent from FANCC (*183*). The two genes are believed to be largely epistatic: even double knockout mice show a phenotype no more severe than either single knockout (*184*). Additionally, of the six FA samples that our laboratory attempted to reprogram in 2008, two were *FANCC-/-* and these two samples failed reprogramming along with the others. However, given the Williams lab's observation, it remains possible that a difference between gene function accounts for the lack of reprogramming defect in our secondary *FANCC*-/- mice.

The other possibility is that our FA cells reprogrammed as well as WT cells because the cause of the published reprogramming defect was absent from our system. A major difference between our system and others' was the method of OSKM expression: our secondary reprogramming was initiated by the simple addition of doxycycline. All previous publications on FA reprogramming defects, and our lab's unpublished experience, used integrating viruses to introduce the four factors. Although it is not yet known whether FA proteins are directly involved in viral integration, DNA repair proteins associated with the FA pathway such as hRad18 and Ku70 are directly involved in the integration process (*168, 185, 186*). Viral infection may therefore affect FA cells differently than it does WT cells.

The data presented here are insufficient to demonstrate conclusively the cause of the published FA reprogramming defect. However, given that FANCA and FANCC are largely epistatic in other contexts and that FA mouse cells reprogrammed well in a non-integrating system, we believe that integration of viruses into the genome is likely to be a contributing cause of the FA reprogramming defect. This new hypothesis predicts that FA cells reprogram more poorly than WT cells only when reprogramming is mediated by virus. We performed a brief follow-up experiment in which non-integrating episomes were used to reprogram human Fanconi fibroblasts. We were indeed able to easily reprogram the cells and establish FA-iPS lines, but the sample size was only a single FA patient.

This question is the most interesting future direction for this project. To properly investigate, one would obtain samples from multiple patients that have different FA genotypes, to control for potential inter-genotype variation. Two experiments should be performed on these and WT samples. First, they should be subjected to episomal reprogramming with and without viral infection: one condition of each sample would be infected by a control virus such as GFP, and the other would not. Reprogramming efficiency should be measured for each condition. If the GFP virus negatively affects the reprogramming efficiency of the FA cells but not the WT cells, this would be evidence that viral infection *per se* impairs FA reprogramming.

Secondly, double knockout of p53 and FA proteins has recently been shown to reduce Fanconi hematopoietic phenotypes (*178*). A reasonable extension of this finding would suggest that the improvement in reprogramming efficiency we observed with the episomal system could be due to its p53 knockdown, not its non-integrating nature. This hypothesis should be tested by direct comparison of reprogramming efficiencies between viral and episomal systems utilizing exactly the same genes, promoters, and 2A spacing sequences. Preparation of these materials

would have to be accomplished from scratch, as there are currently no viral and episomal systems that utilize the same OSKM cassettes. Once the reagents were made, however, this experiment would determine whether the observed facilitation in FA reprogramming efficiency is due to p53 knockdown or the non-integrating nature of the episomal system.

Preparation and execution of these experiments would require additional years of work and expanded access to patient samples. Therefore, they represent excellent starting points for the next scientist interested in the mechanisms of the FA reprogramming defect.

Conclusion

This project was initiated because we believed that the FA reprogramming defect signified a vital role for DNA repair in the reprogramming process. The absence of a severe reprogramming defect in our secondary system suggests that the Fanconi DNA repair pathway is not, in fact, required for efficient reprogramming. Instead, certain FA proteins may be important, or the FA pathway may be called upon to aid cellular recovery from viral integration. We hope that the work described in this chapter will contribute to more thorough understanding of the Fanconi pathway in the reprogramming process.

Chapter 5: Discussion and Future Directions of the Field

Genetic diseases must be studied in the affected cell type

Cellular identity is often invoked in cancer research, but much less frequently in discussion of genetic disorders. The mutation is present in every cell of the body, so genetic diseases are often investigated in patients' easy-to-access blood or skin cells. But these systems do not take into account the effect of cellular identity on gene function and cellular phenotype, so they cannot provide the most accurate information on genetic diseases.

A mutation in a given gene will cause vastly different effects in different cell types: the gene's expression levels may be different, it may be crucial or dispensable, and there may be other proteins present that amplify or negate its effects. This was underscored by the three Dravet syndrome papers described above, where the true effect of a sodium channel mutation was completely misunderstood until it was finally studied in neurons (*145-147*). The same effect can be seen even more clearly in the mitochondrial field: when fused to wild-type nuclei with different cellular identities, a single mutant mtDNA genome produces very different phenotypes (*102, 103*).

iPS cell-based models have the potential to solve this problem. If scientists can create a differentiation protocol for the type of cell affected by the disease, the mutation can be studied in the proper cellular context. This may not only lead to a better understanding of how the mutation causes symptoms, but also suggest novel mechanism-based approaches to therapies.

We employed cellular identity transformations to create the cell types affected by various genetic diseases. This dissertation depicts the progression towards reprogramming models of

three genetic disorders: Pearson syndrome, ring 14 syndrome, and Fanconi anemia. Each of these diseases is at a different stage of its research lifecycle: our Pearson syndrome iPS cells were the first published pluripotent cells to carry deleted mtDNA and we identified a Pearson syndrome-specific phenotype in blood cells; we created iPS cells carrying ring chromosome 14 and generated the first neural cells from a ring 14 patient available for study; we reprogrammed mouse and human Fanconi anemia cells using non-integrating approaches and observed surprisingly robust efficiency. These research advances demonstrate the power of cellular identity manipulation for research on genetic diseases.

Genetic, epigenetic, and environmental factors control cellular identity *in vivo*

Unicellular organisms all have a single goal, to survive long enough to reproduce. The difference between these basic organisms and multicellular creatures like humans is simple: in complex organisms, different cells play different roles. A neuron will express neuronal genes but will never express liver-specific genes; a melanocyte will produce melanin after exposure to UV light but a fibroblast will not. These cell types all contain the same genetic sequence, but the differences in their responses are determined by which regions of the DNA are accessible to transcription. In complex organisms, the epigenome maintains cellular identity by carefully allowing certain genes and non-coding RNAs to be expressed in a given cell type, while simultaneously blocking access to other regions of the genome.

As a human zygote cleaves, and through subsequent rounds of cell division develops into a complex organism, cells transition inexorably from one identity to another. Gene expression from a single genome evolves and adapts via a carefully choreographed and directed set of

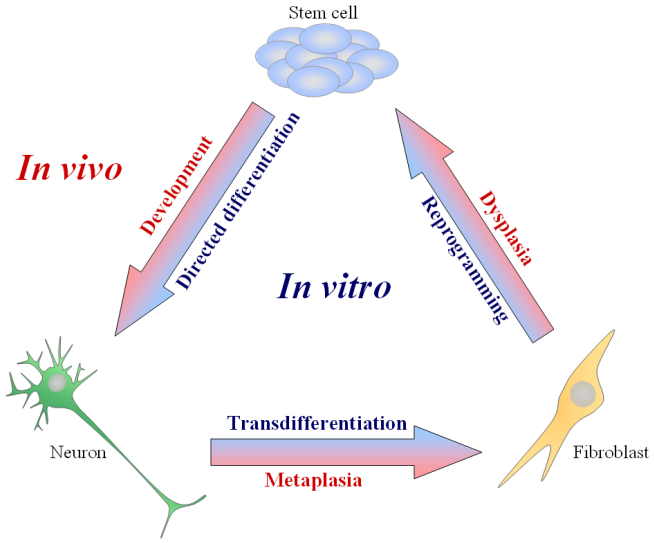

Figure 5.1: Cellular identity transformations. Blue are *in vivo* transformations; red are the corresponding *in vitro* transformations.

inductive and selective events, until lineages become segregated and tissue fates are determined. Evolution has invested heavily in maintaining and restricting cellular identities in mammals: once a mammalian cell has progressed through its natural developmental transitions, its final specialized state is sustained by a loss of self-renewal and inevitable senescence.

Occasionally, genetic, epigenetic, or environmental changes can cause cell identity to change. *In vivo* cellular identity changes are called dysplasia (Figure 5.1). Dysplasia often leads to malignancy, in which cellular identities have changed so completely that the cancer cells behave like single-celled organisms, surviving and reproducing regardless of the needs of the whole person.

The most common cause of dysplasia is genetic mutation. Cancer-causing mutations often manipulate cellular identity by affecting genes related to self-renewal and senescence (*187*). For example, when normal hematopoietic precursors acquire mutations that allow them to self-renew, they are quickly transformed into leukemic stem cells (*188*).

Epigenetic alterations can lead to dysplasia by changing the transcriptional accessibility of certain genes, especially those related to metastasis. For example, hypomethylation of the pro-metastasis gene *SNCG* has been shown to play a causal role in metastasis of breast and ovarian tumors (*189*).

More rarely, transformation of cellular identity is brought about as a reaction to extreme environmental conditions. For example, metaplasia and subsequent adenocarcinoma can occur when esophogeal tissue is repeatedly exposed to stomach acid (*190*). Likewise, in January of this year, two surprising papers showed the conversion of somatic cells into pluripotent cells by transient exposure to acidic conditions (*191, 192*). Although their findings may or may not be repeated by other laboratories, the papers sparked much scientific discussion of the influence that a cell's environment—pH, physical stresses, oxygen tension, hyperglycemia, toxins, UV exposure, or nutrient deprivation—can have on its identity.

Researchers are now co-opting these three methods of cellular identity transformation to reprogram cells to pluripotency. Reprogramming provides the cell with extra copies of genes that encourage self-renewal and prevent senescence. These factors erase the old epigenetic cellular identity and establish a pluripotency epigenetic network in its place. Finally, a few days into the reprogramming process, the cellular environment is adjusted by changing the media to fit the nutritional and signaling requirements of pluripotent stem cells. This was the recipe for cellular identity manipulation that Dr. Yamanaka created.

The future of iPS cell-based modeling: complex disorders

The same three factors that control cellular identity can also be the underlying causes of illness. Genetic diseases occur when a DNA mutation causes a clinical phenotype, such as Pearson syndrome, ring 14 syndrome, or Fanconi anemia. Epigenetic disorders occur from improper regulation of genes, such as imprinting syndromes. Environmental ailments are caused

by outside forces, such as a skin burn caused by boiling water. But most disorders do not fall neatly into one of these three categories.

The vast majority of disorders affecting the human population have genetic, epigenetic, and environmental predispositions. For example, identical twins are often discordant for complex diseases such as schizophrenia, type II diabetes, or autism (*193*). Between monozygotic twins, the difference in phenotype cannot be genetic so must be caused by the different environments the twins' cells have experienced as they aged and the resulting changes in epigenetics and cellular behavior. Additionally, many complex disorders manifest at late ages: early-twenties for bipolar disorder, mid-seventies for Alzheimer's disease. Stochastic epigenetic and environmental events that occur over decades of life can profoundly affect cellular function, creating a permissive backdrop upon which disease phenotypes can be expressed (*194*).

During reprogramming of somatic cells to pluripotency, epigenetic histories are erased and standard tissue culture conditions normalize all environmental differences. Of the genetic, environmental, and epigenetic variation that leads to complex disease, the only source of variation likely to be faithfully maintained in iPS cell lines is the genetic variation. In order to create a complete *in vitro* model of complex disorders, scientists must find a way to induce the epigenetic and environmental factors in their system.

In a notable attempt to induce complex disease phenotypes by mimicking aged cells, researchers from the Sloan-Kettering Institute recently overexpressed a truncated version of the gene *LMNA* in fibroblasts and neurons (*195*). This mutant protein, known as PROGERIN, is responsible for the aging syndrome progeria. The researchers noted that after *PROGERIN* expression, cell nuclei, gene expression, and methylation markers were similar to those seen in cells from elderly individuals, so they wondered whether this "aged" cellular backdrop could

allow complex disease phenotypes to manifest. They found that in cells receiving PROGERIN, but not cells receiving GFP, genetic mutations associated with Parkinson's disease caused appreciable cellular PD phenotypes. These included reduced dendrite length and a dramatic reduction in the number of tyrosine hydroxylase positive cells produced *in vivo*. Although this paper did not perform any specific or measured manipulations of epigenetics or environmental stimuli to induce PD, it is a groundbreaking example of how manipulating the cellular environment can affect the penetrance of a genetic disease predisposition.

To model a complex disorder even more accurately, researchers should induce the specific epigenetic and environmental events that lead to expression of the disease phenotype. For example, in Barrett's esophagus, exposure to acidic pH induces esophogeal cells to take on characteristics of the lower gut. Genetic predisposition, gene regulation, and acid exposure all contribute to the appearance of Barrett's esophagus (heritability is estimated at 0.35) (*196*). A reprogramming-based model of this condition would start by differentiating patient-specific iPS cells into esophogeal cells, and then model the disease by exposing them to repeated bouts of acid. In this case the genetic component would include the individual's predisposition to metaplasia, and the cells' epigenomes would reflect the previous acid exposures. Finally, duration and intensity of the acidic solution would affect severity of the resulting phenotype. A reprogramming-based model of Barrett's esophagus would need to take all three of these factors into account in order to reproduce a physiologically accurate *in vitro* model. This leads to a well-controlled triad experimental model: as long as two of the three variables are held constant, the third can be manipulated to test hypotheses about metaplasia and the disease mechanism. These types of experiments will provide a much-needed tool to investigate the effects of epigenetic manipulations on cellular disease states. They will also be useful for teasing apart

genotype by environment or genotype by epigenome effects, because the behavior of cells with various genetic backgrounds can be directly compared.

Our recent appreciation for the plasticity of cellular identity makes this area one of the most exciting topics in modern biology. Dr. Yamanaka's seminal publication has compelled a new and creative open-mindedness about cellular identity, and paved the way for the development of iPS cell-based disease models, drug screens, and transplantation. Full realization of the promise of cellular therapies is still on the horizon, but use of reprogramming technology for disease modeling and drug testing has already begun to show us the possibilities.

Conclusion

Medical genetics has advanced to the point where Pearson syndrome, ring 14 syndrome, and Fanconi anemia are likely to be diagnosed at a young age. An accurate diagnosis is a blessing to families, as it gives them information about their child's probable future and allows them to reach out to other families for support. But along with these diagnoses comes bad news: their child's disease has no treatment.

Our laboratory's long-term goal is to create models that reveal disease mechanisms and suggest novel therapeutic approaches to rare genetic disorders. In this dissertation, we describe work towards this goal for three diseases. We generated the iPS cells that carry a mtDNA deletion and identified a pathognomonic signature of Pearson syndrome in erythroid progenitors bearing the mutation. For the same child, we also derived a patient-specific iPS line that was completely free of disease, a technique that could be used in the future to create cells for transplantation. In ring 14 syndrome, the inability to study the ring chromosome in neurons has

been an insurmountable hurdle for researchers. We reprogrammed cells from patients with ring chromosome 14 and differentiated the resulting iPS cells down a neuronal pathway. The resulting cells are the first neural cells from a ring 14 patient available for investigation. Even better, since they come from a pluripotent stem cell line, more neural cells can be generated at will. Finally, we reprogrammed mouse and human Fanconi anemia cells using non-integrating methods. The secondary FA mouse cells reprogrammed nearly as well as the WT cells, and our human sample reprogrammed easily with episomes. These surprisingly robust findings lead us to believe that the FA pathway is not as indispensible to the reprogramming process as we had hypothesized, and suggest more experiments to investigate how FA cells respond to viral infection.

All of this work has taken advantage of cellular identity changes. By providing exogenous transcription factors and manipulating the environmental conditions, we have been able to generate pluripotent cells and direct their differentiation into hematopoietic and neuronal lineages. Dr. Yamanaka's breakthrough paper was published less than ten years ago, and its rewards have already been rich. In the next ten years, hopefully it will bear fruit for the families expectantly waiting on new treatment approaches and therapeutics.

Appendix: mRNA Transfection

Reprogramming can be accomplished by many approaches. Early publications used retroviruses, which quickly gave way to more versatile lentiviral vectors (*197-199*). But both of these systems shared a fatal flaw: the reprogramming factors integrated into the host genome. Low titer lentiviral systems with floxed monovector cassettes came close to resolving this issue by removing the transcription factors, but they still left behind a genetic scar (*200, 201*). Such a scar is unlikely to be approved for clinical-grade cells, so much work has gone into finding other reprogramming methods that do not involve permanent genetic modification.

Laboratories have reprogrammed cells using protein transfection, mRNA transfection, episomal expression, and forms of non-integrating viruses such as AAV and Sendai (*202-211*). Multiple laboratories have reported partial success using chemicals to supplement the reprogramming process, and a few recent papers report that cellular stress can reprogram cells under rare circumstances (*191, 192, 212, 213*).

At the time that our *FANCC*-/- secondary reprogramming mouse system was in development, reprogramming via mRNA transfection had just been published. The reported efficiency was an astoundingly high 4%. We suspected that the Fanconi reprogramming defect was not an absolute barrier, but rather one of efficiency, so we were quite interested in utilizing the mRNA reprogramming platform to investigate the FA reprogramming defect.

In order to obtain such high efficiencies, Dr. Derek Rossi's group had optimized a very complex protocol. The mRNA was *in vitro* transcribed with multiple modifications to prevent activating the cellular immune response, and then transfected into the reprogramming cells for four hours each day (*202*). Anticipating *FANCC*-/- reprogramming experiments, we set out to

design and create a modified mRNA encoding a rescue copy of *FANCC*. We began with the human *FANCC* ORF, and added a Kozak sequence immediately 5' of its translational start site, along with 5' and 3' UTR sequence, and then cloned this construct into a plasmid. To generate the DNA sequence of the complete mRNA (5' UTR, Kozak, ORF, 3' UTR, and poly-A tail), we performed PCR off of the template using a primer encoding a poly-A tail. This template was then used for *in vitro* transcription, including 5-methyl cytidine and pseudouridine as described in Warren et al. for reduced immune reaction.

The one part of an mRNA transcript that cannot easily be added is the 5' guanine cap. This cap is a specially-modified guanine base, and has to be encoded into the RNA during transcription. In order to make sure that some of the resulting mRNA molecules carried the 5' cap, we included these di-guanosine cap analogs at a 4:1 ratio with normal guanine in the transcription mix. The analogs cannot be incorporated into a growing mRNA chain, so guanine was the limiting reagent for mRNA synthesis (*214*). The 4:1 ratio ensured that about 80% of the resulting mRNA molecules carried a 5' cap. The resulting mix of mRNA was treated with a phosphotase to remove the 20% of free 5' phosphates, as these can cause immune response in the cells (*202*).

We obtained late-passage Fanconi patient fibroblasts from a cell repository to test whether our new *FANCC* mRNA could rescue the Fanconi pathway in human cells. When the FA pathway is active, the FANCD2 protein becomes ubiquitinated. On western blots, it appears as a heavier band, called FANCD2-L. Upon addition of hydroxyurea, in WT cells the FA pathway is activated and so the long:short ratio increases. We transfected the *FANCC* mRNA into *FANCC*-/- human fibroblasts daily and exposed some of the cells to hydroxyurea. As seen

in Figure App.1, transfection of the *FANCC* mRNA effectively rescued activity of the FA pathway in human Fanconi anemia cells.

In the paper published by the Rossi group, a constant amount of reprogramming mRNA was transfected daily, while the number of cells grew exponentially. At the time, it was not known how the ratio of mRNA micrograms to cell number affected transfection. On one hand, it could be that all mRNA molecules always entered the cells, such that any variation in cell number would strongly affect the number of mRNA molecules received by each cell. On the other, it could be that mRNA molecules were present in such excess that the cell number was irrelevant to the per-cell dosage—or anywhere in between these two extremes. We set out to quantify this phenomenon.

Fibroblasts were plated at four different densities and transfected with various amounts of *in vitro* transcribed, low-immunogenic mRNA coding for GFP. FACS analysis was used to measure mean fluorescence intensity (MFI; a proxy for the number of GFP mRNA molecules received by the cell), the raw number of GFP positive cells, and the percentage of cells that were GFP positive (Figure App.2).

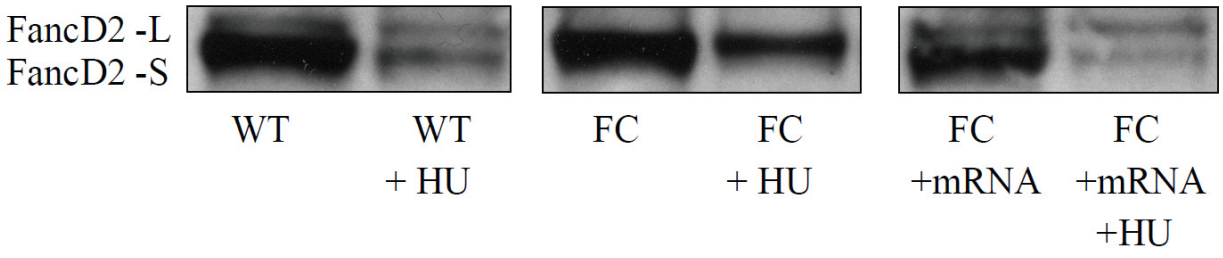

Figure App.1: Western blot showing mRNA functional correction of FA pathway. Each panel is a condition, with or without addition of hydroxyurea (HU). FANCC knockout cells (FC) do not have the long form of FANCD2. FANCC knockout cells plus the FANCC mRNA show the long form.

Larger quantities of mRNA resulted in more mRNA molecules per cell and more cells transfected (Figure App.2 A and B). Surprisingly, at the highest cell density, 160 ng mRNA was required to achieve the same percentage GFP positive cells as the lowest density shows with 20 ng mRNA (Figure App.2 C). This suggests that the percentage of cells that receive mRNA per RNA nanogram decreases strongly with increasing cell numbers (Figure App.2 D).

Interestingly, at any given level of RNA input, higher numbers of cells result in lower MFI (Figure App.2 E). This demonstrates that higher cellular densities cause each cell to receive fewer copies of the mRNA molecule. Finally, we also observed that at the lowest amount of RNA, there was no difference in the number of GFP positive cells between densities: 20 ng of RNA causes about 20,000 cells to become fluorescent, and no more (Figure App.2 F). This suggests that 1,000 cells is the upper limit of the number of cells that can become fluorescent from 1 nanogram of mRNA.

Our conclusion from this analysis is that the amount of mRNA received by a cell varies greatly depending on the cell density. Thus, in order to maintain a constant level of mRNA transfection during reprogramming, the total amount of mRNA added should increase with cell numbers.

In addition to transfection of mRNA into fibroblasts, we investigated transfection of modified mRNA into human pluripotent cells. Specifically, we wondered whether mRNA transfection would be more efficient in iPS cells grown on murine feeder cells or cultured on matrigel. We transfected human iPS cells with varying amounts of modified GFP mRNA, as described above. As can be seen in Figure App.3, iPS cells grown on matrigel proved to be far easier to transfect than those grown on MEFs.

Figure App.2, on following page: Characterization of cell density effect on mRNA transfection. (A) Effect of increasing mRNA concentrations on mean fluorescence intensity (proxy for mRNA copies per cell). (B) Effect of increasing mRNA concentrations on percentage of transfected cells. (C) Effect of cell density on percentage of transfected cells. (D) Effect of cell density on "bang for your buck," the percentage fluorescent cells acquired per ng of mRNA. (E) Inverse relationship of cell density and mean fluorescence intensity, regardless of mRNA concentration. (F) Effect of cell density on the absolute number of transfected cells.

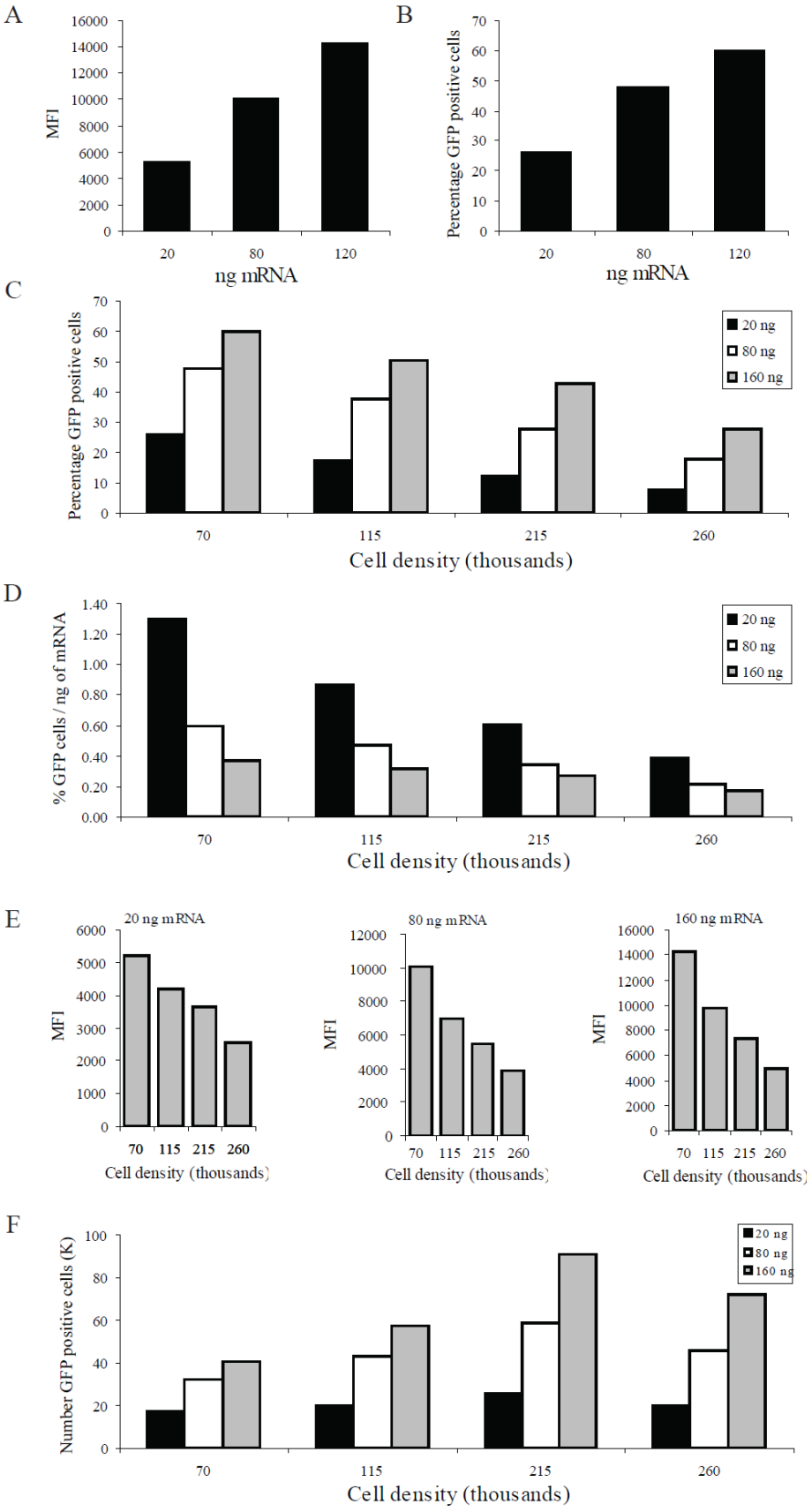

Figure App.2: Characterization of cell density effect on mRNA transfection (Continued)

We attempted to reprogram cells using mRNA multiple times. Unfortunately, our laboratory and many others found the procedure highly variable. Multiple crucial reagents were subject to inter-lot variability, and shortage of key components of the *in vitro* transcription reaction cut short reprogramming attempts. Our laboratory and the Boston Children's Hospital stem cell core have since concluded that mRNA is a hit-or-miss reprogramming method: about one in three tries is highly successful, but two out of three attempts fail entirely. Given the variable reprogramming efficiency inherent in this approach, we decided it was not a good system for pursuing investigations of Fanconi reprogramming efficiency.

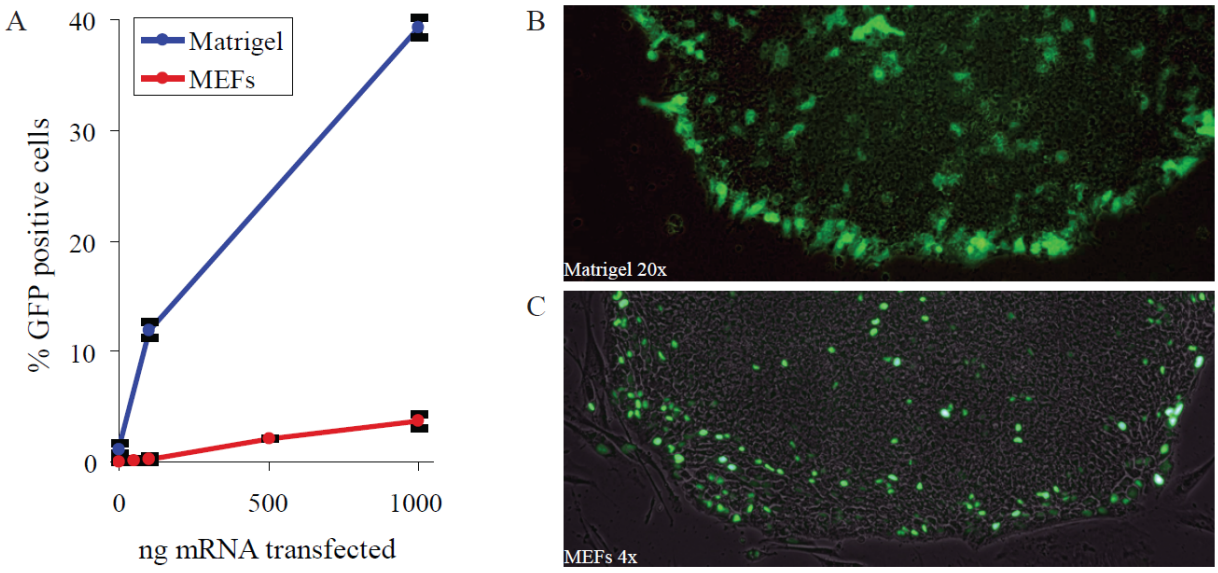

Figure App.3: Transfection of mRNA into human iPS colonies. (A) Comparison of mRNA transfection into iPS cells grown on matrigel and MEFs. (B) Combined brightfield and fluorescent image of 1 ug of GFP mRNA transfected into iPS cells grown on Matrigel. (C) Combined brightfield and fluorescent image of 1 ug of GFP mRNA transfected into iPS cells grown on MEFs.

Citations

1. J. A. Thomson, J. Itskovitz-Eldor, S. S. Shapiro, M. A. Waknitz, J. J. Swiergiel, V. S. Marshall, J. M. Jones, *Embryonic stem cell lines derived from human blastocysts*. **Science** 282, 1145. (Nov, 1998).

2. H. Gottweis, B. Prainsack, *Emotion in political discourse: contrasting approaches to stem cell governance in the USA, UK, Israel and Germany*. **Regenerative Medicine** 1, 823. (Nov, 2006).

3. K. Takahashi, S. Yamanaka, *Induction of pluripotent stem cells from mouse embryonic and adult fibroblast cultures by defined factors*. **Cell** 126, 663. (Aug, 2006).

4. R. L. Davis, H. Weintraub, A. B. Lassar, *Expression of a single transfected cDNA converts fibroblasts to myoblasts* **Cell** 51, 987. (Dec, 1987).

5. M. Wernig, A. Meissner, R. Foreman, T. Brambrink, M. C. Ku, K. Hochedlinger, B. E. Bernstein, R. Jaenisch, *In vitro reprogramming of fibroblasts into a pluripotent ES-cell-like state*. **Nature** 448, 318. (Jul, 2007).

6. K. Okita, T. Ichisaka, S. Yamanaka, *Generation of germline-competent induced pluripotent stem cells*. **Nature** 448, 313. (Jul, 2007).

7. X. Y. Zhao, W. Li, Z. Lv, L. Liu, M. Tong, T. Hai, J. Hao, C. L. Guo, Q. W. Ma, L. Wang, F. Y. Zeng, Q. Zhou, *iPS cells produce viable mice through tetraploid complementation*. **Nature** 461, 86. (Sep, 2009).

8. M. J. Boland, J. L. Hazen, K. L. Nazor, A. R. Rodriguez, W. Gifford, G. Martin, S. Kupriyanov, K. K. Baldwin, *Adult mice generated from induced pluripotent stem cells*. **Nature** 461, 91. (Sep, 2009).

9. J. T. Dimos, K. T. Rodolfa, K. K. Niakan, L. M. Weisenthal, H. Mitsumoto, W. Chung, G. F. Croft, G. Saphier, R. Leibel, R. Goland, H. Wichterle, C. E. Henderson, K. Eggan, *Induced pluripotent stem cells generated from patients with ALS can be differentiated into motor neurons*. **Science** 321, 1218. (Aug, 2008).

10. I. H. Park, N. Arora, H. Huo, N. Maherali, T. Ahfeldt, A. Shimamura, M. W. Lensch, C. Cowan, K. Hochedlinger, G. Q. Daley, *Disease-specific induced pluripotent stem cells*. **Cell** 134, 877. (Sep, 2008).

11. K. Takahashi, K. Tanabe, M. Ohnuki, M. Narita, T. Ichisaka, K. Tomoda, S. Yamanaka, *Induction of pluripotent stem cells from adult human fibroblasts by defined factors*. **Cell** 131, 861. (Nov, 2007).

12. K. R. Denton, L. Lei, J. Grenier, V. Rodionov, C. Blackstone, X. J. Li, *Loss of Spastin Function Results in Disease-Specific Axonal Defects in Human Pluripotent Stem Cell-Based Models of Hereditary Spastic Paraplegia*. **Stem Cells** 32, 414. (Feb, 2014).

13. I. H. Park, P. H. Lerou, R. Zhao, H. G. Huo, G. Q. Daley, *Generation of human-induced pluripotent stem cells*. **Nature Protocols** 3, 1180. (2008).

14. K. McNagny, T. Graf, *Making eosinophils through subtle shifts in transcription factor expression*. **Journal of Experimental Medicine** 195, f43. (Jun, 2002).

15. S. L. Nutt, B. Heavey, A. G. Rolink, M. Busslinger, *Commitment to the B-lymphoid lineage depends on the transcription factor Pax5*. **Nature** 401, 556. (Oct, 1999).

16. K. Kim, A. Doi, B. Wen, K. Ng, R. Zhao, P. Cahan, J. Kim, M. J. Aryee, H. Ji, L. I. R. Ehrlich, A. Yabuuchi, A. Takeuchi, K. C. Cunniff, H. Hongguang, S. McKinney-Freeman, O. Naveiras, T. J. Yoon, R. A. Irizarry, N. Jung, J. Seita, J. Hanna, P. Murakami, R. Jaenisch, R. Weissleder, S. H. Orkin, I. L. Weissman, A. P. Feinberg, G. Q. Daley, *Epigenetic memory in induced pluripotent stem cells*. **Nature** 467, 285. (Sep, 2010).

17. A. Doi, I. H. Park, B. Wen, P. Murakami, M. J. Aryee, R. Irizarry, B. Herb, C. Ladd-Acosta, J. S. Rho, S. Loewer, J. Miller, T. Schlaeger, G. Q. Daley, A. P. Feinberg, *Differential methylation of tissue- and cancer-specific CpG island shores distinguishes human induced pluripotent stem cells, embryonic stem cells and fibroblasts*. **Nature Genetics** 41, 1350. (Dec, 2009).

18. J. M. Polo, S. Liu, M. E. Figueroa, W. Kulalert, S. Eminli, K. Y. Tan, E. Apostolou, M. Stadtfeld, Y. S. Li, T. Shioda, S. Natesan, A. J. Wagers, A. Melnick, T. Evans, K. Hochedlinger, *Cell type of origin influences the molecular and functional properties of mouse induced pluripotent stem cells*. **Nature Biotechnology** 28, 848. (Aug, 2010).

19. R. D. Hawkins, G. C. Hon, L. K. Lee, Q. Ngo, R. Lister, M. Pelizzola, L. E. Edsall, S. Kuan, Y. Luu, S. Klugman, J. Antosiewicz-Bourget, Z. Ye, C. Espinoza, S. Agarwahl, L. Shen, V. Ruotti, W. Wang, R. Stewart, J. A. Thomson, J. R. Ecker, B. Ren, *Distinct Epigenomic Landscapes of Pluripotent and Lineage-Committed Human Cells*. **Cell Stem Cell** 6, 479. (May, 2010).

20. M. H. Chin, M. J. Mason, W. Xie, S. Volinia, M. Singer, C. Peterson, G. Ambartsumyan, O. Aimiuwu, L. Richter, J. Zhang, I. Khvorostov, V. Ott, M. Grunstein, N. Lavon, N. Benvenisty, C. M. Croce, A. T. Clark, T. Baxter, A. D. Pyle, M. A. Teitell, M. Pelegrini, K. Plath, W. E. Lowry, *Induced Pluripotent Stem Cells and Embryonic Stem Cells Are Distinguished by Gene Expression Signatures*. **Cell Stem Cell** 5, 111. (Jul, 2009).

21. M. G. Guenther, G. M. Frampton, F. Soldner, D. Hockemeyer, M. Mitalipova, R. Jaenisch, R. A. Young, *Chromatin Structure and Gene Expression Programs of Human Embryonic and Induced Pluripotent Stem Cells*. **Cell Stem Cell** 7, 249. (Aug, 2010).

22. M. Alikani, S. Munne, *Nonviable human pre-implantation embryos as a source of stem cells for research and potential therapy*. **Stem Cell Reviews** 1, 337. (2005).

23. P. Tropel, J. Tournois, J. Come, C. Varela, C. Moutou, P. Fragner, M. Cailleret, Y. Laabi, M. Peschanski, S. Viville, *High-efficiency derivation of human embryonic stem cell lines following pre-implantation genetic diagnosis*. **In Vitro Cellular & Developmental Biology-Animal** 46, 376. (Apr, 2010).

24. R. Siller, S. Greenhough, I. H. Park, G. J. Sullivan, *Modelling Human Disease with Pluripotent Stem Cells*. **Curr. Gene Ther.** 13, 99. (Apr, 2013).

25. S. Nishikawa, R. A. Goldstein, C. R. Nierras, *The promise of human induced pluripotent stem cells for research and therapy*. **Nature Reviews Molecular Cell Biology** 9, 725. (Sep, 2008).

26. P. H. Lerou, G. Q. Daley, *Therapeutic potential of embryonic stem cells*. **Blood Reviews** 19, 321. (Nov, 2005).

27. A. B. C. Cherry, G. Q. Daley, *Reprogrammed Cells for Disease Modeling and Regenerative Medicine*. **Annu. Rev. Med.** 64, 277. (2013).

28. M. W. Kalichman, P. H. Schwartz, *Guidelines for Embryonic Stem Cell Research Oversight (ESCRO) Committees*. **Human Stem Cell Manual: A Laboratory Guide**, 437. (2007).

29. Y. Heled, *On presidents, agencies, and the stem cells between them: A legal analysis of president Bush's and the federal government's policy on the funding of research involving human embryonic stem cells*. **Adm. Law Rev.** 60, 65. (Win, 2008).

30. A. B. C. Cherry, G. Q. Daley, *Reprogramming Cellular Identity for Regenerative Medicine*. **Cell** 148, 1110. (Mar, 2012).

31. W. Q. Zhang, J. Qu, K. Suzuki, G. H. Liu, J. C. I. Belmonte, *Concealing cellular defects in pluripotent stem cells*. **Trends in Cell Biology** 23, 587. (Dec, 2013).

32. S. Agarwal, Y. H. Loh, E. M. McLoughlin, J. J. Huang, I. H. Park, J. D. Miller, H. G. Huo, M. Okuka, R. M. dos Reis, S. Loewer, H. H. Ng, D. L. Keefe, F. D. Goldman, A. J. Klingelhutz, L. Liu, G. Q. Daley, *Telomere elongation in induced pluripotent stem cells from dyskeratosis congenita patients*. **Nature** 464, 292. (Mar, 2010).

33. M. F. Burkhardt, F. J. Martinez, S. Wright, C. Ramos, D. Volfson, M. Mason, J. Garnes, V. Dang, J. Lievers, U. Shoukat-Mumtaz, R. Martinez, H. Gai, R. Blake, E. Vaisberg, M. Grskovic, C. Johnson, S. Irion, J. Bright, B. Cooper, L. Nguyen, I. Griswold-Prenner, A. Javaherian, *A cellular model for sporadic ALS using patient-derived induced pluripotent stem cells*. **Molecular and Cellular Neuroscience** 56, 355. (Sep, 2013).

34. P. Seibler, J. Graziotto, H. Jeong, F. Simunovic, C. Klein, D. Krainc, *Mitochondrial Parkin Recruitment Is Impaired in Neurons Derived from Mutant PINK1 Induced Pluripotent Stem Cells*. **J Neurosci** 31, 5970. (2011).

35. M. A. Israel, S. H. Yuan, C. Bardy, S. M. Reyna, Y. L. Mu, C. Herrera, M. P. Hefferan, S. Van Gorp, K. L. Nazor, F. S. Boscolo, C. T. Carson, L. C. Laurent, M. Marsala, F. H. Gage, A. M. Remes, E. H. Koo, L. S. B. Goldstein, *Probing sporadic and familial Alzheimer's disease using induced pluripotent stem cells*. **Nature** 482, 216. (Feb, 2012).

36. A. Tulpule, J. M. Kelley, M. W. Lensch, J. McPherson, I. H. Park, O. Hartung, T. Nakamura, T. M. Schlaeger, A. Shimamura, G. Q. Daley, *Pluripotent stem cell models of Shwachman-Diamond syndrome reveal a common mechanism for pancreatic and hematopoietic dysfunction*. **Cell Stem Cell** 12, 727. (Jun 6, 2013).

37. G. A. MacLean, T. F. Menne, G. J. Guo, D. J. Sanchez, I. H. Park, G. Q. Daley, S. H. Orkin, *Altered hematopoiesis in trisomy 21 as revealed through in vitro differentiation of isogenic human pluripotent cells*. **Proceedings of the National Academy of Sciences of the United States of America** 109, 17567. (Oct, 2012).

38. A. Nasu, M. Ikeya, T. Yamamoto, A. Watanabe, Y. H. Jin, Y. Matsumoto, K. Hayakawa, N. Amano, S. Sato, K. Osafune, T. Aoyama, T. Nakamura, T. Kato, J. Toguchida, *Genetically Matched Human iPS Cells Reveal that Propensity for Cartilage and Bone Differentiation Differs with Clones, not Cell Type of Origin*. **PLoS One** 8. (Jan, 2013).

39. K. D. Choi, J. Yu, K. Smuga-Otto, G. Salvagiotto, W. Rehrauer, M. Vodyanik, J. Thomson, I. Slukvin, *Hematopoietic and Endothelial Differentiation of Human Induced Pluripotent Stem Cells*. **Stem Cells** 27, 559. (2009).

40. J. A. Mills, K. Wang, P. Paluru, L. Ying, L. Lu, A. M. Galvao, D. B. Xu, Y. Yao, S. K. Sullivan, L. M. Sullivan, H. Mac, A. Omari, J. C. Jean, S. Shen, A. Gower, A. Spira, G. Mostoslavsky, D. N. Kotton, D. L. French, M. J. Weiss, P. Gadue, *Clonal genetic and hematopoietic heterogeneity among human-induced pluripotent stem cell lines*. **Blood** 122, 2047. (Sep, 2013).

41. P. R. G. Zen, F. N. d. Moraes, R. F. M. Rosa, C. Graziadio, G. A. Paskulin, *Características clínicas de pacientes com anemia de Fanconi*. **Revista Paulista de Pediatria** 29, 392. (2011).

42. M. Zollino, E. Ponzi, G. Gobbi, G. Neri, *The ring 14 syndrome*. **Eur. J. Med. Genet.** 55, 374. (May, 2012).

43. H. T. Hogberg, J. Bressler, K. M. Christian, G. Harris, G. Makri, C. O'Driscoll, D. Pamies, L. Smirnova, Z. X. Wen, T. Hartung, *Toward a 3D model of human brain development for studying gene/environment interactions*. **Stem Cell Res. Ther.** 4. (Dec, 2013).

44. J. H. Zhang, G. F. Wilson, A. G. Soerens, C. H. Koonce, J. Y. Yu, S. P. Palecek, J. A. Thomson, T. J. Kamp, *Functional Cardiomyocytes Derived From Human Induced Pluripotent Stem Cells*. **Circulation Research** 104, E30. (Feb, 2009).

45. F. Zanella, R. C. Lyon, F. Sheikh, *Modeling heart disease in a dish: From somatic cells to disease-relevant cardiomyocytes*. **Trends in Cardiovascular Medicine** 24, 32. (Jan, 2014).

46. D. W. Zhang, M. Pekkanen-Mattila, M. O. Shahsavani, A. Falk, A. I. Teixeira, A. Herland, *A 3D Alzheimer's disease culture model and the induction of P21-activated kinase mediated sensing in iPSC derived neurons*. **Biomaterials** 35, 1420. (Feb, 2014).

47. L. Adamo, O. Naveiras, P. L. Wenzel, S. McKinney-Freeman, P. J. Mack, J. Gracia-Sancho, A. Suchy-Dicey, M. Yoshimoto, M. W. Lensch, M. C. Yoder, G. Garcia-Cardena, G. Q. Daley, *Biomechanical forces promote embryonic haematopoiesis*. **Nature** 459, 1131. (Jun, 2009).

48. E. Kroon, L. A. Martinson, K. Kadoya, A. G. Bang, O. G. Kelly, S. Eliazer, H. Young, M. Richardson, N. G. Smart, J. Cunningham, A. D. Agulnick, K. A. D'Amour, M. K. Carpenter, E. E. Baetge, *Pancreatic endoderm derived from human embryonic stem cells generates glucose-responsive insulin-secreting cells in vivo*. **Nature Biotechnology** 26, 443. (Apr, 2008).

49. D. H. Zhang, W. Jiang, M. Liu, X. Sui, X. L. Yin, S. Chen, Y. Shi, H. K. Deng, *Highly efficient differentiation of human ES cells and iPS cells into mature pancreatic insulin-producing cells*. **Cell Research** 19, 429. (Apr, 2009).

50. K. J. Brennand, *Inducing Cellular Aging: Enabling Neurodegeneration-in-a-Dish*. **Cell Stem Cell** 13, 635. (Dec, 2013).

51. C. Y. Ivashchenko, G. C. Pipes, I. M. Lozinskaya, Z. J. Lin, X. P. Xu, S. Needle, E. T. Grygielko, E. D. Hu, J. R. Toomey, J. J. Lepore, R. N. Willette, *Human-induced pluripotent stem cell-derived cardiomyocytes exhibit temporal changes in phenotype*. **American Journal of Physiology-Heart and Circulatory Physiology** 305, H913. (Sep, 2013).

52. J. Mariani, M. V. Simonini, D. Palejev, L. Tomasini, G. Coppola, A. M. Szekely, T. L. Horvath, F. M. Vaccarino, *Modeling human cortical development in vitro using induced pluripotent stem cells*. **Proceedings of the National Academy of Sciences of the United States of America** 109, 12770. (Jul, 2012).

53. D. X. Zhao, S. Chen, S. G. Duo, C. G. Xiang, J. Jia, M. N. Guo, W. Lai, S. C. Lu, H. K. Deng, *Promotion of the efficient metabolic maturation of human pluripotent stem cell-derived hepatocytes by correcting specification defects*. **Cell Research** 23, 157. (Jan, 2013).

54. M. Ieda, J. D. Fu, P. Delgado-Olguin, V. Vedantham, Y. Hayashi, B. G. Bruneau, D. Srivastava, *Direct Reprogramming of Fibroblasts into Functional Cardiomyocytes by Defined Factors*. **Cell** 142, 375. (Aug, 2010).

55. L. Qian, Y. Huang, C. I. Spencer, A. Foley, V. Vedantham, L. Liu, S. J. Conway, J. D. Fu, D. Srivastava, *In vivo reprogramming of murine cardiac fibroblasts into induced cardiomyocytes*. **Nature** 485, 593. (May, 2012).

56. K. H. Song, Y. J. Nam, X. Luo, X. X. Qi, W. Tan, G. N. Huang, A. Acharya, C. L. Smith, M. D. Tallquist, E. G. Neilson, J. A. Hill, R. Bassel-Duby, E. N. Olson, *Heart repair by reprogramming non-myocytes with cardiac transcription factors*. **Nature** 485, 599. (May, 2012).

57. W. F. Lim, T. Inoue-Yokoo, K. S. Tan, M. I. Lai, D. Sugiyama, *Hematopoietic cell differentiation from embryonic and induced pluripotent stem cells*. **Stem Cell Res. Ther.** 4. (Jun, 2013).

58. A. Moretti, M. Bellin, A. Welling, C. B. Jung, J. T. Lam, L. Bott-Flugel, T. Dorn, A. Goedel, C. Hohnke, F. Hofmann, M. Seyfarth, D. Sinnecker, A. Schomig, K. L. Laugwitz, *Patient-Specific Induced Pluripotent Stem-Cell Models for Long-QT Syndrome*. **New England Journal of Medicine** 363, 1397. (Oct, 2010).

59. I. Itzhaki, L. Maizels, I. Huber, L. Zwi-Dantsis, O. Caspi, A. Winterstern, O. Feldman, A. Gepstein, G. Arbel, H. Hammerman, M. Boulos, L. Gepstein, *Modelling the long QT syndrome with induced pluripotent stem cells*. **Nature** 471, 225. (Mar, 2011).

60. L. M. Panicker, D. Miller, T. S. Park, B. Patel, J. L. Azevedo, O. Awad, M. A. Masood, T. D. Veenstra, E. Goldin, B. K. Stubblefield, N. Tayebi, S. K. Polumuri, S. N. Vogel, E. Sidransky, E. T. Zambidis, R. A. Feldman, *Induced pluripotent stem cell model recapitulates pathologic hallmarks of Gaucher disease*. **Proceedings of the National Academy of Sciences of the United States of America** 109, 18054. (Oct, 2012).

61. R. Maehr, S. B. Chen, M. Snitow, T. Ludwig, L. Yagasaki, R. Goland, R. L. Leibel, D. A. Melton, *Generation of pluripotent stem cells from patients with type 1 diabetes*. **Proceedings of the National Academy of Sciences of the United States of America** 106, 15768. (Sep, 2009).

62. P. McGonigle, B. Ruggeri, *Animal models of human disease: Challenges in enabling translation*. **Biochemical Pharmacology** 87, 162. (Jan, 2014).

63. A. Mathur, P. Loskill, S. Hong, J. Y. Lee, S. G. Marcus, L. Dumont, B. R. Conklin, H. Willenbring, L. P. Lee, K. E. Healy, *Human induced pluripotent stem cell-based microphysiological tissue models of myocardium and liver for drug development*. **Stem Cell Res. Ther.** 4. (Dec, 2013).

64. K. Yoshizato, C. Tateno, *A mouse with humanized liver as an animal model for predicting drug effects and for studying hepatic viral infection: where to next?* **Expert Opinion on Drug Metabolism & Toxicology** 9, 1419. (Nov, 2013).

65. M. Z. Chow, K. R. Boheler, R. A. Li, *Human pluripotent stem cell-derived cardiomyocytes for heart regeneration, drug discovery and disease modeling: from the genetic, epigenetic, and tissue modeling perspectives*. **Stem Cell Res. Ther.** 4. (Aug, 2013).

66. R. Stoner, M. L. Chow, M. P. Boyle, S. M. Sunkin, P. R. Mouton, S. Roy, A. Wynshaw-Boris, S. A. Colamarino, E. S. Lein, E. Courchesne, *Patches of disorganization in the neocortex of children with autism*. **N Engl J Med** 370, 1209. (Mar 27, 2014).

67. E. D. Thomas, H. L. Lochte, Jr., J. H. Cannon, O. D. Sahler, J. W. Ferrebee, *Supralethal whole body irradiation and isologous marrow transplantation in man*. **J Clin Invest** 38, 1709. (Oct, 1959).

68. E. Thomas, R. Storb, R. A. Clift, A. Fefer, F. L. Johnson, P. E. Neiman, K. G. Lerner, H. Glucksberg, C. D. Buckner, *Bone-marrow transplantation (first of two parts)*. **N Engl J Med** 292, 832. (Apr 17, 1975).

69. E. D. Thomas, R. Storb, R. A. Clift, A. Fefer, L. Johnson, P. E. Neiman, K. G. Lerner, H. Glucksberg, C. D. Buckner, *Bone-marrow transplantation (second of two parts)*. **N Engl J Med** 292, 895. (Apr 24, 1975).

70. E. A. Copelan, *Medical progress: Hematopoietic stem-cell transplantation*. **New England Journal of Medicine** 354, 1813. (Apr, 2006).

71. R. Martino, S. Iacobelli, R. Brand, T. Jansen, A. van Biezen, J. Finke, A. Bacigalupo, D. Beelen, J. Reiffers, A. Devergie, E. Alessandrino, G. J. Mufti, R. Barge, J. Sierra, T. Ruutu, M. Boogaerts, M. Falda, J. P. Jouet, D. Niederwieser, T. de Witte, s. Myelodysplastic Syndrome, *Retrospective comparison of reduced-intensity conditioning and conventional high-dose conditioning for allogeneic hematopoietic stem cell transplantation using BLA-identical sibling donors in myelodysplastic syndromes*. **Blood** 108, 836. (Aug, 2006).

72. M. Goerner, T. Gooley, M. E. D. Flowers, K. M. Sullivan, H. P. Kiem, J. E. Sanders, P. J. Martin, R. Storb, *Morbidity and mortality of chronic GVHD after hematopoietic stem cell transplantation from HLA-identical siblings for patients with aplastic or refractory anemias*. **Biology of Blood and Marrow Transplantation** 8, 47. (2002).

73. M. Stern, J. R. Passweg, A. Locasciulli, G. Socie, H. Schrezenmeier, A. N. Bekassy, M. Fuehrer, J. Hows, E. T. Korthof, S. McCann, A. Tichelli, N. C. Zoumbos, J. C. W. Marsh, A. Bacigalupo, A. Gratwohl, T. European Grp Blood Marrow, *Influence of donor/recipient sex matching on outcome of allogeneic hematopoietic stem cell transplantation for aplastic anemia*. **Transplantation** 82, 218. (Jul, 2006).

74. L. Y. Bai, T. J. Chiou, J. H. Liu, C. C. Yen, W. S. Wang, M. H. Yan, L. T. Hsiao, T. C. Chao, P. M. Chen, *Hematopoietic stem cell transplantation for severe aplastic anemia - experience of an institute in Taiwan*. **Annals of Hematology** 83, 38. (Jan, 2004).

75. S. Maury, A. Bacigalupo, P. Anderlini, M. Aljurf, J. Marsh, G. Socie, R. Oneto, J. R. Passweg, B. European Grp, T. Marrow, *Improved outcome of patients older than 30 years receiving HLA-identical sibling hematopoietic stem cell transplantation for severe acquired aplastic anemia using fludarabine-based conditioning: a comparison with conventional conditioning regimen*. **Haematologica-the Hematology Journal** 94, 1312. (Sep, 2009).

76. A. Medvinsky, E. Dzierzak, *Definitive hematopoiesis is autonomously initiated by the AGM region*. **Cell** 86, 897. (Sep, 1996).

77. A. M. Muller, A. Medvinsky, J. Strouboulis, F. Grosveld, E. Dzierzak, *DEVELOPMENT OF HEMATOPOIETIC STEM-CELL ACTIVITY IN THE MOUSE EMBRYO*. **Immunity** 1, 291. (Jul, 1994).

78. M. J. Chen, T. Yokomizo, B. M. Zeigler, E. Dzierzak, N. A. Speck, *Runx1 is required for the endothelial to haematopoietic cell transition but not thereafter*. **Nature** 457, 887. (Feb, 2009).

79. J. Y. Bertrand, N. C. Chi, B. Santoso, S. T. Teng, D. Y. R. Stainier, D. Traver, *Haematopoietic stem cells derive directly from aortic endothelium during development*. **Nature** 464, 108. (Mar, 2010).

80. K. Kissa, P. Herbomel, *Blood stem cells emerge from aortic endothelium by a novel type of cell transition*. **Nature** 464, 112. (Mar, 2010).

81. P. Kumaravelu, L. Hook, A. M. Morrison, J. Ure, S. L. Zhao, S. Zuyev, J. Ansell, A. Medvinsky, *Quantitative developmental anatomy of definitive haematopoietic stem cells long-term repopulating units (HSC/RUs): role of the aorta-gonad-mesonephros (AGM) region and the yolk sac in colonisation of the mouse embryonic liver*. **Development** 129, 4891. (Nov, 2002).

82. C. Gekas, F. Dieterlen-Lievre, S. H. Orkin, H. K. A. Mikkola, *The placenta is a niche for hematopoietic stem cells*. **Developmental Cell** 8, 365. (Mar, 2005).

83. J. L. Christensen, D. E. Wright, A. J. Wagers, I. L. Weissman, *Circulation and chemotaxis of fetal hematopoietic stem cells*. **Plos Biology** 2, 368. (Mar, 2004).

84. M. H. Ledran, A. Krassowska, L. Armstrong, I. Dimmick, J. Renstrom, R. Lang, S. Yung, M. Santibanez-Coref, E. Dzierzak, M. Stojkovic, R. A. J. Oostendorp, L. Forrester, M. Lako, *Efficient hematopoietic differentiation of human embryonic stem cells on stromal cells derived from hematopoietic niches*. **Cell Stem Cell** 3, 85. (Jul, 2008).

85. E. S. Ng, R. P. Davis, L. Azzola, E. G. Stanley, A. G. Elefanty, *Forced aggregation of defined numbers of human embryonic stem cells into embryoid bodies fosters robust, reproducible hematopoietic differentiation*. **Blood** 106, 1601. (Sep, 2005).

86. S. Pilat, S. Carotta, B. Schiedlmeier, K. Kamino, A. Mairhofer, E. Will, U. Modlich, P. Steinlein, W. Ostertag, C. Baum, H. Beug, H. Klump, *HOXB4 enforces equivalent fates of ES-cell-derived and adult hematopoietic cells*. **Proceedings of the National Academy of Sciences of the United States of America** 102, 12101. (Aug, 2005).

87. L. S. Wang, P. Menendez, F. Shojaei, L. Li, F. Mazurier, J. E. Dick, C. Cerdan, K. Levac, M. Bhatia, *Generation of hematopoietic repopulating cells from human embryonic stem cells independent of ectopic HOXB4 expression*. **Journal of Experimental Medicine** 201, 1603. (May, 2005).

88. M. Kyba, R. C. R. Perlingeiro, G. Q. Daley, *HoxB4 confers definitive lymphoid-myeloid engraftment potential on embryonic stem cell and yolk sac hematopoietic progenitors*. **Cell** 109, 29. (Apr, 2002).

89. K. M. Bowles, L. Vallier, J. R. Smith, M. R. J. Alexander, R. A. Pedersen, *HOXB4 overexpression promotes hematopoietic development by human embryonic stem cells*. **Stem Cells** 24, 1359. (May, 2006).

90. J. F. Ji, K. Vijayaragavan, M. Bosse, K. Weisel, M. Bhatia, *OP9 Stroma Augments Survival of Hematopoietic Precursors and Progenitors During Hematopoietic Differentiation from Human Embryonic Stem Cells*. **Stem Cells** 26, 2485. (2008).

91. S. DiMauro, *Mitochondrial DNA medicine*. **Biosci. Rep.** 27, 5. (Jun, 2007).

92. L. I. Grossman, E. A. Shoubridge, *Mitochondrial genetics and human disease*. **Bioessays** 18, 983. (Dec, 1996).

93. E. A. Schon, *Mitochondrial genetics and disease*. **Trends in Biochemical Sciences** 25, 555. (Nov, 2000).

94. S. Navarro, V. Moleiro, F. J. Molina-Estevez, M. L. Lozano, R. Chinchon, E. Almarza, O. Quintana-Bustamante, G. Mostoslavsky, T. Maetzig, M. Galla, N. Heinz, B. Schiedlmeier, Y. Torres, U. Modlich, E. Samper, P. Rio, J. C. Segovia, A. Raya, G. Guenechea, J. C. Izpisua-Belmonte, J. A. Bueren, *Generation of iPSCs from Genetically Corrected Brca2 Hypomorphic Cells: Implications in Cell Reprogramming and Stem Cell Therapy*. **Stem Cells** 32, 436. (Feb, 2014).

95. R. H. Swerdlow, *Mitochondrial DNA-related mitochondrial dysfunction in neurodegenerative diseases*. **Archives of Pathology & Laboratory Medicine** 126, 271. (Mar, 2002).

96. P. F. Chinnery, M. A. Johnson, T. M. Wardell, R. Singh-Kler, C. Hayes, D. T. Brown, R. W. Taylor, L. A. Bindoff, D. M. Turnbull, *The epidemiology of pathogenic mitochondrial DNA mutations*. **Ann. Neurol.** 48, 188. (Aug, 2000).

97. L. Kobari, F. Yates, N. Oudrhiri, A. Francina, L. Kiger, C. Mazurier, S. Rouzbeh, W. El-Nemer, N. Hebert, M. C. Giarratana, S. Francois, A. Chapel, H. Lapillonne, D. Luton, A. Bennaceur-Griscelli, L. Douay, *Human induced pluripotent stem cells can reach complete terminal maturation: in vivo and in vitro evidence in the erythropoietic differentiation model*. **Haematologica-the Hematology Journal** 97, 1795. (Dec, 2012).

98. H. A. Pearson, J. S. Lobel, S. A. Kocoshis, J. L. Naiman, J. Windmiller, A. T. Lammi, R. Hoffman, J. C. Marsh, *NEW SYNDROME OF REFRACTORY SIDEROBLASTIC ANEMIA WITH VACUOLIZATION OF MARROW PRECURSORS AND EXOCRINE PANCREATIC DYSFUNCTION*. **Journal of Pediatrics** 95, 976. (1979).

99. M. I. Koster, J. Dinella, J. L. Chen, C. O'Shea, P. J. Koch, *Integrating Animal Models and In Vitro Tissue Models to Elucidate the Role of Desmosomal Proteins in Diseases*. **Cell Commun. Adhes.** 21, 55. (Feb, 2014).

100. S. R. Bacman, C. T. Moraes, in *Mitochondria, 2nd Edition,* L. A. Pon, E. A. Schon, Eds. (Elsevier Academic Press Inc, San Diego, 2007), vol. 80, pp. 503-524.

101. R. H. Swerdlow, *Mitochondria in cybrids containing mtDNA from persons with mitochondriopathies*. **Journal of Neuroscience Research** 85, 3416. (Nov, 2007).

102. H. R. Cock, S. J. Tabrizi, J. M. Cooper, A. H. V. Schapira, *The influence of nuclear background on the biochemical expression of 3460 Leber's hereditary optic neuropathy*. **Ann. Neurol.** 44, 187. (Aug, 1998).

103. D. R. Dunbar, P. A. Moonie, H. T. Jacobs, I. J. Holt, *DIFFERENT CELLULAR BACKGROUNDS CONFER A MARKED ADVANTAGE TO EITHER MUTANT OR WILD-TYPE MITOCHONDRIAL GENOMES*. **Proceedings of the National Academy of Sciences of the United States of America** 92, 6562. (Jul, 1995).

104. H. Landgren, P. Sartipy, *Can stem-cell-derived models revolutionize drug discovery?* **Expert. Opin. Drug Discov.** 9, 9. (Jan, 2014).

105. W. K. Porteous, A. M. James, P. W. Sheard, C. M. Porteous, M. A. Packer, S. J. Hyslop, J. V. Melton, C. Y. Pang, Y. H. Wei, M. P. Murphy, *Bioenergetic consequences of accumulating the common 4977-bp mitochondrial DNA deletion*. **European Journal of Biochemistry** 257, 192. (Oct, 1998).

106. W. E. Lowry, L. Richter, R. Yachechko, A. D. Pyle, J. Tchieu, R. Sridharan, A. T. Clark, K. Plath, *Generation of human induced pluripotent stem cells from dermal fibroblasts*. **Proceedings of the National Academy of Sciences of the United States of America** 105, 2883. (Feb, 2008).

107. Z. Ma, S. Koo, M. A. Finnegan, P. Loskill, N. Huebsch, N. C. Marks, B. R. Conklin, C. P. Grigoropoulos, K. E. Healy, *Three-dimensional filamentous human diseased cardiac tissue model*. **Biomaterials** 35, 1367. (Feb, 2014).

108. M. P. C. vandeCorput, J. M. W. vandenOuweland, R. W. Dirks, L. M. tHart, G. J. Bruining, J. A. Maassen, A. K. Raap, *Detection of mitochondrial DNA deletions in human skin fibroblasts of patients with Pearson's syndrome by two-color fluorescence in situ hybridization*. **J. Histochem. Cytochem.** 45, 55. (Jan, 1997).

109. T. Vazin, K. A. Ball, H. Lu, H. Park, Y. Ataeijannati, T. Head-Gordon, M. M. Poo, D. V. Schaffer, *Efficient derivation of cortical glutamatergic neurons from human pluripotent stem cells: A model system to study neurotoxicity in Alzheimer's disease*. **Neurobiology of Disease** 62, 62. (Feb, 2014).

110. C. Y. Lo, Y. W. Tjong, J. C. Y. Ho, C. W. Siu, S. Y. Cheung, N. L. Tang, S. Yu, H. F. Tse, X. Q. Yao, *An Upregulation in the Expression of Vanilloid Transient Potential Channels 2 Enhances Hypotonicity-Induced Cytosolic Ca2+ Rise in Human Induced Pluripotent Stem Cell Model of Hutchinson Gillford Progeria*. **PLoS One** 9. (Jan, 2014).

111. D. N. Kotton, J. Rossant, *Modeling Pulmonary Alveolar Proteinosis with Induced Pluripotent Stem Cells*. **Am. J. Respir. Crit. Care Med.** 189, 124. (Jan, 2014).

112. C. D. L. Folmes, T. J. Nelson, A. Martinez-Fernandez, D. K. Arrell, J. Z. Lindor, P. P. Dzeja, Y. Ikeda, C. Perez-Terzic, A. Terzic, *Somatic Oxidative Bioenergetics Transitions into Pluripotency-Dependent Glycolysis to Facilitate Nuclear Reprogramming*. **Cell Metab.** 14, 264. (Aug, 2011).

113. A. Prigione, B. Fauler, R. Lurz, H. Lehrach, J. Adjaye, *The Senescence-Related Mitochondrial/Oxidative Stress Pathway is Repressed in Human Induced Pluripotent Stem Cells*. **Stem Cells** 28, 721. (Apr, 2010).

114. S. Varum, A. S. Rodrigues, M. B. Moura, O. Momcilovic, C. A. Easley, J. Ramalho-Santos, B. Van Houten, G. Schatten, *Energy Metabolism in Human Pluripotent Stem Cells and Their Differentiated Counterparts*. **PLoS One** 6. (Jun, 2011).

115. A. D. Panopoulos, O. Yanes, S. Ruiz, Y. S. Kida, D. Diep, R. Tautenhahn, A. Herrerias, E. M. Batchelder, N. Plongthongkum, M. Lutz, W. T. Berggren, K. Zhang, R. M. Evans, G. Siuzdak, J. C. I. Belmonte, *The metabolome of induced pluripotent stem cells reveals metabolic changes occurring in somatic cell reprogramming*. **Cell Research** 22, 168. (Jan, 2012).

116. T. Saric, M. Halbach, M. Khalil, F. Er, *Induced pluripotent stem cells as cardiac arrhythmic in vitro models and the impact for drug discovery*. **Expert. Opin. Drug Discov.** 9, 55. (Jan, 2014).

117. G. Tiscornia, E. L. Vivas, L. Matalonga, I. Berniakovich, M. B. Monasterio, C. Eguizabal, L. Gort, F. Gonzalez, C. O. Mellet, J. M. G. Fernandez, A. Ribes, A. Veiga, J. C. I. Belmonte, *Neuronopathic Gaucher's disease: induced pluripotent stem cells for disease modelling and testing chaperone activity of small compounds (vol 22, pg 633, 2013)*. **Human Molecular Genetics** 23, 281. (Jan, 2014).

118. J. Zhang, I. Khvorostov, J. S. Hong, Y. Oktay, L. Vergnes, E. Nuebel, P. N. Wahjudi, K. Setoguchi, G. Wang, A. Do, H. J. Jung, J. M. McCaffery, I. J. Kurland, K. Reue, W. N. P. Lee, C. M. Koehler, M. A. Teitell, *UCP2 regulates energy metabolism and differentiation potential of human pluripotent stem cells*. **Embo Journal** 30, 4860. (Dec, 2011).

119. C. D. L. Folmes, A. Martinez-Fernandez, E. Perales-Clemente, X. Li, A. McDonald, D. Oglesbee, S. C. Hrstka, C. Perez-Terzic, A. Terzic, T. J. Nelson, *Disease-Causing Mitochondrial Heteroplasmy Segregated Within Induced Pluripotent Stem Cell Clones Derived from a Patient with MELAS*. **Stem Cells** 31, 1298. (Jul, 2013).

120. C. Aguer, D. Gambarotta, R. J. Mailloux, C. Moffat, R. Dent, R. McPherson, M. E. Harper, *Galactose Enhances Oxidative Metabolism and Reveals Mitochondrial Dysfunction in Human Primary Muscle Cells*. **PLoS One** 6. (Dec, 2011).

121. H. K. Rajasimha, P. F. Chinnery, D. C. Samuels, *Selection against pathogenic mtDNA mutations in a stem cell population leads to the loss of the 3243A -> G mutation in blood*. **American Journal of Human Genetics** 82, 333. (Feb, 2008).

122. A. Sharma, J. C. Wu, S. M. Wu, *Induced pluripotent stem cell-derived cardiomyocytes for cardiovascular disease modeling and drug screening*. **Stem Cell Res. Ther.** 4. (Dec, 2013).

123. K. Weber, J. N. Wilson, L. Taylor, E. Brierley, M. A. Johnson, D. M. Turnbull, L. A. Bindoff, *A new mtDNA mutation showing accumulation with time and restriction to skeletal muscle*. **American Journal of Human Genetics** 60, 373. (Feb, 1997).

124. K. Fu, R. Hartlen, T. Johns, A. Genge, G. Karpati, E. A. Shoubridge, *A novel heteroplasmic tRNA(leu(CUN)) mtDNA point mutation in a sporadic patient with mitochondrial encephalomyopathy segregates rapidly in skeletal muscle and suggests an approach to therapy*. **Human Molecular Genetics** 5, 1835. (Nov, 1996).

125. Gilgenkrantz.S, C. Cabrol, Lausecke.C, M. E. Hartleyb, B. Bohe, *DR SYNDROME REPORT OF NEW CASE (46,XX,14R)*. **Ann. Genet.** 14, 23. (1971).

126. M. Zollino, L. Seminara, D. Orteschi, G. Gobbi, S. Giovannini, E. D. Giustina, D. Frattini, A. Scarano, G. Neril, *The Ring 14 Syndrome: Clinical and Molecular Definition*. **American Journal of Medical Genetics Part A** 149A, 1116. (Jun, 2009).

127. N. Specchio, M. Trivisano, D. Serino, S. Cappelletti, A. Carotenuto, D. Claps, C. E. Marras, L. Fusco, M. Elia, F. Vigevano, *Epilepsy in ring 14 chromosome syndrome*. **Epilepsy Behav.** 25, 585. (Dec, 2012).

128. B. Ricard-Mousnier, S. N'Guyen, F. Dubas, F. Pouplard, A. Guichet, *Ring chromosome 17 epilepsy may resemble that of ring chromosome 20 syndrome*. **Epileptic Disord.** 9, 327. (Sep, 2007).

129. R. Moavero, R. Cusmai, M. C. Roberti, F. Vigevano, P. Curatolo, *Clinical Reasoning: A girl presenting with stiffness episodes during sleep, cafe-au-lait spots, and flecked retina*. **Neurology** 80, E42. (Jan, 2013).

130. A. Lo-Castro, N. El-Malhany, C. Galasso, A. Verrotti, A. M. Nardone, D. Postorivo, C. Palmieri, P. Curatolo, *De novo mosaic ring chromosome 18 in a child with mental retardation, epilepsy and immunological problems*. **Eur. J. Med. Genet.** 54, 329. (May-Jun, 2011).

131. E. Brodtkorb, T. Torbergsen, K. O. Nakken, K. Andersen, R. Gimse, O. Sjaastad, *EPILEPTIC SEIZURES, ARTHROGRYPOSIS, AND MIGRATIONAL BRAIN DISORDERS - A SYNDROME*. **Acta Neurol. Scand.** 90, 232. (Oct, 1994).

132. A. Shahwan, A. J. Green, A. Carey, T. L. Stallings, O. C. O'Flaherty, M. D. King, *Malignant refractory epilepsy in identical twins mosaic for a supernumerary ring chromosome 19*. **Epilepsia** 45, 997. (Aug, 2004).

133. Y. Inoue, T. Fujiwara, K. Matsuda, H. Kubota, M. Tanaka, K. Yagi, K. Yamamori, Y. Takahashi, *Ring chromosome 20 and nonconvulsive status epilepticus - A new epileptic syndrome*. **Brain** 120, 939. (Jun, 1997).

134. A. Biraben, F. Semah, M. J. Ribeiro, G. Douaud, P. Remy, A. Depaulis, *PET evidence for a role of the basal ganglia in patients with ring chromosome 20 epilepsy*. **Neurology** 63, 73. (Jul, 2004).

135. P. B. Augustijn, J. Parra, C. H. Wouters, P. Joosten, D. Lindhout, W. V. Boas, *Ring chromosome 20 epilepsy syndrome in children: Electroclinical features*. **Neurology** 57, 1108. (Sep, 2001).

136. H. Z. Zhang, F. Xu, M. Seashore, P. Li, *Unique Genomic Structure and Distinct Mitotic Behavior of Ring Chromosome 21 in Two Unrelated Cases*. **Cytogenetic and Genome Research** 136, 180. (2012).

137. R. S. Guilherme, V. D. A. Meloni, C. P. Sodre, D. M. Christofolini, R. Pellegrino, C. B. de Mello, L. K. Conlin, A. L. Hutchinson, N. B. Spinner, D. Brunoni, L. D. Kulikowski, M. I. Melaragno, *Cytogenetic and Molecular Evaluation and 20-Year Follow-Up of a Patient With Ring Chromosome 14*. **American Journal of Medical Genetics Part A** 152A, 2865. (Nov, 2010).

138. C. D. M. van Karnebeek, S. Quik, S. Sluijter, M. M. F. Hulsbeek, J. M. N. Hoovers, R. C. M. Hennekam, *Further delineation of the chromosome 14q terminal deletion syndrome*. **American Journal of Medical Genetics** 110, 65. (Jun, 2002).

139. K. Schlade-Bartusiak, T. Costa, A. M. Summers, M. J. M. Nowaczyk, D. W. Cox, *FISH-mapping of telomeric 14q32 deletions: Search for the cause of seizures*. **American Journal of Medical Genetics Part A** 138A, 218. (Oct, 2005).

140. K. Schlade-Bartusiak, H. Ardinger, D. W. Cox, *A Child With Terminal 14q Deletion Syndrome: Consideration of Genotype-Phenotype Correlations*. **American Journal of Medical Genetics Part A** 149A, 1012. (May, 2009).

141. E. Torgyekes, A. L. Shanske, K. Anyane-Yeboa, O. Nahum, S. Pirzadeh, E. Blumfield, V. Jobanputra, D. Warburton, B. Levy, *The Proximal Chromosome 14q Microdeletion Syndrome: Delineation of the Phenotype Using High Resolution SNP Oligonucleotide Microarray Analysis (SOMA) and Review of the Literature*. **American Journal of Medical Genetics Part A** 155A, 1884. (Aug, 2011).

142. S. M. Chambers, C. A. Fasano, E. P. Papapetrou, M. Tomishima, M. Sadelain, L. Studer, *Highly efficient neural conversion of human ES and iPS cells by dual inhibition of SMAD signaling*. **Nature Biotechnology** 27, 275. (Mar, 2009).

143. A. M. Maroof, S. Keros, J. A. Tyson, S. W. Ying, Y. M. Ganat, F. T. Merkle, B. Liu, A. Goulburn, E. G. Stanley, A. G. Elefanty, H. R. Widmer, K. Eggan, P. A. Goldstein, S. A. Anderson, L. Studer, *Directed Differentiation and Functional Maturation of Cortical Interneurons from Human Embryonic Stem Cells*. **Cell Stem Cell** 12, 559. (May, 2013).

144. M. Bershteyn, Y. Hayashi, G. Desachy, E. C. Hsiao, S. Sami, K. M. Tsang, L. A. Weiss, A. R. Kriegstein, S. Yamanaka, A. Wynshaw-Boris, *Cell-autonomous correction of ring chromosomes in human induced pluripotent stem cells*. **Nature** 507, 99. (Mar, 2014).

145. N. Higurashi, T. Uchida, C. Lossin, Y. Misumi, Y. Okada, W. Akamatsu, Y. Imaizumi, B. Zhang, K. Nabeshima, M. X. Mori, S. Katsurabayashi, Y. Shirasaka, H. Okano, S. Hirose, *A human Dravet syndrome model from patient induced pluripotent stem cells*. **Mol. Brain** 6. (May, 2013).

146. J. Jiao, Y. Y. Yang, Y. W. Shi, J. Y. Chen, R. Gao, Y. Fan, H. Yao, W. P. Liao, X. F. Sun, S. R. Gao, *Modeling Dravet syndrome using induced pluripotent stem cells (iPSCs) and directly converted neurons*. **Human Molecular Genetics** 22, 4241. (Nov, 2013).

147. Y. Liu, L. F. Lopez-Santiago, Y. Yuan, J. M. Jones, H. Zhang, H. A. O'Malley, G. A. Patino, J. E. O'Brien, R. Rusconi, A. Gupta, R. C. Thompson, M. R. Natowicz, M. H. Meisler, L. L. Isom, J. M. Parent, *Dravet Syndrome Patient-Derived Neurons Suggest a Novel Epilepsy Mechanism*. **Ann. Neurol.** 74, 128. (Jul, 2013).

148. M. D. Tischkowitz, S. V. Hodgson, *Fanconi anaemia*. **Journal of Medical Genetics** 40, 1. (Jan, 2003).

149. F. Fares, K. Badarneh, M. Abosaleh, A. Harari-Shaham, R. Diukman, M. David, *Carrier frequency of autosomal-recessive disorders in the Ashkenazi Jewish population: should the rationale for mutation choice for screening be reevaluated?* **Prenatal Diagnosis** 28, 236. (Mar, 2008).

150. G. L. Moldovan, A. D. D'Andrea, in *Annual Review of Genetics*. (2009), vol. 43, pp. 223-249.

151. A. M. Ali, T. R. Singh, A. R. Meetei, *FANCM-FAAP24 and FANCJ: FA proteins that metabolize DNA*. **Mutation Research-Fundamental and Molecular Mechanisms of Mutagenesis** 668, 20. (Jul, 2009).

152. J. P. de Winter, H. Joenje, *The genetic and molecular basis of Fanconi anemia*. **Mutation Research-Fundamental and Molecular Mechanisms of Mutagenesis** 668, 11. (Jul, 2009).

153. H. Kim, A. D. D'Andrea, *Regulation of DNA cross-link repair by the Fanconi anemia/BRCA pathway*. **Genes & Development** 26, 1393. (Jul, 2012).

154. F. Langevin, G. P. Crossan, I. V. Rosado, M. J. Arends, K. J. Patel, *Fancd2 counteracts the toxic effects of naturally produced aldehydes in mice*. **Nature** 475, 53. (Jul, 2011).

155. C. L. Garcia, M. Mechilli, L. P. De Santis, A. Schinoppi, K. Kobos, F. Palitti, *Relationship between DNA lesions, DNA repair and chromosomal damage induced by acetaldehyde*. **Mutation Research-Fundamental and Molecular Mechanisms of Mutagenesis** 662, 3. (Mar, 2009).

156. A. Hira, H. Yabe, K. Yoshida, Y. Okuno, Y. Shiraishi, K. Chiba, H. Tanaka, S. Miyano, J. Nakamura, S. Kojima, S. Ogawa, K. Matsuo, M. Takata, M. Yabe, *Variant ALDH2 is associated with accelerated progression of bone marrow failure in Japanese Fanconi anemia patients*. **Blood** 122, 3206. (Oct, 2013).

157. A. D. Auerbach, R. G. Allen, *LEUKEMIA AND PRELEUKEMIA IN FANCONI ANEMIA PATIENTS - A REVIEW OF THE LITERATURE AND REPORT OF THE INTERNATIONAL FANCONI ANEMIA REGISTRY*. **Cancer Genetics and Cytogenetics** 51, 1. (Jan, 1991).

158. A. Butturini, R. P. Gale, P. C. Verlander, B. Adlerbrecher, A. P. Gillio, A. D. Auerbach, *HEMATOLOGIC ABNORMALITIES IN FANCONI-ANEMIA - AN INTERNATIONAL FANCONI-ANEMIA REGISTRY STUDY*. **Blood** 84, 1650. (Sep, 1994).

159. P. F. Giampietro, P. C. Verlander, J. G. Davis, A. D. Auerbach, *Diagnosis of Fanconi anemia in patients without congenital malformations: An international Fanconi anemia registry study*. **American Journal of Medical Genetics** 68, 58. (Jan, 1997).

160. P. F. Kelly, S. Radtke, C. von Kalle, B. Balcik, K. Bohn, R. Mueller, T. Schuesler, M. Haren, L. Reeves, J. A. Cancelas, T. Leemhuis, R. Harris, A. D. Auerbach, F. O. Smith, S. M. Davies, D. A. Williams, *Stem cell collection and gene transfer in Fanconi anemia*. **Molecular Therapy** 15, 211. (Jan, 2007).

161. P. S. Rosenberg, M. H. Greene, B. P. Alter, *Cancer incidence in persons with Fanconi anemia*. **Blood** 101, 822. (Feb, 2003).

162. B. P. Alter, M. H. Greene, I. Velazquez, P. S. Rosenberg, *Cancer in Fanconi anemia*. **Blood** 101, 2072. (Mar, 2003).

163. A. Raya, I. Rodriguez-Piza, G. Guenechea, R. Vassena, S. Navarro, M. J. Barrero, A. Consiglio, M. Castella, P. Rio, E. Sleep, F. Gonzalez, G. Tiscornia, E. Garreta, T. Aasen, A. Veiga, I. M. Verma, J. Surralles, J. Bueren, J. C. I. Belmonte, *Disease-corrected haematopoietic progenitors from Fanconi anaemia induced pluripotent stem cells*. **Nature** 460, 53. (Jul, 2009).

164. L. U. W. Mueller, M. D. Milsom, C. E. Harris, R. Vyas, K. M. Brumme, K. Parmar, L. A. Moreau, A. Schambach, I.-H. Park, W. B. London, K. Strait, T. Schlaeger, A. L. DeVine, E. Grassman, A. D'Andrea, G. Q. Daley, D. A. Williams, *Overcoming reprogramming resistance of Fanconi anemia cells*. **Blood** 119, 5449. (Jun 7, 2012).

165. T. Kawamura, J. Suzuki, Y. V. Wang, S. Menendez, L. B. Morera, A. Raya, G. M. Wahl, J. C. I. Belmonte, *Linking the p53 tumour suppressor pathway to somatic cell reprogramming*. **Nature** 460, 1140. (Aug, 2009).

166. F. Gonzalez, D. Georgieva, F. Vanoli, Z. D. Shi, M. Stadtfeld, T. Ludwig, M. Jasin, D. W. Huangfu, *Homologous Recombination DNA Repair Genes Play a Critical Role in Reprogramming to a Pluripotent State*. **Cell Reports** 3, 651. (Mar, 2013).

167. E. M. Kass, M. Jasin, *Collaboration and competition between DNA double-strand break repair pathways*. **Febs Letters** 584, 3703. (Sep, 2010).

168. P. Pace, G. Mosedale, M. R. Hodskinson, I. V. Rosado, M. Sivasubramaniam, K. J. Patel, *Ku70 Corrupts DNA Repair in the Absence of the Fanconi Anemia Pathway*. **Science** 329, 219. (Jul, 2010).

169. A. Adamo, S. J. Collis, C. A. Adelman, N. Silva, Z. Horejsi, J. D. Ward, E. Martinez-Perez, S. J. Boulton, A. La Volpe, *Preventing Nonhomologous End Joining Suppresses DNA Repair Defects of Fanconi Anemia*. **Molecular Cell** 39, 25. (Jul, 2010).

170. H. Li, M. Collado, A. Villasante, K. Strati, S. Ortega, M. Canamero, M. A. Blasco, M. Serrano, *The Ink4/Arf locus is a barrier for iPS cell reprogramming*. **Nature** 460, 1136. (Aug, 2009).

171. H. Hong, K. Takahashi, T. Ichisaka, T. Aoi, O. Kanagawa, M. Nakagawa, K. Okita, S. Yamanaka, *Suppression of induced pluripotent stem cell generation by the p53-p21 pathway*. **Nature** 460, 1132. (Aug, 2009).

172. R. M. Marion, K. Strati, H. Li, M. Murga, R. Blanco, S. Ortega, O. Fernandez-Capetillo, M. Serrano, M. A. Blasco, *A p53-mediated DNA damage response limits reprogramming to ensure iPS cell genomic integrity*. **Nature** 460, 1149. (Aug, 2009).

173. M. Stadtfeld, N. Maherali, M. Borkent, K. Hochedlinger, *A reprogrammable mouse strain from gene-targeted embryonic stem cells*. **Nature Methods** 7, 53. (Jan, 2010).

174. B. W. Carey, S. Markoulaki, C. Beard, J. Hanna, R. Jaenisch, *Single-gene transgenic mouse strains for reprogramming adult somatic cells*. **Nature Methods** 7, 56. (Jan, 2010).

175. J. Hanna, K. Saha, B. Pando, J. van Zon, C. J. Lengner, M. P. Creyghton, A. van Oudenaarden, R. Jaenisch, *Direct cell reprogramming is a stochastic process amenable to acceleration*. **Nature** 462, 595. (Dec, 2009).

176. Q. Waisfisz, N. V. Morgan, M. Savino, J. P. de Winter, C. G. M. van Berkel, M. E. Hoatlin, L. Ianzano, R. A. Gibson, F. Arwert, A. Savoia, C. G. Mathew, J. C. Pronk, H. Joenje, *Spontaneous functional correction of homozygous Fanconi anaemia alleles reveals novel mechanistic basis for reverse mosaicism*. **Nature Genetics** 22, 379. (Aug, 1999).

177. M. Gross, H. Hanenberg, S. Lobitz, R. Friedl, S. Herterich, R. Dietrich, B. Gruhn, D. Schindler, H. Hoehn, *Reverse mosaicism in Fanconi anemia: natural gene therapy via molecular self-correction*. **Cytogenetic and Genome Research** 98, 126. (2002).

178. R. Ceccaldi, K. Parmar, E. Mouly, M. Delord, J. M. Kim, M. Regairaz, M. Pla, N. Vasquez, Q. S. Zhang, C. Pondarre, R. P. de Latour, E. Gluckman, M. Cavazzana-Calvo, T. Leblanc, J. Larghero, M. Grompe, G. Socie, A. D. D'Andrea, J. Soulier, *Bone Marrow Failure in Fanconi Anemia Is Triggered by an Exacerbated p53/p21 DNA Damage Response that Impairs Hematopoietic Stem and Progenitor Cells*. **Cell Stem Cell** 11, 36. (Jul, 2012).

179. Q. S. Zhang, K. Watanabe-Smith, K. Schubert, A. Major, A. M. Sheehan, L. Marquez-Loza, A. E. H. Newell, E. Benedetti, E. Joseph, S. Olson, M. Grompe, *Fancd2 and p21 function independently in maintaining the size of hematopoietic stem and progenitor cell pool in mice*. **Stem Cell Research** 11, 687. (Sep, 2013).

180. L. U. W. Muller, M. D. Milsom, C. E. Harris, R. Vyas, K. M. Brumme, K. Parmar, L. A. Moreau, A. Schambach, I. H. Park, W. B. London, K. Strait, T. Schlaeger, A. L. DeVine, E. Grassman, A. D'Andrea, G. Q. Daley, D. A. Williams, *Overcoming reprogramming resistance of Fanconi anemia cells*. **Blood** 119, 5449. (Jun, 2012).

181. S. Ruiz, A. D. Panopoulos, A. Herrerias, K. D. Bissig, M. Lutz, W. T. Berggren, I. M. Verma, J. C. I. Belmonte, *A High Proliferation Rate Is Required for Cell Reprogramming and Maintenance of Human Embryonic Stem Cell Identity*. **Current Biology** 21, 45. (Jan, 2011).

182. S. Q. Guo, X. Y. Zi, V. P. Schulz, J. J. Cheng, M. Zhong, S. H. J. Koochaki, C. M. Megyola, X. H. Pan, K. Heydari, S. M. Weissman, P. G. Gallagher, D. S. Krause, R. Fan, J. Lu, *Nonstochastic Reprogramming from a Privileged Somatic Cell State*. **Cell** 156, 649. (Feb, 2014).

183. J. I. Garaycoechea, K. J. Patel, *Why does the bone marrow fail in Fanconi anemia?* **Blood** 123, 26. (Jan, 2014).

184. M. Noll, K. P. Battaile, R. Bateman, T. P. Lax, K. Rathbun, C. Reifsteck, G. Bagby, M. Finegold, S. Olson, M. Grompe, *Fanconi anemia group A and C double-mutant mice: Functional evidence for a multi-protein Fanconi anemia complex*. **Experimental Hematology** 30, 679. (Jul, 2002).

185. Y. F. Zheng, X. J. Yao, *Posttranslational Modifications of HIV-1 Integrase by Various Cellular Proteins during Viral Replication*. **Viruses-Basel** 5, 1787. (Jul, 2013).

186. L. Y. Geng, C. J. Huntoon, L. M. Karnitz, *RAD18-mediated ubiquitination of PCNA activates the Fanconi anemia DNA repair network*. **Journal of Cell Biology** 191, 249. (Oct, 2010).

187. S. H. He, D. Nakada, S. J. Morrison, in *Annual Review of Cell and Developmental Biology*. (Annual Reviews, Palo Alto, 2009), vol. 25, pp. 377-406.

188. A. V. Krivtsov, D. Twomey, Z. H. Feng, M. C. Stubbs, Y. Z. Wang, J. Faber, J. E. Levine, J. Wang, W. C. Hahn, D. G. Gilliland, T. R. Golub, S. A. Armstrong, *Transformation from committed progenitor to leukaemia stem cell initiated by MLL-AF9*. **Nature** 442, 818. (Aug, 2006).

189. A. Gupta, A. K. Godwin, L. Vanderveer, A. P. Lu, J. W. Liu, *Hypomethylation of the Synuclein gamma gene CpG island promotes its aberrant expression in breast carcinoma and ovarian carcinoma*. **Cancer Research** 63, 664. (Feb, 2003).

190. J. Lagergren, R. Bergstrom, A. Lindgren, O. Nyren, *Symptomatic gastroesophageal reflux as a risk factor for esophageal adenocarcinoma*. **New England Journal of Medicine** 340, 825. (Mar, 1999).

191. H. Obokata, Y. Sasai, H. Niwa, M. Kadota, M. Andrabi, N. Takata, M. Tokoro, Y. Terashita, S. Yonemura, C. A. Vacanti, T. Wakayama, *Bidirectional developmental potential in reprogrammed cells with acquired pluripotency*. **Nature** 505, 676. (Jan 30, 2014).

192. H. Obokata, T. Wakayama, Y. Sasai, K. Kojima, M. P. Vacanti, H. Niwa, M. Yamato, C. A. Vacanti, *Stimulus-triggered fate conversion of somatic cells into pluripotency*. **Nature** 505, 641. (Jan 30, 2014).

193. J. T. Bell, T. D. Spector, *DNA methylation studies using twins: what are they telling us?* **Genome Biology** 13. (2012).

194. J. M. P. Freije, C. Lopez-Otin, *Reprogramming aging and progeria*. **Current Opinion in Cell Biology** 24, 757. (Dec, 2012).

195. J. D. Miller, Y. M. Ganat, S. Kishinevsky, R. L. Bowman, B. Liu, E. Y. Tu, P. K. Mandal, E. Vera, J. W. Shim, S. Kriks, T. Taldone, N. Fusaki, M. J. Tomishima, D. Krainc, T. A. Milner, D. J. Rossi, L. Studer, *Human iPSC-Based Modeling of Late-Onset Disease via Progerin-Induced Aging*. **Cell Stem Cell** 13, 691. (Dec, 2013).

196. W. E. Ek, D. M. Levine, M. D'Amato, N. L. Pedersen, P. K. E. Magnusson, F. Bresso, L. E. Onstad, P. T. Schmidt, H. Tornblom, H. Nordenstedt, Y. Romero, W. H. Chow, L. J. Murray, M. D. Gammon, G. Liu, L. Bernstein, A. G. Casson, H. A. Risch, N. J. Shaheen, N. C. Bird, B. J. Reid, D. A. Corley, L. J. Hardie, W. M. Ye, A. H. Wu, M. Zucchelli, T. D. Spector, P. Hysi, T. L. Vaughan, D. C. Whiteman, S. MacGregor, A. Mayo Clinic Esophageal, C. Barretts Esophagus Registry, B. S. Investigators, *Germline Genetic Contributions to Risk for Esophageal Adenocarcinoma, Barretts Esophagus, and Gastroesophageal Reflux*. **JNCI-. Natl. Cancer Inst.** 105, 1711. (Nov, 2013).

197. L. J. Shao, W. Feng, Y. Sun, H. Bai, J. Liu, C. Currie, J. J. Kim, R. Gama, Z. Wang, Z. J. Qian, L. Liaw, W. S. Wu, *Generation of iPS cells using defined factors linked via the self-cleaving 2A sequences in a single open reading frame*. **Cell Research** 19, 296. (Mar, 2009).

198. A. Schambach, E. Warlich, T. Cantz, M. Brugman, T. Matzig, H. Scholer, C. Baum, *Lentiviral vectors for reprogramming of somatic cells into induced pluripotent stem (iPS) cells*. **Human Gene Therapy** 19, 1087. (Oct, 2008).

199. C. A. Sommer, M. Stadtfeld, G. J. Murphy, K. Hochedlinger, D. N. Kotton, G. Mostoslavsky, *Induced Pluripotent Stem Cell Generation Using a Single Lentiviral Stem Cell Cassette*. **Stem Cells** 27, 543. (2009).

200. A. Somers, J. C. Jean, C. A. Sommer, A. Omari, C. C. Ford, J. A. Mills, L. Ying, A. G. Sommer, J. M. Jean, B. W. Smith, R. Lafyatis, M. F. Demierre, D. J. Weiss, D. L. French, P. Gadue, G. J. Murphy, G. Mostoslavsky, D. N. Kotton, *Generation of*

Transgene-Free Lung Disease-Specific Human Induced Pluripotent Stem Cells Using a Single Excisable Lentiviral Stem Cell Cassette. **Stem Cells** 28, 1728. (Oct, 2010).

201. C. W. Chang, Y. S. Lai, K. M. Pawlik, K. Liu, C. W. Sun, C. Li, T. R. Schoeb, T. M. Townes, *Polycistronic Lentiviral Vector for "Hit and Run" Reprogramming of Adult Skin Fibroblasts to Induced Pluripotent Stem Cells*. **Stem Cells** 27, 1042. (2009).

202. L. Warren, P. D. Manos, T. Ahfeldt, Y. H. Loh, H. Li, F. Lau, W. Ebina, P. K. Mandal, Z. D. Smith, A. Meissner, G. Q. Daley, A. S. Brack, J. J. Collins, C. Cowan, T. M. Schlaeger, D. J. Rossi, *Highly Efficient Reprogramming to Pluripotency and Directed Differentiation of Human Cells with Synthetic Modified mRNA*. **Cell Stem Cell** 7, 618. (Nov, 2010).

203. H. J. Cho, C. S. Lee, Y. W. Kwon, J. S. Paek, S. H. Lee, J. Hur, E. J. Lee, T. Y. Roh, I. S. Chu, S. H. Leem, Y. Kim, H. J. Kang, Y. B. Park, H. S. Kim, *Induction of pluripotent stem cells from adult somatic cells by protein-based reprogramming without genetic manipulation*. **Blood** 116, 386. (Jul, 2010).

204. K. Okita, Y. Matsumura, Y. Sato, A. Okada, A. Morizane, S. Okamoto, H. Hong, M. Nakagawa, K. Tanabe, K. Tezuka, T. Shibata, T. Kunisada, M. Takahashi, J. Takahashi, H. Saji, S. Yamanaka, *A more efficient method to generate integration-free human iPS cells*. **Nature Methods** 8, 409. (May, 2011).

205. M. Thier, B. Munst, S. Mielke, F. Edenhofer, *Cellular Reprogramming Employing Recombinant Sox2 Protein*. **Stem Cells Int.** (2012).

206. J. Y. Yu, K. J. Hu, K. Smuga-Otto, S. L. Tian, R. Stewart, Slukvin, II, J. A. Thomson, *Human Induced Pluripotent Stem Cells Free of Vector and Transgene Sequences*. **Science** 324, 797. (May, 2009).

207. E. Senis, E. Kienle, C. A. Fajardo, I. Aydin, D. Grimm, *An AAV Vector-Based Toolbox for Somatic Reprogramming and for iPS Cell Tracking and Purging*. **Molecular Therapy** 20, S204. (May, 2012).

208. E. Senis, D. Grimm, *Efficient somatic cell reprogramming using low doses of self-complementary AAV-DJ vectors*. **Human Gene Therapy** 24, A105. (Dec, 2013).

209. L. Ye, M. O. Muench, N. Fusaki, A. I. Beyer, J. M. Wang, Z. X. Qi, J. W. Yu, Y. W. Kan, *Blood Cell-Derived Induced Pluripotent Stem Cells Free of Reprogramming Factors Generated by Sendai Viral Vectors*. **Stem Cells Transl. Med.** 2, 558. (Aug, 2013).

210. N. Fusaki, H. Ban, A. Nishiyama, K. Saeki, M. Hasegawa, *Efficient induction of transgene-free human pluripotent stem cells using a vector based on Sendai virus, an RNA virus that does not integrate into the host genome*. **Proceedings of the Japan Academy Series B-Physical and Biological Sciences** 85, 348. (Oct, 2009).

211. Y. C. Kudva, S. Ohmine, L. V. Greder, J. R. Dutton, A. Armstrong, J. G. De Lamo, Y. K. Khan, T. Thatava, M. Hasegawa, N. Fusaki, J. M. W. Slack, Y. Ikeda, *Transgene-Free Disease-Specific Induced Pluripotent Stem Cells from Patients with Type 1 and Type 2 Diabetes*. **Stem Cells Transl. Med.** 1, 451. (Jun, 2012).

212. J. K. Ichida, J. Blanchard, K. Lam, E. Y. Son, J. E. Chung, D. Egli, K. M. Loh, A. C. Carter, F. P. Di Giorgio, K. Koszka, D. W. Huangfu, H. Akutsu, D. R. Liu, L. L. Rubin, K. Eggan, *A Small-Molecule Inhibitor of Tgf-beta Signaling Replaces Sox2 in Reprogramming by Inducing Nanog*. **Cell Stem Cell** 5, 491. (Nov, 2009).

213. T. T. Onder, N. Kara, A. Cherry, A. U. Sinha, N. Zhu, K. M. Bernt, P. Cahan, B. O. Mancarci, J. Unternaehrer, P. B. Gupta, E. S. Lander, S. A. Armstrong, G. Q. Daley, *Chromatin-modifying enzymes as modulators of reprogramming*. **Nature** 483, 598. (Mar, 2012).

214. J. K. Yisraeli, D. A. Melton, *Synthesis of long, capped transcripts in vitro by SP6 and T7 RNA polymerases*. **Methods Enzymol** 180, 42. (1989).